

1981

# An Experimental Evaluation of Neuber's Cyclic Relation at Room and Elevated Temperature.

Michael Wade Guillot

*Louisiana State University and Agricultural & Mechanical College*

Follow this and additional works at: [https://digitalcommons.lsu.edu/gradschool\\_disstheses](https://digitalcommons.lsu.edu/gradschool_disstheses)

---

## Recommended Citation

Guillot, Michael Wade, "An Experimental Evaluation of Neuber's Cyclic Relation at Room and Elevated Temperature." (1981). *LSU Historical Dissertations and Theses*. 3598.

[https://digitalcommons.lsu.edu/gradschool\\_disstheses/3598](https://digitalcommons.lsu.edu/gradschool_disstheses/3598)

This Dissertation is brought to you for free and open access by the Graduate School at LSU Digital Commons. It has been accepted for inclusion in LSU Historical Dissertations and Theses by an authorized administrator of LSU Digital Commons. For more information, please contact [gradetd@lsu.edu](mailto:gradetd@lsu.edu).

## **INFORMATION TO USERS**

**This was produced from a copy of a document sent to us for microfilming. While the most advanced technological means to photograph and reproduce this document have been used, the quality is heavily dependent upon the quality of the material submitted.**

**The following explanation of techniques is provided to help you understand markings or notations which may appear on this reproduction.**

- 1. The sign or "target" for pages apparently lacking from the document photographed is "Missing Page(s)". If it was possible to obtain the missing page(s) or section, they are spliced into the film along with adjacent pages. This may have necessitated cutting through an image and duplicating adjacent pages to assure you of complete continuity.**
- 2. When an image on the film is obliterated with a round black mark it is an indication that the film inspector noticed either blurred copy because of movement during exposure, or duplicate copy. Unless we meant to delete copyrighted materials that should not have been filmed, you will find a good image of the page in the adjacent frame.**
- 3. When a map, drawing or chart, etc., is part of the material being photographed the photographer has followed a definite method in "sectioning" the material. It is customary to begin filming at the upper left hand corner of a large sheet and to continue from left to right in equal sections with small overlaps. If necessary, sectioning is continued again—beginning below the first row and continuing on until complete.**
- 4. For any illustrations that cannot be reproduced satisfactorily by xerography, photographic prints can be purchased at additional cost and tipped into your xerographic copy. Requests can be made to our Dissertations Customer Services Department.**
- 5. Some pages in any document may have indistinct print. In all cases we have filmed the best available copy.**

**University  
Microfilms  
International**

**300 N. ZEEB ROAD, ANN ARBOR, MI 48106  
18 BEDFORD ROW, LONDON WC1R 4EJ, ENGLAND**

8117628

GUILLOT, MICHAEL WADE

AN EXPERIMENTAL EVALUATION OF NEUBER'S CYCLIC RELATION AT  
ROOM AND ELEVATED TEMPERATURE

*The Louisiana State University and Agricultural and Mechanical Col.*    PH.D. 1981

University  
Microfilms  
International 300 N. Zeeb Road, Ann Arbor, MI 48106

**PLEASE NOTE:**

In all cases this material has been filmed in the best possible way from the available copy.  
Problems encountered with this document have been identified here with a check mark ✓.

1. Glossy photographs or pages \_\_\_\_\_
2. Colored illustrations, paper or print \_\_\_\_\_
3. Photographs with dark background \_\_\_\_\_
4. Illustrations are poor copy \_\_\_\_\_
5. Pages with black marks, not original copy \_\_\_\_\_
6. Print shows through as there is text on both sides of page \_\_\_\_\_
7. Indistinct, broken or small print on several pages ✓
8. Print exceeds margin requirements \_\_\_\_\_
9. Tightly bound copy with print lost in spine \_\_\_\_\_
10. Computer printout pages with indistinct print ✓
11. Page(s) \_\_\_\_\_ lacking when material received, and not available from school or author.
12. Page(s) \_\_\_\_\_ seem to be missing in numbering only as text follows.
13. Two pages numbered \_\_\_\_\_. Text follows.
14. Curling and wrinkled pages \_\_\_\_\_
15. Other \_\_\_\_\_

AN EXPERIMENTAL EVALUATION OF NEUBER'S  
CYCLIC RELATION AT ROOM AND  
ELEVATED TEMPERATURE

A Dissertation

Submitted to the Graduate Faculty of the  
Louisiana State University and  
Agricultural and Mechanical College  
in partial fulfillment of the  
requirements for the degree of  
Doctor of Philosophy

in

The Department of Mechanical Engineering

by  
Michael Wade Guillot  
B.S., Louisiana State University, 1972  
M.S., Louisiana State University, 1976  
May, 1981

## ACKNOWLEDGEMENT

The author wishes to express his appreciation to Dr. M. Sabbaghian for serving as chairman of his advisory committee and to Dr. D. E. Thompson, Dr. R. L. Thoms and Professor A. J. McPhate for participating on the committee. Also, a special acknowledgement is given to Dr. W. N. Sharpe, Jr., for the careful guidance and extreme patience shown during the entire research program.

The author is greatly indebted to the National Science Foundation, whose funding permitted this research to be carried out. The Air Force Materials Lab also provided funds for the machining of the test specimens. Appreciation is expressed to the Ethyl Corporation for permitting the author the freedom to pursue an advanced degree.

Finally, a special thanks is given to my wife, Ladonna, for the patience and encouragement she provided during this endeavor.

## FOREWORD

This research was supported by the National Science Foundation (NSF) under grant number ENG77 13872. It was originally granted jointly to W. N. Sharpe, Jr., and J. F. Martin, both of Michigan State University (MSU). However, shortly after receiving the grant, Sharpe accepted a position as Chairman of the Mechanical Engineering Department at Louisiana State University (LSU). At that time an agreement between Sharpe and Martin was made to divide both the research and funds from the NSF. The decision was that Martin would perform all of the room temperature experiments at MSU, while Sharpe would conduct the elevated temperature portion at LSU. Also, it was agreed that Martin would select and purchase all specimen material for both experiments. This agreement was adhered to by Martin, resulting in the thesis by Bofferding, reference 11. For the sake of insuring a good data base to use in evaluating the elevated temperature data, both room and elevated temperature tests were conducted by LSU. Funds for some of the specimen machining were provided by the Air Force Materials Laboratory.

## TABLE OF CONTENTS

	Page
ACKNOWLEDGEMENTS . . . . .	ii
FOREWORD . . . . .	iii
LIST OF TABLES . . . . .	vi
LIST OF FIGURES . . . . .	vii
ABSTRACT . . . . .	x
 Chapter	
I. INTRODUCTION . . . . .	1
1.1 Overview of Fatigue . . . . .	1
1.2 Literature Survey . . . . .	2
1.3 Objective . . . . .	6
II. SPECIMEN DESIGN . . . . .	9
2.1 Geometry . . . . .	9
2.2 Materials . . . . .	17
2.3 Temperature . . . . .	21
III. TEST APPARATUS . . . . .	27
3.1 Interferometric Strain Gage . . . . .	27
3.2 Extensometer . . . . .	30
3.3 Grips . . . . .	35
3.4 Heater and Temperature Controller . . . . .	37
3.5 Computer-Testing Machine Interface . . . . .	41



Chapter	Page
IV. SOFTWARE . . . . .	44
4.1 Notched Specimen Programs . . . . .	44
4.2 Smooth Specimen Programs . . . . .	54
4.3 Data Reduction Programs . . . . .	57
V. EXPERIMENTAL PROCEDURES . . . . .	60
5.1 Notched Specimen Tests . . . . .	61
5.2 Smooth Specimen Tests . . . . .	66
5.3 Elevated Temperature Tests . . . . .	68
5.4 Experimental Accuracy . . . . .	69
VI. RESULTS . . . . .	72
6.1 Specimen Log . . . . .	72
6.2 Notch Strain vs. Remote Stress . . . . .	75
6.3 Notch Strain vs. Notch Stress . . . . .	77
6.4 Notch Strain vs. Neuber's Parameter . . . . .	81
6.5 Concentration Factors vs. Cycles . . . . .	85
6.6 Fatigue Notch Factor vs. Cycles . . . . .	105
VII. CONCLUSIONS . . . . .	112
BIBLIOGRAPHY . . . . .	114
APPENDIXES	
A. Strain Gage Specifications for the Extensometer . . . . .	116
B. Computer Program Listing NOTCH6.FOR . . . . .	118
C. Computer Program Listing SMOOTH.FOR . . . . .	125
D. Data Reduction Programs . . . . .	128
VITA . . . . .	141

## LIST OF TABLES

Table	Page
2.1 Material Properties . . . . .	21
6.1 Specimen List . . . . .	73

## LIST OF FIGURES

Figure	Page
2.1 Notched Specimen - Hole . . . . .	11
2.2 Notched Specimen - Original Design of Ellipse . . . . .	12
2.3 Notched Specimen - Slot . . . . .	14
2.4 Smooth Specimen . . . . .	16
2.5 Specimen Layout - 7475 Aluminum . . . . .	18
2.6 Specimen Layout - 2024 Aluminum . . . . .	19
2.7 Specimen Layout - 1018 CRS . . . . .	20
2.8 Stress - Strain Curve - 7475 Aluminum . . . . .	22
2.9 Stress - Strain Curve - 2024 Aluminum . . . . .	23
2.10 Stress - Strain Curve - 1018 C.R.S. . . . .	24
3.1 Interferometric Strain Gage Principles . . . . .	28
3.2 Interferometric Strain Gage Equipment . . . . .	31
3.3 Photomultiplier Tube Voltage Signal . . . . .	32
3.4 Extensometer Assembly . . . . .	34
3.5 Grips Assembly . . . . .	36
3.6 Smooth Specimen Grip Adaptor . . . . .	38
3.7 Furnace Assembly . . . . .	39
4.1 Flowchart of NOTCH6 . . . . .	50-51
4.2 Flowchart of SMOOTH . . . . .	55
5.1 Calibration Curve for the Interferometric Strain Gage . . .	63
5.2 Calibration Curve for the Extensometer . . . . .	67

Figure	Page
6.1 Notch Strain vs. Remote Stress . . . . .	76
6.2 Notch Strain vs. Notch Stress - AL 2024 . . . . .	78
6.3 Notch Strain vs. Notch Stress - Steel 1018 . . . . .	79
6.4 Notch Strain vs. Notch Stress - AL 7475 . . . . .	80
6.5 Stress Concentration vs. Notch Strain- 1st Quarter Cycle . .	82
6.6 Strain Concentration vs. Notch Strain- 1st Quarter Cycle . .	83
6.7 Neuber's Parameter vs. Notch Strain- 1st Quarter Cycle . . .	84
6.8 AL 2024 - Hole - Stress Concentration vs. Cycles . . . . .	87
6.9 AL 2024 - Slot - Stress Concentration vs. Cycles . . . . .	88
6.10 AL 2024 - Hole - Strain Concentration vs. Cycles . . . . .	89
6.11 AL 2024 - Slot - Strain Concentration vs. Cycles . . . . .	90
6.12 AL 2024 - Hole - Neuber's Parameter vs. Cycles . . . . .	91
6.13 AL 2024 - Slot - Neuber's Parameter vs. Cycles . . . . .	92
6.14 CRS 1018 - Hole - Stress Concentration vs. Cycles . . . . .	93
6.15 CRS 1018 - Slot - Stress Concentration vs. Cycles . . . . .	94
6.16 CRS 1018 - Hole - Strain Concentration vs. Cycles . . . . .	95
6.17 CRS 1018 - Slot - Strain Concentration vs. Cycles . . . . .	96
6.18 CRS 1018 - Hole - Neuber's Parameter vs. Cycles . . . . .	97
6.19 CRS 1018 - Slot - Neuber's Parameter vs. Cycles . . . . .	98
6.20 AL 7475 - Hole - Stress Concentration vs. Cycles . . . . .	99
6.21 AL 7475 - Slot - Stress Concentration vs. Cycles . . . . .	100
6.22 AL 7475 - Hole - Strain Concentration vs. Cycles . . . . .	101
6.23 AL 7475 - Slot - Strain Concentration vs. Cycles . . . . .	102
6.24 AL 7475 - Hole - Neuber's Parameter vs. Cycles . . . . .	103
6.25 AL 7475 - Slot - Neuber's Parameter vs. Cycles . . . . .	104

Figure	Page
6.26 Neuber's Parameter vs. Fatigue Notch Factor - AL 2024 . . .	107
6.27 Neuber's Parameter vs. Fatigue Notch Factor - Steel 1018 .	108
6.28 Neuber's Parameter vs. Fatigue Notch Factor - AL 7475 . . .	109
6.29 Neuber's Parameter vs. Fatigue Notch Factor - AL 2024 . . .	110

## ABSTRACT

Neuber's rule which relates the stress and strain concentration factor at a notch to the theoretical stress concentration factor for a monotonic loading case. It is currently being used in a modified form to analyze cyclic loading cases. The purpose of this research was to experimentally measure the four quantities incorporated in Neuber's cyclic relation so that a direct evaluation of the relation could be made. Three of the parameters were measured during tests lasting a thousand cycles on notched specimens run under completely reversed load control. These three were the stress and strain in the specimen far removed from the notch and the strain at the edge of the notch. The latter value was obtained using a novel laser based interferometric technique. The fourth parameter, stress at the notch, was inferred from load data taken on a small, smooth specimen which was subjected to the strains measured at the notch. These measurements were conducted on specimens manufactured from three different materials, with two notch geometries, and run at both room and elevated temperatures. After having recorded this data, Neuber's rule was used to compute a value for numerous cycles of each test which was then compared to the theoretical stress concentration factor. Results showed that Neuber's parameter was generally less than the stress concentration factor regardless of material, notch geometry or temperature and is, therefore, a conservative design criterion.

## CHAPTER I

### INTRODUCTION

The decade of the seventies has brought about a changing philosophy in the design of structures and machine components. Due to rapidly rising costs and expanding computer-aided design techniques, the philosophy of making a machine part so that it would last forever has been replaced with the requirement that a structure be designed for a specific lifetime. This philosophy is fine in concept, but problems unencountered in the older design methods suddenly surface. One of the problems is that of fatigue, which can cause sudden catastrophic failures. The goal of the research presented in this dissertation is to evaluate experimentally a technique which is in current use as a design tool that considers fatigue in the initial analysis. Before discussing this experimental evaluation, a brief description of the fatigue process and some of the earlier research will be reviewed.

#### 1.1 Overview of Fatigue

Fatigue is defined by the American Society for Testing and Materials[1]\* as:

The process of progressive localized permanent structural change occurring in a material subjected to conditions which produce fluctuating stresses and strains at some point or points and which may

---

\*Number in brackets refers to bibliography.

culminate in cracks or complete fracture after a sufficient number of fluctuations.

This definition sums up what has been learned about fatigue since August Wohler first began his systematic investigation of railway axle failures during the 1850's and 1860's. One of the three main points stated in the definition is that fatigue is a progressive change, which means that the material properties are cyclicly dependent. Therefore, this presents a serious problem to the design engineer since a component which is subjected to a fluctuating load and sees a continual material properties change cannot be evaluated by a simple strength of materials approach. Also, a second problem is that fatigue results in a permanent structural change which means the component goes beyond the elastic limit at least in a localized area. These last two points of the definition are interesting since they are exactly what Neuber considered analytically in his paper in 1961.

## 1.2 Literature Survey

Neuber's<sup>[2]</sup> 1961 paper is a continuation of his famous 1958 work entitled Kerbspannungslehre<sup>[3]</sup> on the theory of notch stresses. In his paper, the shear stress distribution is computed mathematically for a prismatic body containing a notch and loaded statically. The difference in this analysis from the theory of elasticity is that the material is considered to obey an arbitrary nonlinear stress-strain relation. In analyzing this problem, Neuber used a stress concentration factor and a strain concentration factor. The stress concentration factor is defined as the local stress at the notch divided by the remote stress. The latter factor is defined in a similar manner as being the local



notch strain divided by the strain far removed from the notch. The conclusions from this generalized analysis was that the geometrical mean value of the stress and strain concentration factors for any stress-strain law is equal to the theoretical stress concentration factor as determined by the theory of elasticity.

This has become known as Neuber's rule:

$$K_t = (K_\epsilon K_\sigma)^{1/2} = (\epsilon/e \times \sigma/S)^{1/2}$$

where  $K$  = theoretical stress concentration factor

$\epsilon$  = local strain at a notch

$e$  = remote strain

$\sigma$  = local stress at a notch

$S$  = remote strain

When the material at the edge of a notch is in the elastic region and obeys Hooke's law, Neuber's rule simply reduces to the definition of the stress concentration factor. However, when the stress near the notch goes above the elastic range according to Neuber's rule the stress concentration factor decreases as more load is applied while the strain concentration increases.

Neuber's rule is a great aid for analyzing the stresses and strains at a notch, but it is only valid for the static case. Since the definition of fatigue states that permanent structural change must exist, then one must consider that this may affect Neuber's rule. This was first investigated by Topper<sup>[4]</sup> et al. in a paper published in 1969. In this paper some modifications were made to Neuber's rule in order to apply it to fatigue. The modified Neuber's rule is:

$$K_f = (\Delta\sigma/\Delta S \times \Delta\epsilon/\Delta e)^{1/2}$$

where

$K_f$  = fatigue notch factor

$$K_f = \frac{\text{fatigue strength, unnotched specimen}}{\text{fatigue strength, notched specimen}}$$

$\Delta\sigma$  = localized stress range

$\Delta S$  = remote stress range

$\Delta\epsilon$  = localized strain range

$\Delta e$  = remote strain range

The major changes in Neuber's rule are that the theoretical stress concentration factor has been replaced by the fatigue notch factor and the stresses and strains have been replaced by ranges of stresses and strains. Topper et al. did try to experimentally evaluate this modification, not by measuring the stresses and strains at the notch, but by a technique of generating a set of life vs.  $(\Delta\sigma \times \Delta\epsilon)^{1/2}$  curves using smooth specimens of two aluminum materials and then comparing this to the lives of notched specimens. Good agreement was found, and it was concluded that the new Neuber's rule for fatigue was accurate for aluminum alloy plates subjected to completely reversed loading.

Several other investigators have attempted to evaluate Neuber's rule experimentally by actually measuring the parameters of stress and strain. The general trend in the experimental investigations of Leis<sup>[5]</sup> et al., Crews and Hardrath<sup>[6]</sup>, Kremp<sup>[7,8,9]</sup> and, Conle and Nowack<sup>[10]</sup> has been to test a specimen containing a notch under either load or strain control and measure the remote stress and strain with load cells and extensometers while measuring the strain at the notch by either strain gages or photoelastic coatings. The stress at the notch is then inferred by subjecting an unnotched specimen to the notch strains measured. Using these quantities and the theoretical stress concentration factor, Neuber's rule is evaluated.

This technique has been partially successful; however, several problems have existed in trying to measure the large plastic strains at the notch for tests of any duration. Crews and Hardrath, who used both photo-elastic coatings and strain gages at the notch, stated that use of the former "required extremely tedious observations and was subject to errors . . . ." Leis, et al., in speaking on the use of strain gages, commented that ". . . the problem inherent in the use of strain gages result in deviations of measured strain . . . ." Krempf, who ran tests at both room temperature and 550° F, had trouble with the gages lasting just one cycle at room temperature and for the elevated temperature tests remarked, "due to the lack of suitable strain gage sensors, notch root strain measurements were not feasible at these temperatures." Also, the smallest strain gages used were .030", which can result in significant errors due to the high strain gradient near a sharp notch. However, one other technique for measuring the notch strain has been used by Bofferding<sup>[11]</sup>, which permits gage lengths on the order of .004". This technique, known as the interferometric strain gage, has been demonstrated to be an accurate method and readily applied to measurements of this type. Bofferding's work consisted of evaluating two notch geometries and three materials at room temperature for agreement with Neuber's rule. Again, both the notched and unnotched specimens were used.

Based on the data developed by these and other researchers, it has been concluded that Neuber's cyclic rule is generally conservative for the data considered. In fact, it is currently being used in the design process as described by Fuchs and Stephens<sup>[12]</sup>, and is written into at least one design code, the ASME code<sup>[13]</sup>, Section III for the design of nuclear reactors. This latter application is extremely

interesting because it deals exclusively with materials undergoing cyclic loads at elevated temperatures. Also, there is some question by Maiya<sup>[14]</sup>, and Severud<sup>[15]</sup> on the specifics of using Neuber's rule in this application.

### 1.3 Objective

Even though this relation has become popular due to its simplicity, much is still not understood about various parameters affecting Neuber's rule. Therefore, the purpose of this research was to evaluate in detail Neuber's cyclic rule at room and elevated temperature for two different notch geometries and three different materials. This would permit the applicability of Neuber's rule to be directly evaluated for several conditions.

The measurements needed to make the evaluation required using both a notched and unnotched specimen as other researchers have done. Recalling Neuber's rule,  $K_t = (\sigma/S \times \epsilon/e)^{1/2}$ , it is apparent that five parameters must be obtained.  $K_t$ , which is the theoretical stress concentration factor, was obtained by using the curves contained in Peterson's<sup>[16]</sup> book on stress concentration factors. These curves were obtained by both analytical and photoelastic means and have been shown to be quite accurate. The other four parameters  $\sigma$ ,  $S$ ,  $\epsilon$ , and  $e$  all must be obtained by experimental means.

Three of the four parameters: remote stress, remote strain, and local strain were measured on the notched specimen. The tests were run on a computer-controlled electrohydraulic testing machine under load control starting from zero load and going into tension to a preset value, and then reversing the load into compression to the same load

value before returning to zero load. The remote stress on the notched member was obtained by recording the load on the specimen at sixty points during the cycle and dividing the load by the gross cross-sectional area. In setting up the experiments, care was taken to insure that the maximum cross section stresses on the specimens were below the proportional limit of the material. Because of this, the remote strains were computed from the remote stresses using Hooke's law. The third parameter to be measured on the notched specimen was local strain at the notch, and this was accomplished using an interferometric strain gage. This technique was developed by W. N. Sharpe and is described in more detail later in this report. However, it permitted the local strains to be measured no further than .002" away from the edge of the notch with a gage length of between .004" to .006". As those three pieces of data were collected, they were stored by a minicomputer on a magnetic disk for use later. Tests on the notched specimens continued for a maximum of 1000 complete cycles or until the specimen cracked to a point where no further measurements of local strain were practical.

After completing the notched specimen test, only one parameter of Neuber's rule remained unknown, the local stress. This stress value was obtained using smooth specimen simulation. A specimen containing no notches was subjected to the same strains as were measured near the notch in the notched specimen. By measuring the load for each imposed strain, the local stress was computed by dividing this load by the smooth specimen's cross-sectional area. In this case the minicomputer was used to record the strains for each cycle and subsequently directed the electro-hydraulic test machine to load the specimen until that strain was reached; the computer then recorded on the magnetic disk the computed local stress.

Therefore, with the acquisition of this piece of data, everything that was needed to evaluate Neuber's rule had been measured.

This procedure was followed on specimens from three different materials: 7475 aluminum, 2024 aluminum and 1018 steel. Each of the three materials were tested with two notch geometries and at both room temperature and a moderately elevated temperature. The details of the specimen design are found in Chapter II.

Chapter III describes the various test apparatus needed to obtain all measurements. The software written to control the various pieces of equipment simultaneously is detailed in Chapter IV. Procedures used in conducting all of the tests are listed in Chapter V, while Chapter VI presents the results of these tests. Conclusions based upon the data obtained comprise Chapter VII.

## CHAPTER II

### SPECIMEN DESIGN

Neuber's relation as described in the previous chapter is very general and is currently being used in the fatigue analysis of many different materials, geometries and temperatures; however, it has only been evaluated experimentally in a very few cases by various researchers. In an effort to evaluate Neuber's rule and to understand the influence of these various parameters, a series of tests, in which the three parameters of material, geometry, and temperature are varied, were run. This chapter describes the design of the specimens for these tests and the reasoning behind the selection of the parameters. It should be noted that since this effort was funded by the LSU and split between two universities, the specimen designs were somewhat constrained so that both universities' data would be comparable.

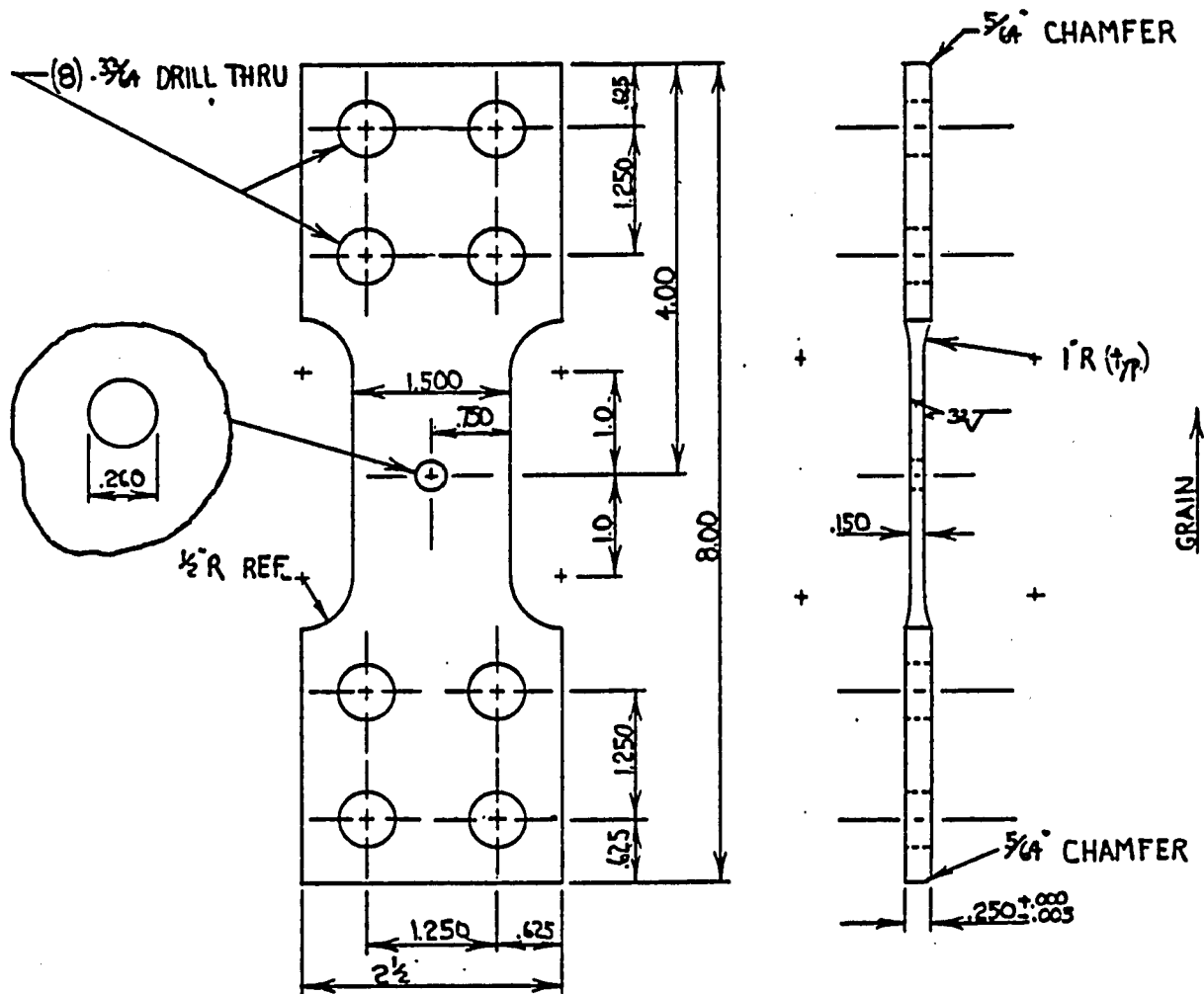
#### 2.1 Geometry

One of the big advantages of using Neuber's relation in fatigue design is that it can be applied to any notch geometry. Therefore, in the design process, data based on a particular material can be obtained by testing smooth specimens easy to fabricate. This data can then be used in fatigue calculations of structures containing extremely complex notch geometries. Because of this fact, it was felt that different geometries should be looked at very carefully. Initially two notch

geometries were to be considered which were similar to those used by Bofferding.<sup>[11]</sup> They were a circular hole in a thin plate and an elliptical hole in a thin plate. The LSU design of the circular hole in specimen is shown in Figure 2.1. The blank for the specimen is a  $\frac{1}{4}$ " thick plate,  $2\frac{1}{2}$ " wide and eight inches long and contains the bolt holes for the grips. The long axis of the blank is oriented parallel to the rolling direction of the plate or flat bar. This blank is then machined in the center to a thickness of .150", a width of 1.50", and a gage length of two inches containing a .260" diameter hole placed in the center. This hole was bored rather than drilled to insure a more uniform diameter. The theoretical stress concentration factor based upon gross cross-sectional area for this geometry was obtained from Peterson as 3.1, and is equal to that used in the Bofferding specimens.

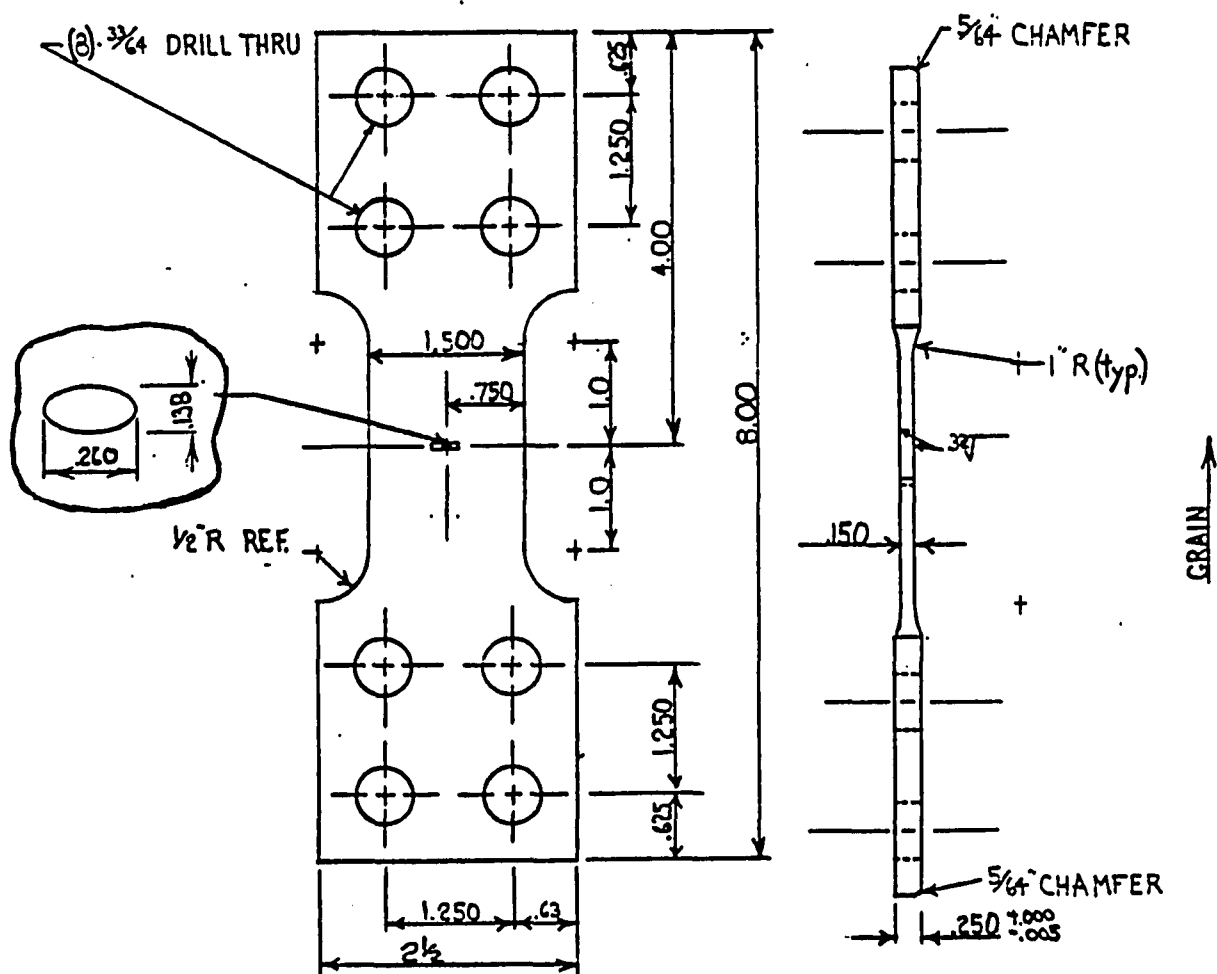
The design of the original elliptical hole in the thin plate is very similar to that of the circular hole specimen. The same blank is used for both. The only difference is that instead of a circular hole, an ellipse with the major and minor axes of .260" and .138", respectively, was used. For this geometry, the major axis is oriented perpendicular to the longitudinal axis of the specimen. This geometry is shown in Figure 2.2. The theoretical stress concentration factor for this geometry was found to be 4.92 from Peterson, while the geometry used by Bofferding had a factor of 5.1. A major difference between the specimen containing a circular hole and the ones with an elliptical hole was the actual machining of the discontinuity. The ellipse was considerably harder to machine and since no numerically controlled milling machine was available, it was done manually. The machining process consisted of first milling a hardened single point broach in the form of the required ellipse. Next,





SCALE: HALF

**Figure 2.1. Notched Specimen - Hole**



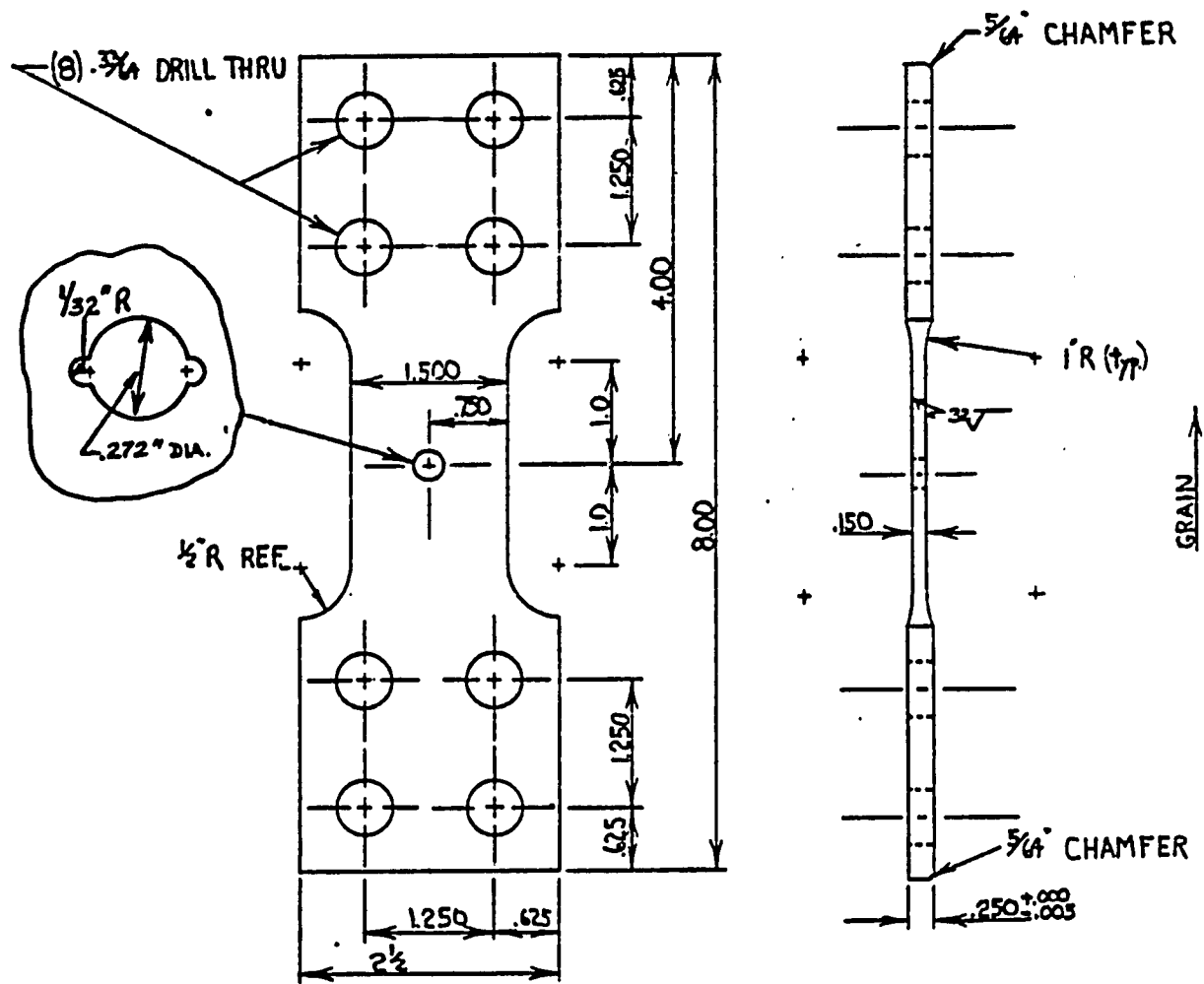
SCALE: HALF

Figure 2.2. Notched Specimen - Original Design of Ellipse

an ellipse was roughed in on the specimen by milling and, finally, the broaching tool was forced through the specimen to form the ellipse. Microscopic inspections of the elliptic notches after machining revealed that there was quite a variance in the shape of the notch, especially at the point having the minimum radius of curvature. Initial calibration testing of these specimens revealed a stress concentration factor of approximately 3.3 instead of the 4.92 desired. Also, fatigue testing of these specimens disclosed erratic results of specimens of the same materials with the same elliptic notch and tested at the same load. Because of this variance, it was felt that the elliptically notched specimens would not furnish data with the desired repeatability between specimens. Therefore, the notch geometry of the elliptical specimens was changed.

The new notch geometry selected was that of a hole containing two smaller diameter half circles machined on both edges of a larger hole. The drawing detailing this geometry is shown in Figure 2.3. The stress concentration factor for this geometry was again obtained from Peterson and found to be 5.92. The dimensions of the notch were chosen so that the already machined elliptical notched specimens could be salvaged by remachining. An "I" drill with a diameter of .272" was used to drill out the ellipse and then the two half circles were placed at the edges of the circles using a 1/16" diameter end mill. Calibration testing of this new geometry revealed an extremely sharp notch at the edge of the two half circle holes.

It should be noted that two other factors influenced the design of the specimens. They were the load capacity of the testing machine and the buckling load of the specimen loading system. In considering the

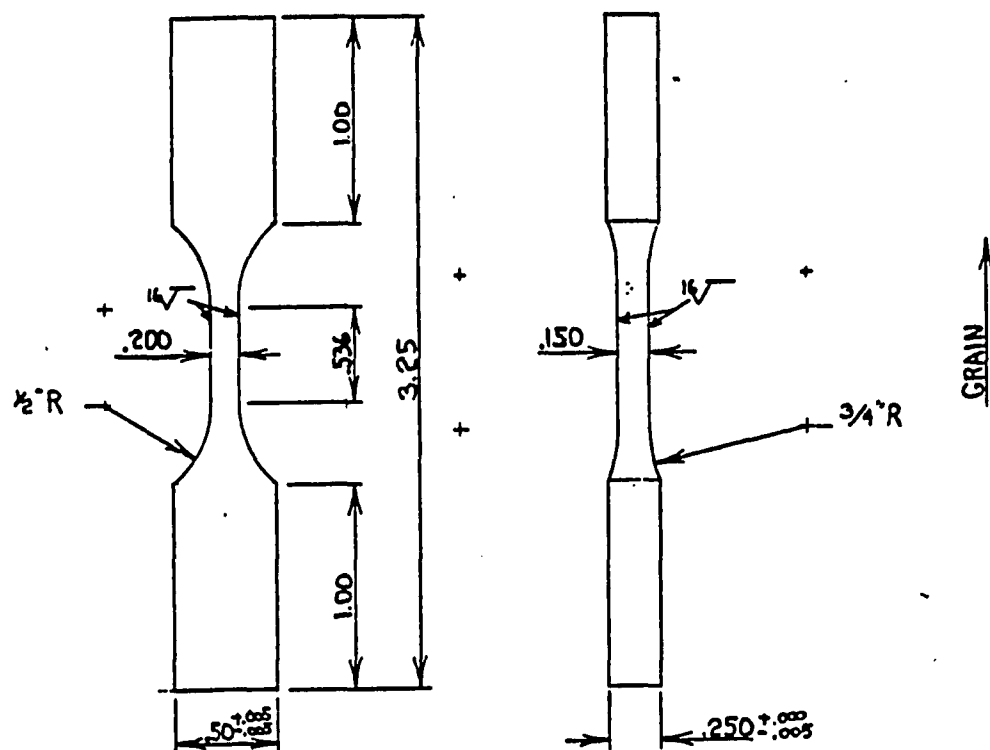


SCALE: HALF

Figure 2.3. Notched Specimen - Slot

20,000 pound load capacity of the testing machine, it was assumed that the ultimate strength of any of the materials would not exceed 100 ksi. Under these conditions, the MTS machine would pull a specimen with a cross-sectional area of .22 square inches to failure. Consequently, a specimen blank having a cross-sectional area of .225 square inches was chosen. The second design criterion, the requirement of elastic stability, was handled by computing the Euler load of the notched specimen. The specimen was considered to be perfectly aligned in two infinitely rigid grips. The critical load for a beam fixed at both ends was computed to be  $P_{cr} = \frac{4\pi^2 EI}{L^2} = 18,500$  pounds. This gives a factor of safety of 2 against failure by buckling if the machine load placed on the specimen does not exceed the expected 40 ksi. Therefore, it was felt that this factor of safety was large enough to allow for any misalignment or flexibility of the grips, so that no notched specimen would fail by buckling when loaded less than the specified maximum.

One other geometry was used in evaluating Neuber's rule and it was that of a smooth specimen. Figure 2.4 illustrates the details of this specimen design. It is cut from the same  $\frac{1}{4}$ " plate as the notched specimen and the blank had the dimensions of  $3\frac{1}{4}$ " long and  $\frac{1}{2}$ " wide. The machined specimen had a necked down region .200" by .150" over a gage length of only .536". This gage length was slightly longer than the .500" length of an extensometer, yet was small enough to reduce the chance of buckling. In considering the two design constraints discussed above for the notched specimens, it becomes apparent that exceeding the load capacity of the machine is of no worry with a specimen having a cross-sectional area of only .030". However, buckling is a major concern, and the computed Euler load for this specimen was 14,200 pounds. The



SCALE: FULL

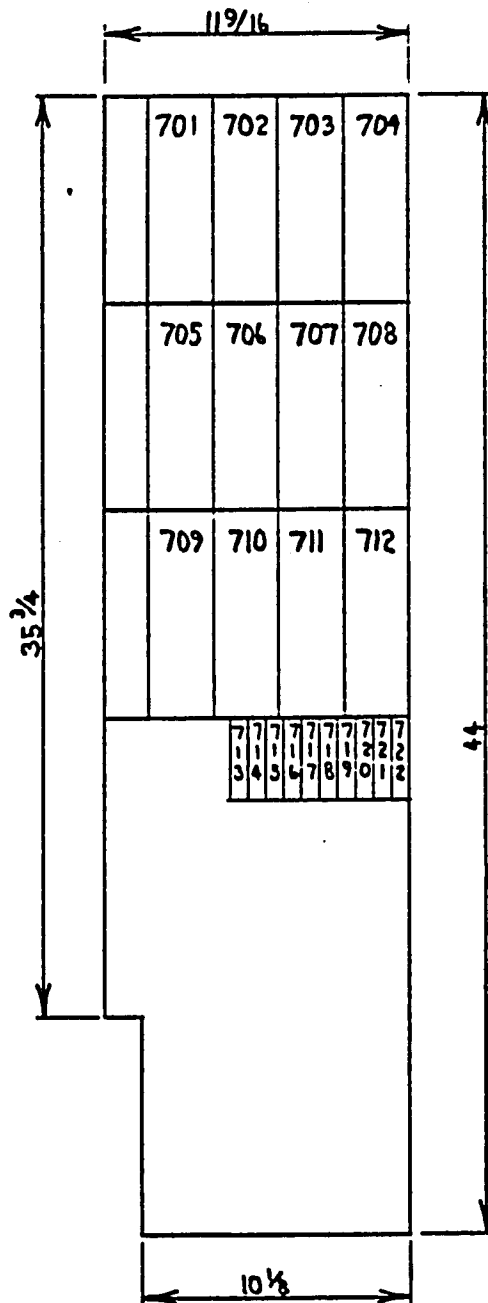
Figure 2.4. Smooth Specimen

factor of safety was lower than before which means the grip alignment became more critical; but, it was large enough so that no major problems were encountered. The reason the smooth specimens were so much smaller was that they are run under the same strains found at the edge of the notch so their failure would correspond to the initiation and growth of a crack at the notch.

## 2.2 Materials

Three different materials were chosen for the tests. They were aluminum 7475-T7351 plate, 2024-T351 plate and 1018 cold-rolled steel flat bar. These materials were originally chosen and purchased by J. F. Martin of Michigan State University. These materials were selected in order that Neuber's rule could be evaluated for materials having differing cyclic properties. The 7475-T7351 aluminum is a high strength aircraft alloy which is cyclicly stable, while the 2024-T351 aluminum is a lower strength alloy having cyclic hardening properties. The 1018 cold roll steel is a common, low carbon steel having a higher elastic modulus than that of the aluminums and can be either cyclic softening, hardening or stable depending upon the strain amplitude. For the tests conducted, the 1018 behaved in a cyclicly softening manner.

As mentioned above, the material for the tests was purchased by Martin and was in the form of  $\frac{1}{4}$ " thick plates. However, Martin ran short on the 1018 CRS, so as a replacement a piece of 1018 flat bar was purchased by LSU. The  $2\frac{1}{2}$ " wide flat bar was chosen because of its availability and size facilitated specimen machining. Details of the size of the plates received from Martin as well as the specimen layouts on all three materials, are shown in Figures 2.5 through 2.7.



SCALE:  $1/8" = 1"$   
 MATERIAL: 7475 ALUM.  
 NOTE: STAMP SPECIMEN  
 NUMBERS PRIOR TO  
 CUTTING SHEET.

Figure 2.5. Specimen Layout - 7475 Aluminum



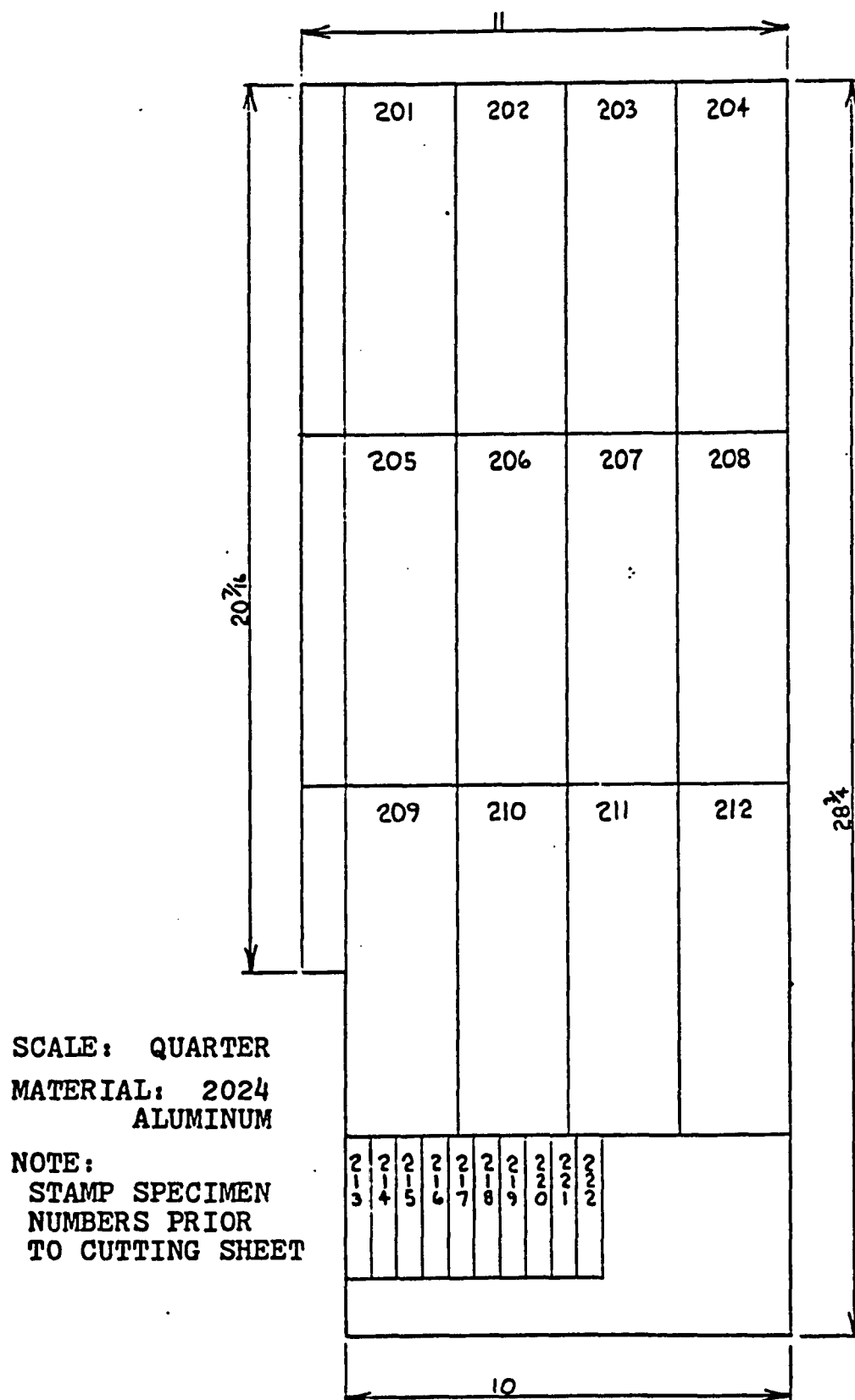
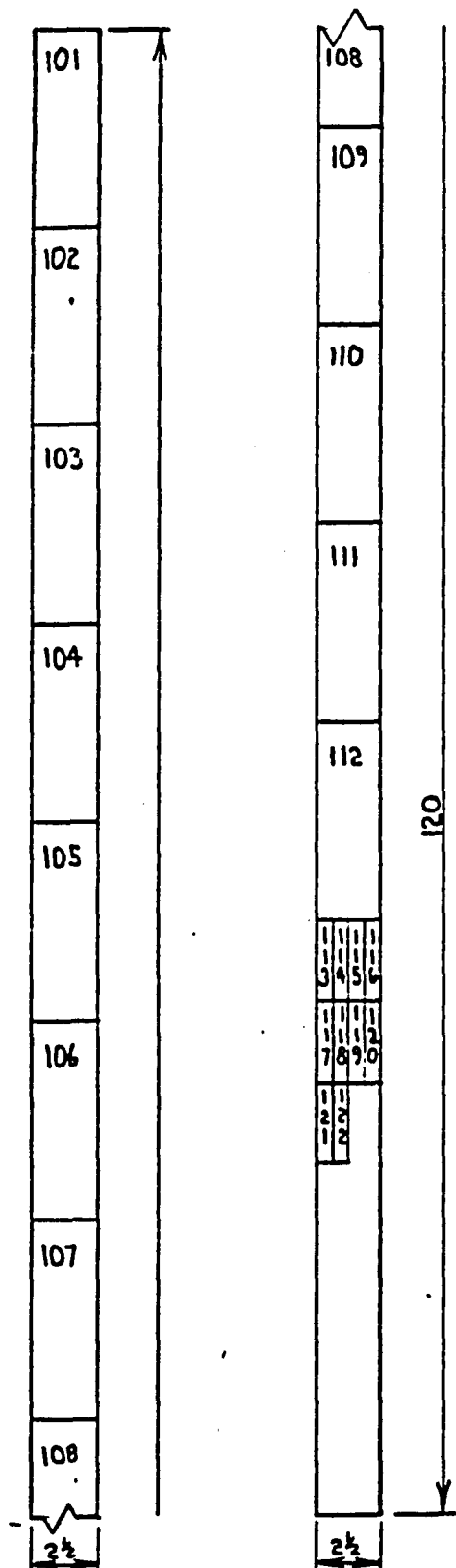


Figure 2.6. Specimen Layout - 2024 Aluminum



SCALE: 1/8" = 1"

MATERIAL: 1018 STEEL

NOTE: STAMP SPECIMEN  
NUMBERS PRIOR TO  
CUTTING STRIP.

Figure 2.7. Specimen Layout - 1018 CRS

In order to characterize these three materials, one smooth specimen of each material was instrumented with a strain gage and a stress-strain curve generated at room temperature. The results of these tests are shown in Figures 2.8 through 2.10 and are summarized in Table 2.1.

Table 2.1  
Material Properties

Material	Proportional Limit KSI	0.2% Yield Strength KSI	Young's Modules KSI
AL 2024T351	44.0	55.5	10.0E3
CRS 1018	70.5	86.0	29.3E3
AL 7475T7351	49.0	57.5	9.8E3

### 2.3 Temperature

The effect that temperature has on the fatigue life of a component is quite important because many highly stressed parts undergoing a cyclic load are operating at elevated temperatures. An example of this is the turbine blade in a jet engine which must withstand the high loads in an extremely hostile environment and at the same time be designed for minimum weight. In applications such as this, Neuber's rule would be extremely useful if it were shown to be valid for elevated temperature environments. Also, a modified form of Neuber's rule written into the ASME code is for components operated at elevated temperatures. Therefore, it was decided to run the same geometries and materials at both room temperature and at a moderately elevated temperature. The elevated temperature selected for each material is

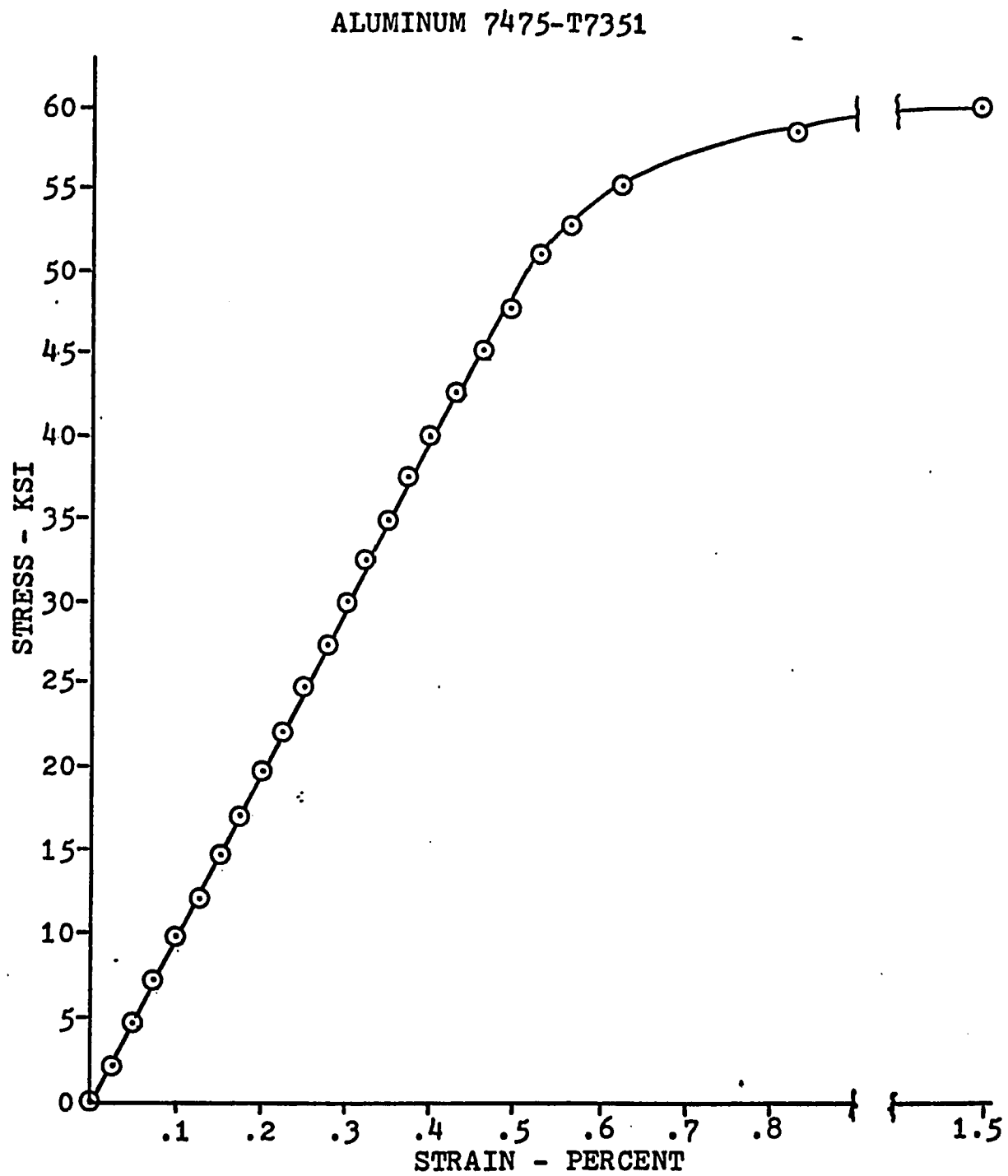


Figure 2.8. Stress - Strain Curve - 7475 Aluminum

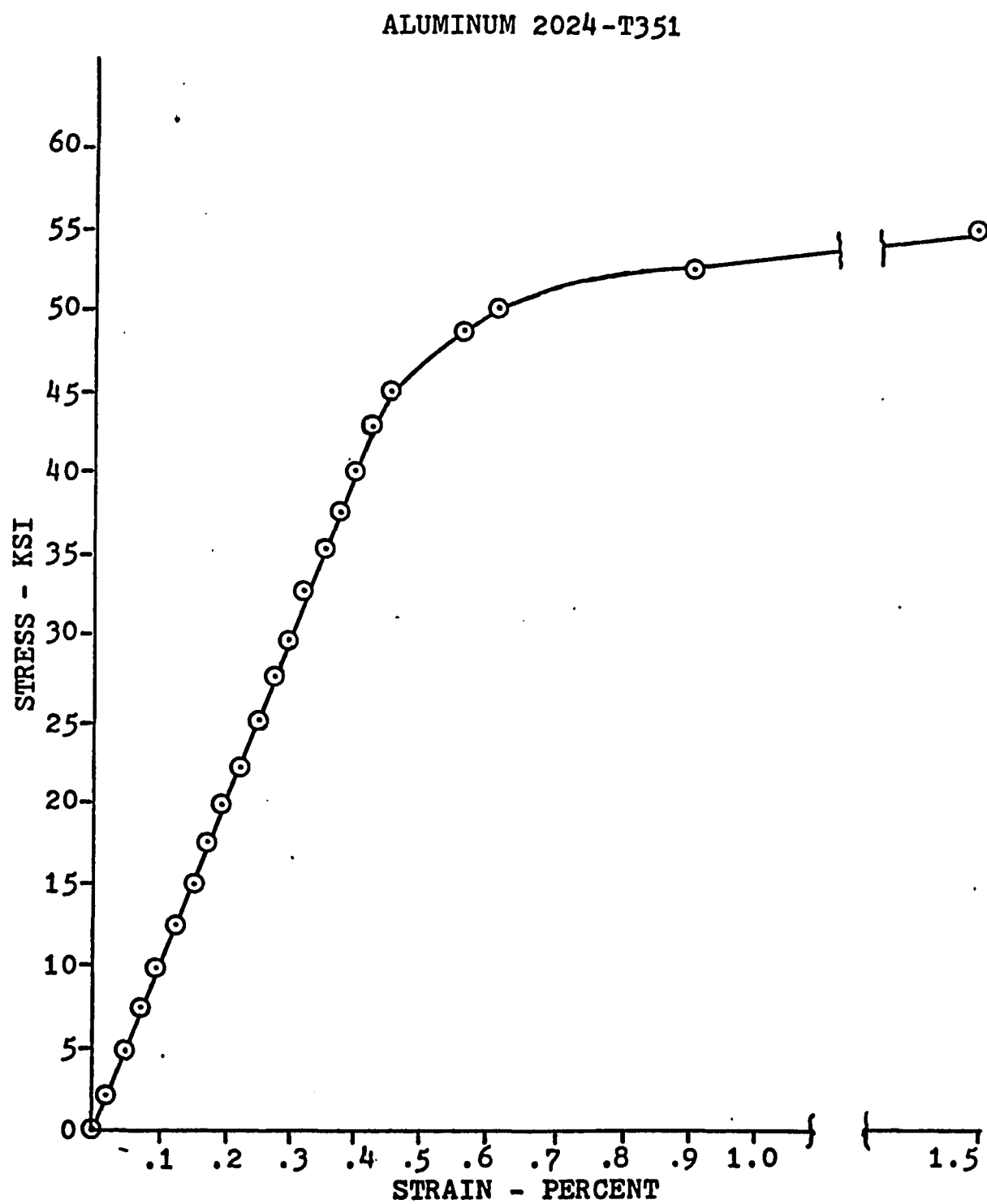


Figure 2.9. Stress - Strain Curve - 2024 Aluminum

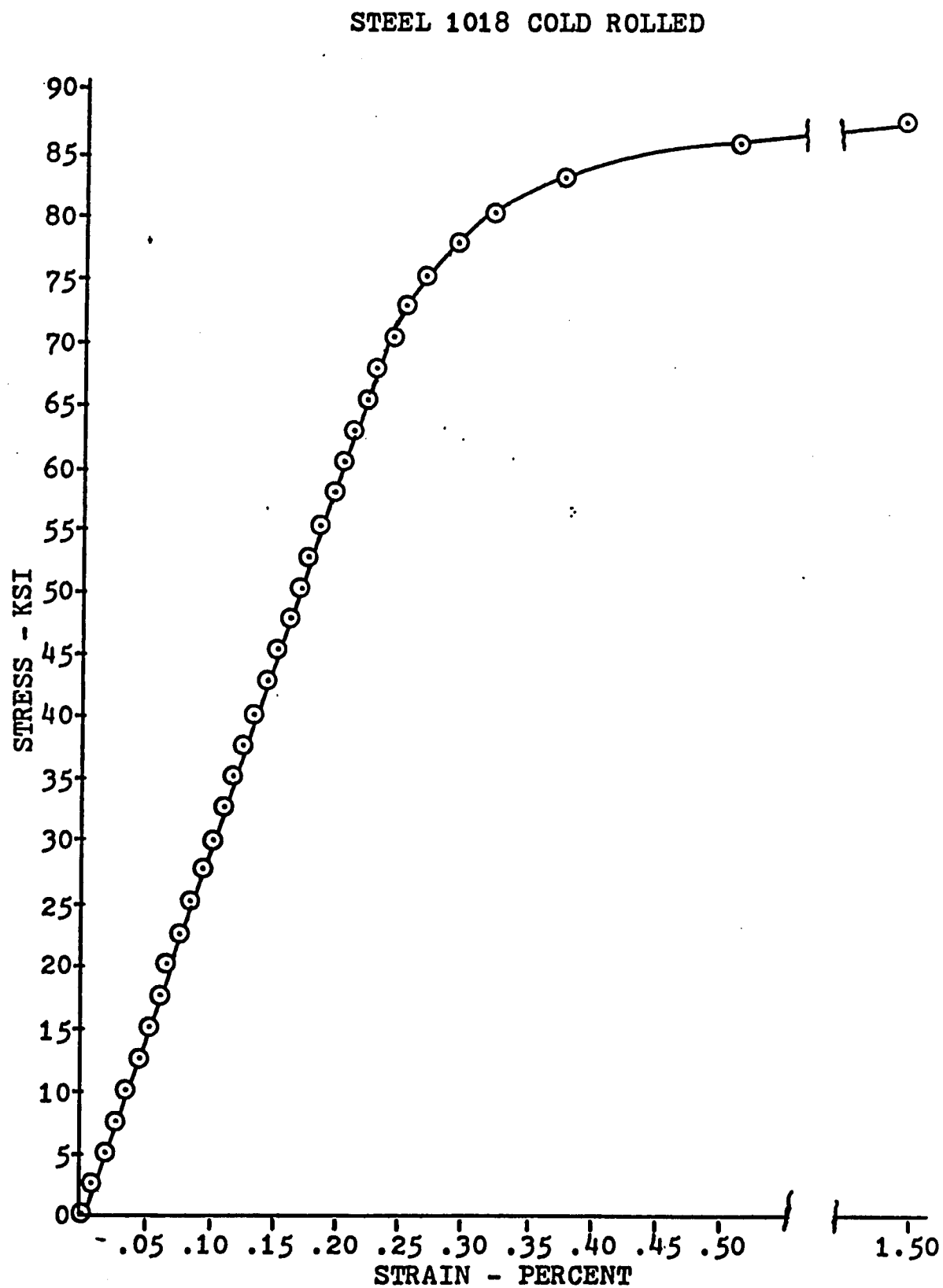


Figure 2.10. Stress - Strain Curve - 1018 CRS

discussed below. It should be observed, however, that this elevated temperature testing was only conducted at LSU and that Bofferding performed only room temperature tests.

The elevated temperature chosen to test both aluminum materials was 300°F. The main reasons this temperature was chosen were because the material properties such as yield strength and tensile strength decrease significantly from those at room temperature and that 300°F is probably the highest normal operating temperature these aluminums would ever be designed for. Also, this temperature does not present any problems for the furnace designed for this purpose and other required instrumentation.

The steel specimens presented more problems for elevated temperature testing because of their increased oxidation rate at the higher temperatures. Since the interferometric strain gage (ISG) operates with light reflected from the specimen surface, excessive oxidation would cause the reflected light to grow dimmer causing measurement problems. In an effort to determine a temperature at which the ISG would function properly for a minimum of four hours, several experiments were conducted. These experiments revealed that the specimen could be held between 550-600°F for six or more hours without seriously degrading the surface. To operate at any temperature above 600°F would require a special coating on the specimen or testing in an inert environment. Therefore, 550°F was initially chosen as the testing temperature; however, in reviewing the peak operating temperature of the extensometer, it was found that 500° was the maximum temperature at which the strain gage adhesive and solder would work. Any higher temperature would result in the use of

special ceramic bonding techniques, the test temperature for the steel specimens was downgraded to 500°F. It is felt, however, that for this common low carbon material, normal design temperatures probably would not exceed this value.



## CHAPTER III

### TEST APPARATUS

The equipment needed to perform the measurements described in the Introduction is explained in detail in this chapter. The test apparatus consists primarily of: (1) the interferometric strain gage, (2) the extensometer, (3) the specimen grips, (4) the heater and temperature controller, and (5) the electrohydraulic testing machine and computer interface.

#### 3.1 Interferometric Strain Gage

The heart of the measurement system is the interferometric strain gage (ISG), which permits the measurement of highly localized strains due to its small gage length. The basic principle of the ISG, which was developed and used by Sharpe[17], is similar to Young's two slit fringe experiment. In this case, however, instead of having two slits, two reflective surfaces were used. These reflecting surfaces are placed into the surface of the specimen through the use of a Vickers hardness tester and are actually pyramidal indentations measuring approximately 17 microns on a side. Coherent light from a helium-neon laser illuminates a pair of these closely spaced indentations (100 microns) and is reflected from their inclined surfaces. This is analogous to having two point sources of coherent light out of phase with each other which results in an interference pattern of light and dark fringes being formed in space. Figure 3.1 shows a schematic of this phenomenon.

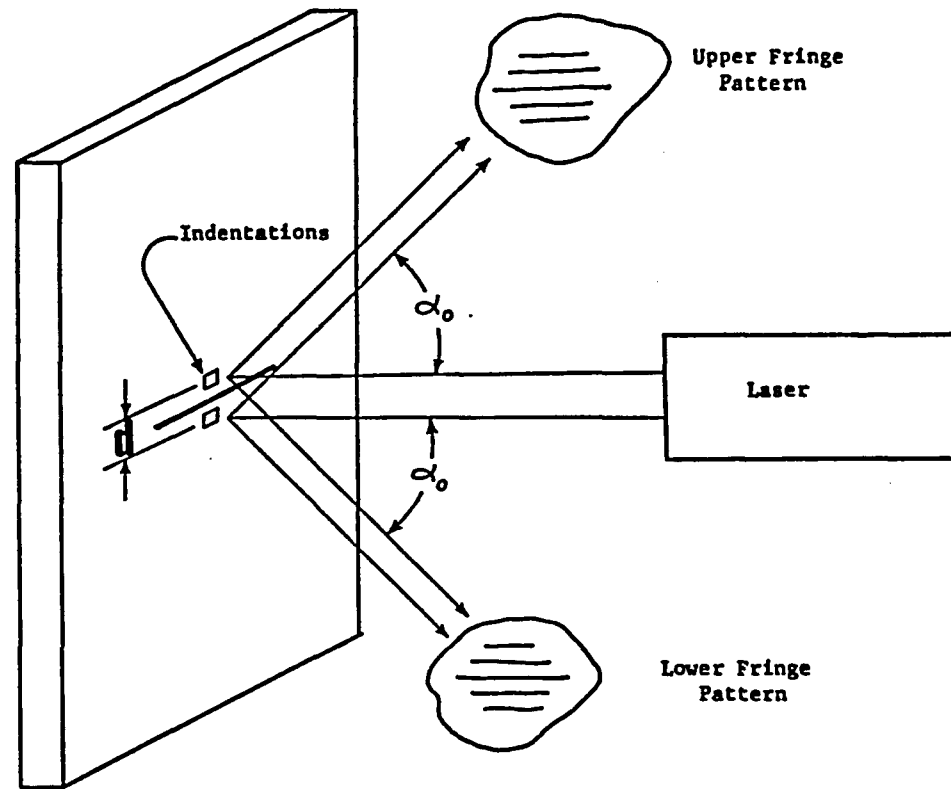


Figure 3.1. Interferometric Strain Gage Principles

From this diagram the basic equation for the interference pattern can be formulated.

$$d \sin \alpha_o = m \lambda; m = 1, 2, 3, \dots \quad 3.1$$

where  $d$  = indentation spacing

$\alpha_o$  = reflected angle

$\lambda$  = wavelength

Three parameters affecting the spacing of these fringes are the distance from the reflecting surface, the wavelength of the coherent light source and the spacing between the indentations. By observing the fringe pattern from a fixed position in space, the relation between displacement of the indentations and fringe motion is found to be:

$$\delta d = (\lambda / \sin \alpha_o) \delta m \quad 3.2$$

where,  $\delta m$  is the number of fringes passing the fixed position. When the two indentations move apart, equation 3.1 states that  $\alpha_o$  must decrease; thus, the reflected beam moves toward the illuminating beam for a tensile load. A second cause of fringe motion is that of rigid body motion of the specimen. This, however, results in one fringe pattern moving toward the initial laser beam with the second moving in the opposite direction. Therefore, in order to filter out the fringe motion resulting from rigid body motion of the specimen, two observation points are used, one above and the other below the incident beam. By averaging the fringe motions obtained at each of these locations, the rigid body motion is eliminated and the displacement is computed by the following equation:

$$\delta d = \lambda (\delta m_1 + \delta m_2 / 2) / \sin \alpha_o \quad 3.3$$

where  $\delta m_1$  = fringe motion of upper channel

$\delta m_2$  = fringe motion of lower channel

The strain is simply computed by dividing  $\delta d$  by the original

spacing  $d$ .

In order to measure the fringe motion so that the strain in the area of the indentations can be obtained, additional equipment is needed. This equipment is shown schematically in Figure 3.2 and consists of a pair of servocontrolled mirrors plus a pair of photomultiplier tubes with narrow apertures across their active region. The main purpose for having the mirrors, and the reason that they are servocontrolled, is to provide some means for sweeping the fringe pattern across the aperture. The photomultiplier tubes serve to convert the light intensity of the fringes into a voltage which can then be amplified and fed into a minicomputer for data reduction.

On the front of the photomultiplier tubes (PMT's) is a filter to screen out any frequencies other than those of the helium-neon laser. This prevents external light sources from affecting the PMT's output; however, as a secondary precaution, all of the room lighting is turned off when the system is in operation, and only a small worklight pointed away from the system is used. Also, across the filter is an aperture in the form of a slit much narrower than the width of a single fringe. This aperture is aligned parallel to the fringes. Consequently, when the mirrors are slowly rotated, the fringe pattern moves across the aperture of the PMT which sends a signal as shown in Figure 3.3. This pattern has been shown by Sharpe to have the appearance of an approximate cosine-squared function. The software which actually transforms this fringe motion into a strain signal is described in the next chapter.

### 3.2 Extensometer

As described in the previous chapter, the strain near the notch

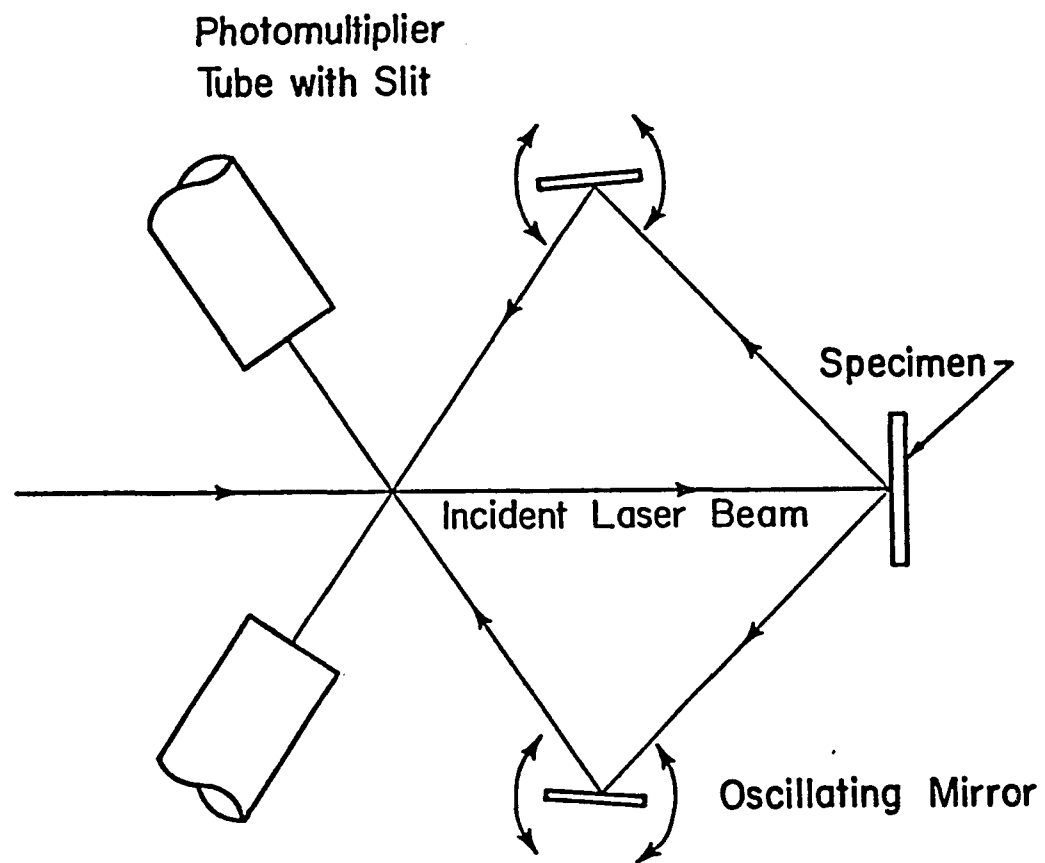


Figure 3.2. Interferometric Strain Gage Equipment

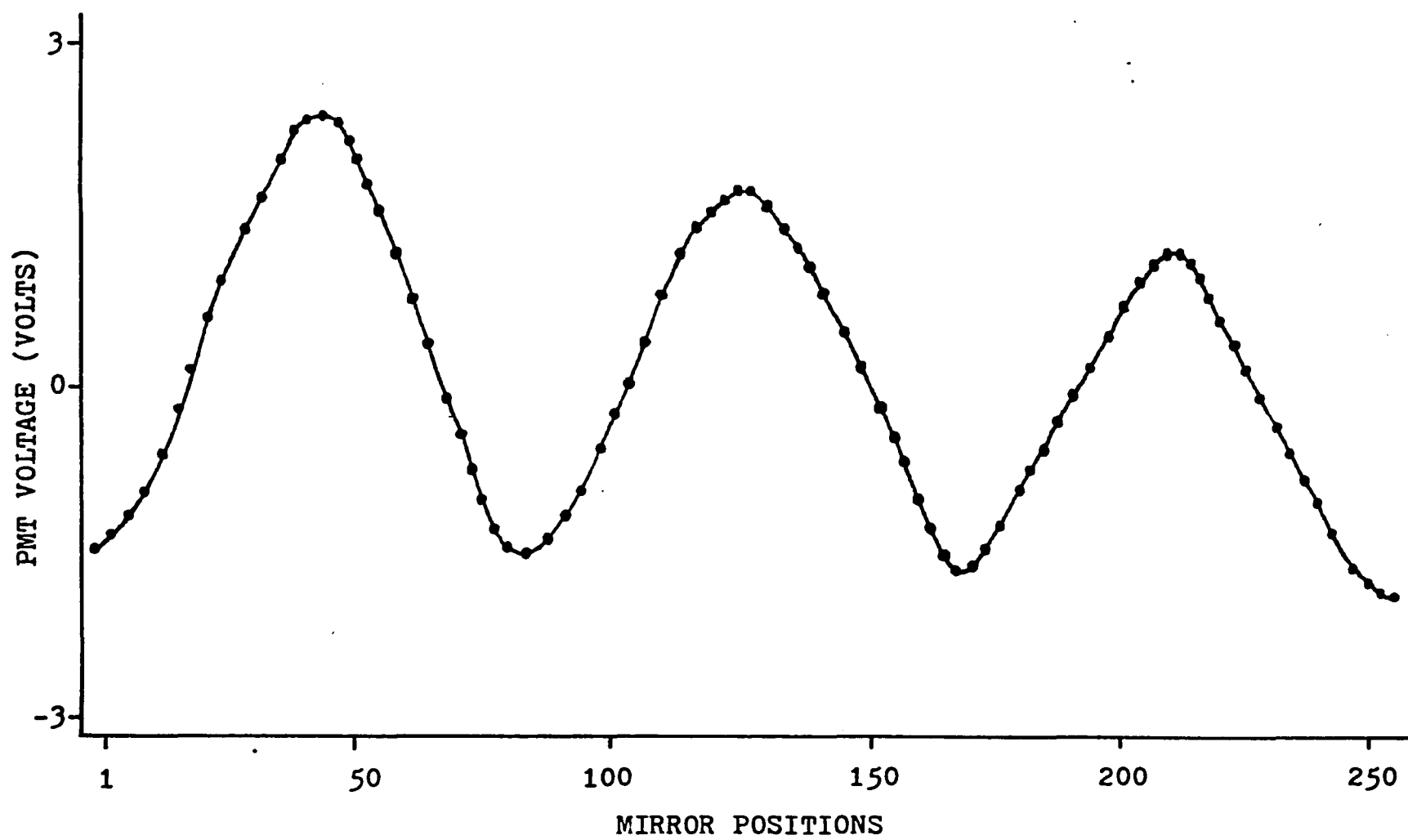
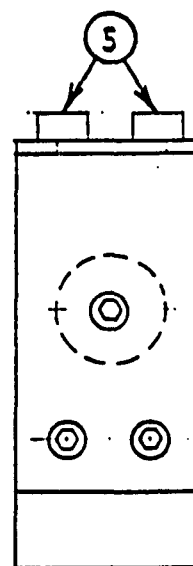
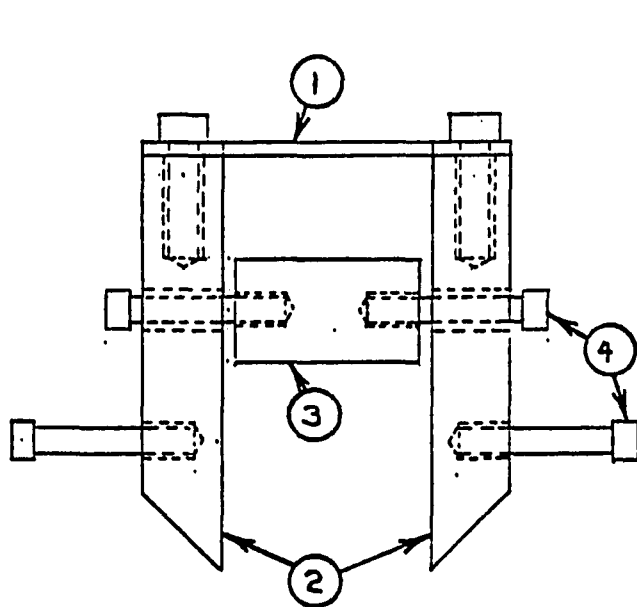
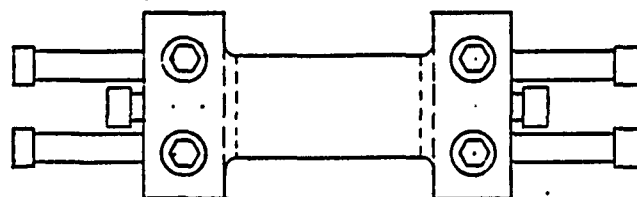


Figure 3.3. Photomultiplier Tube Voltage Signal

is used as a control variable for smooth specimen loading so that the stress corresponding to the measured notch strain can be obtained. In order to incorporate that strain into a feedback loop, a device that provides a voltage proportional to strain was needed. For this purpose an extensometer was designed. Some of the requirements were that it be linear, accurate and operate at the maximum testing temperature of 500°F.

An assembly drawing of the basic design that was fabricated is shown in Figure 3.4. It consisted of three main parts; the knife edges, the bending beam, and the resistance strain gages. The extensometer is attached to the specimen by wrapping springs around the specimen at both knife edges and attaching them to the extended screw heads. This spring force pulls the knife edges into the specimen and holds them there by friction. A voltage signal proportional to the displacement of the knife edges is obtained from the strain gages mounted on the bending beam. Since the ratio of the moments of inertia between the knife edge legs and the bending beam is so great, most of the displacement is obtained from the curvature of the bending beam. The strain gages mounted on the bending beam were arranged in a full bridge pattern; however, problems with the gage installation resulted in only a half-bridge being completed. After putting the gage signal through a strain indicator and amplifier, a calibration constant of 3240  $\mu\text{in/in/volt}$  and 2960  $\mu\text{in/in/volt}$  were obtained for the two-gage installation on the beam. In order to meet the design criterion requiring operation at 500°F, all mechanical components of the extensometer were made of 316 stainless steel. The strain gages and associated equipment chosen to operate at this temperature are described in Appendix A.

PARTS LIST		
ITEM	QTY.	DESCRIPTION
1	1	BENDING BEAM
2	2	KNIFE EDGE LEG
3	1	SAFETY SPACER
4	6	#0-80 UNF S.H.C.S. $\frac{3}{8}$ " LONG
5	4	#1-72 UNF S.H.C.S. $\frac{1}{4}$ " LONG
6	2	EXT. SPRING (NOT SHOWN)
7	2	EXT. SPRING (NOT SHOWN)



SCALE: 2:1

NOTE: ALL PARTS ARE TO BE  
304 or 316 STAINLESS  
STEEL

Figure 3.4. Extensometer Assembly



### 3.3 Grips

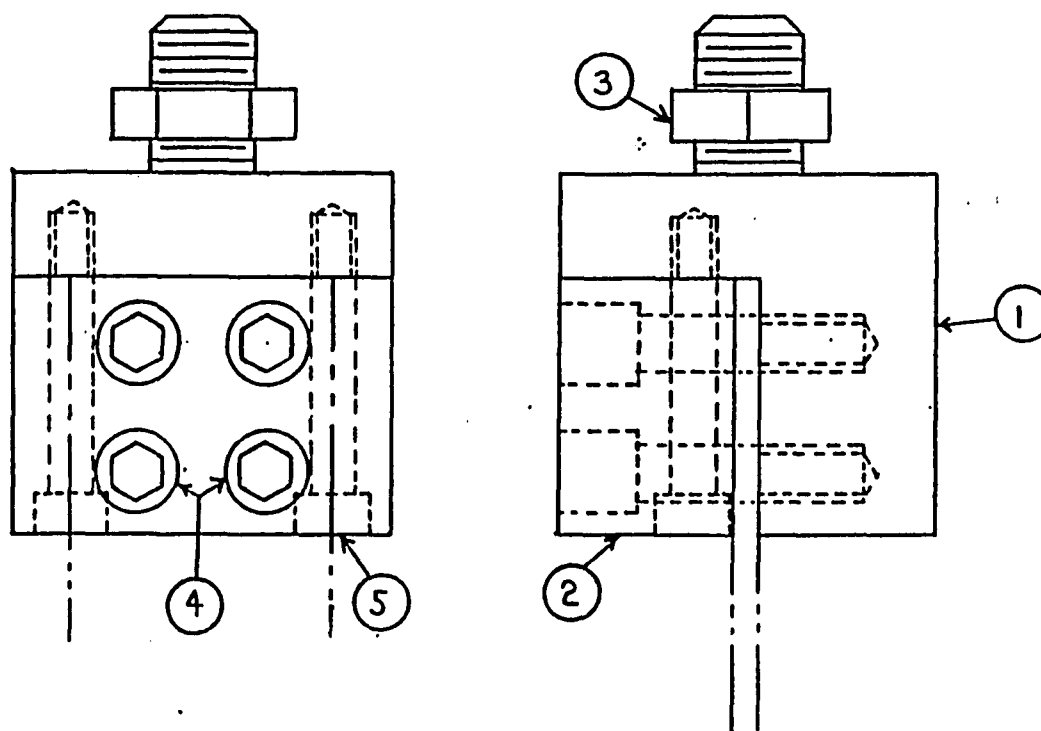
The main objective of the grips is to mechanically hold the specimen during all loading conditions. This must be accomplished without inducing any external forces or moments in the specimen either during specimen installation or specimen loading. They must also operate at 500°F, interface with the existing MTS load cell and ram, and facilitate specimen installation and removal.

The grips which were designed to meet the constraints listed above are shown in an assembly drawing in Figure 3.5. They consist basically of two main parts; an L-shaped bracket and a bolt-on bracket. The grips attach to the MTS machine through the 1"-14 UNS threads on the L-shaped brackets and are torqued to 150 ft.lbs. The notched specimen is gripped by the friction of being sandwiched between the bolt on bracket and the L-shaped bracket by tightening the four  $\frac{1}{2}$ " socket head cap screws. Four bolts were chosen to insure that a uniform pressure is placed over the entire gripping surface.

Two  $\frac{3}{8}$ " socket head cap screws were used to attach the bolt-on bracket to the L-shaped bracket. These bolts, which were placed parallel to the loading axis, prevented bending in the specimen by loading it in double rather than single shear.

An important feature of the grips was that the specimen could easily be removed from just one side by unbolting the six socket head cap screws on both the upper and lower grip. This permitted specimen installation without having to move the ISG. Also, since the specimen could be installed without changing the ram or crosshead position, realignment of the ISG fringe patterns was extraordinarily easy even with the front half of the thermal chamber in position.

PARTS LIST		
ITEM	QTY.	DESCRIPTION
1	2	L-SHAPED BRACKET
2	2	BOLT-ON BRACKET
3	2	JAM NUT
4	8	1/2"-13UNC S.H.C.S. 2" LONG
5	4	3/8"-16UNC S.H.C.S. 2 1/2" LONG



SCALE: HALF

Figure 3.5. Grips Assembly

Another feature was that all of the bolts were countersunk in the grips permitting the thermal chamber to fit snugly around the grip circumference. In order that the same grips could be used for both the smooth and notched specimens, an adaptor plate was fabricated as shown in Figure 3.6. This adaptor plate held a smooth specimen centered in the grips as they were tightened. A heat treated 4140 alloy steel was chosen for the grips because it had good fatigue strength properties for the testing temperature range. The grips, also, did not interfere with the reflected fringe patterns used for the ISG.

#### 3.4 Heater and Temperature Controller

In order to meet the elevated temperature testing needs, a high temperature furnace was designed and fabricated. The basic requirements of the furnace was to heat and maintain the specimen at a maximum temperature of 500°F, with the initial heating period not to exceed one hour. The furnace also had to allow a path for the incident laser beam to reach the specimen and the resulting fringe patterns to exit the furnace, while being as compact as possible.

An assembly drawing of the furnace designed is shown in Figure 3.7. The heat input required to bring the specimen to temperature is supplied by four resistive heating elements, each of 220 watt power at 57½ volts. Calculations revealed that due to the mass of the system, the heater had to be sized for the initial heating requirement, not the operating requirements. A 2½-inch thickness of insulating firebrick with a thermal conductivity of 0.88 BTU in/sq.ft. °F Hr. was placed between the heating elements and the outer frame, which minimized the heat loss from the system. The furnace was split to allow for ease of specimen installation

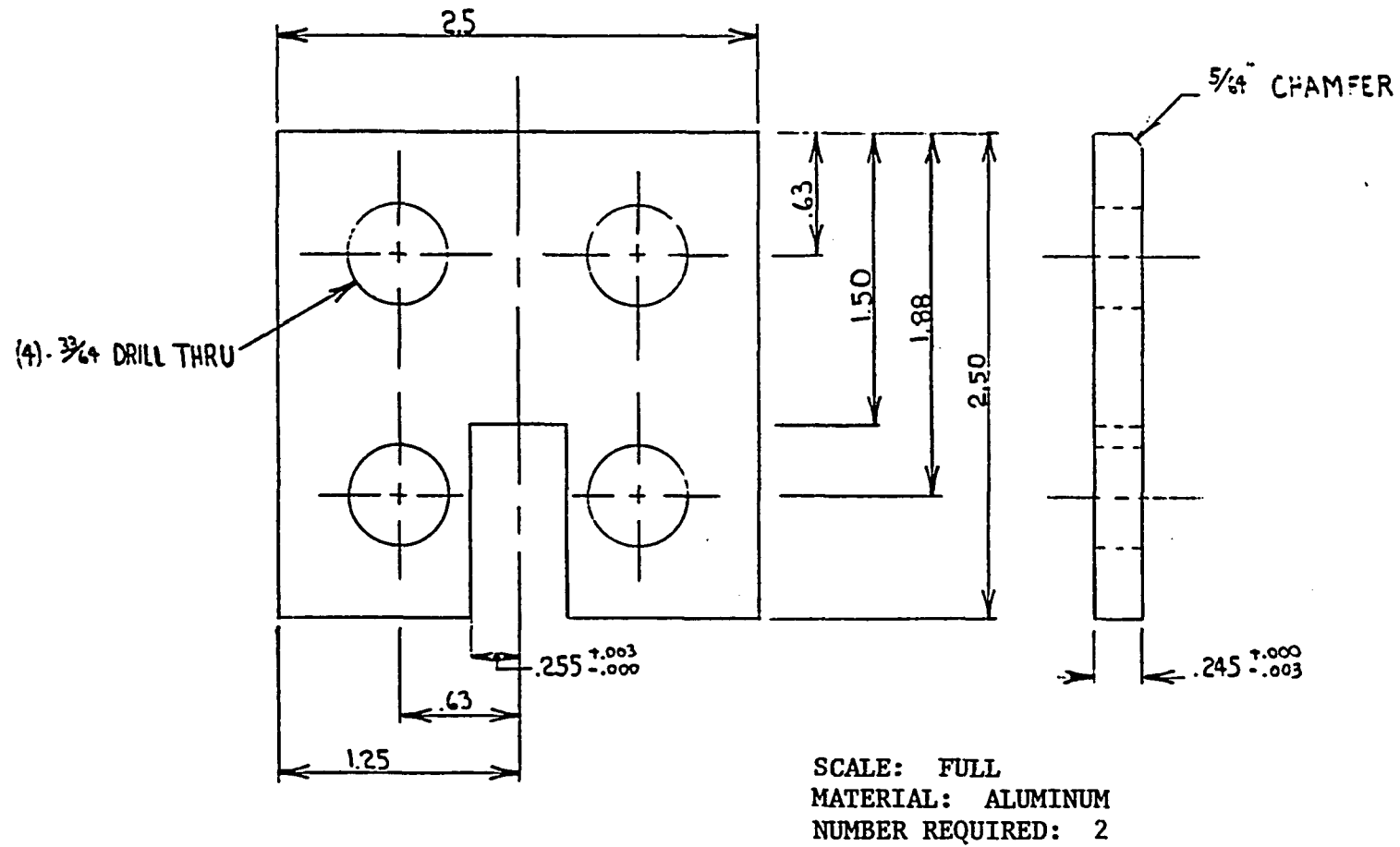
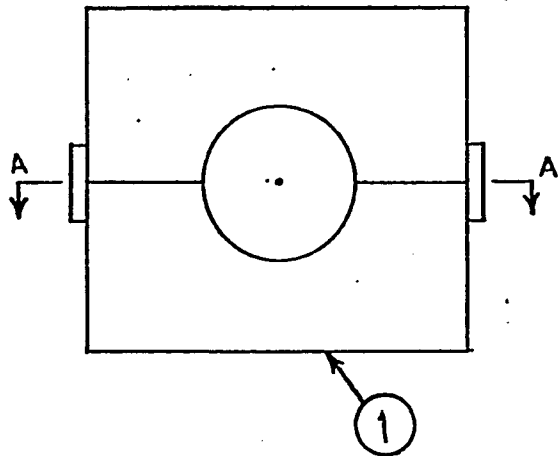
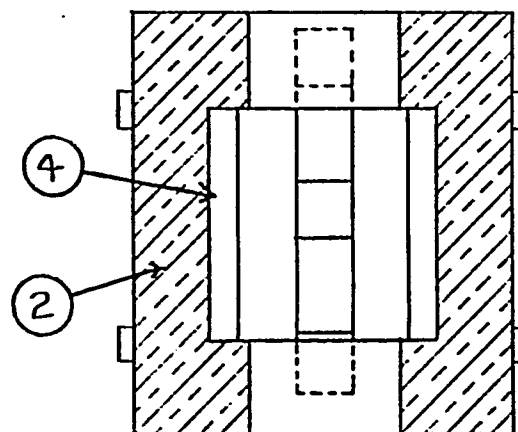
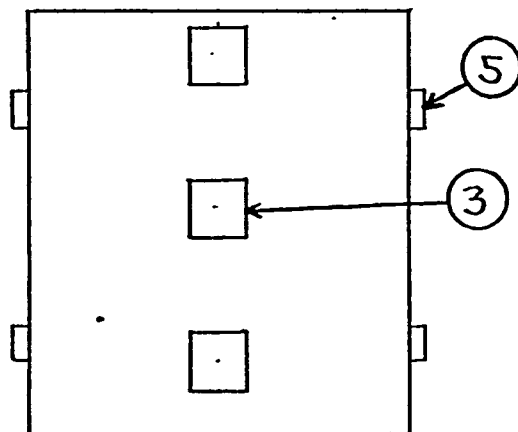


Figure 3.6. Smooth Specimen Grip Adaptor



PARTS LIST		
ITEM	QTY.	DESCRIPTION
1	1	1/16" ALUMINUM SHEET
2	10	2 1/2" x 4 1/2" x 9" FIREBRICK
3	3	2" x 2" x 1/8" FUSED QUARTZ
4	4	220 WATT HEATER
5	4	TOGGLE CLAMP



SCALE: 3/16" = 1"

SECTION A-A

Figure 3.7. Furnace Assembly

and removal. Three fused quartz plates were attached to the outer case and the firebrick behind them removed to allow the incident laser beam and the reflected fringe patterns an optical path to and from the specimen.

Holes, 3 3/4" in diameter, were placed at the top and bottom of the furnace in both the outer aluminum frame and firebrick to fit around the grips when the furnace was buckled together. The furnace was supported at the bottom by two lab jacks placed on either side of the MTS machine's ram. This permitted slight height adjustments of the furnace to be made in order to insure a clear optical path for the incident and reflected laser beams.

Control of the furnace temperature was by a Research Inc. model 624A temperature controller. An input signal was supplied to the temperature controller by a chromel-alumel thermocouple attached to the specimen and fed out of the furnace through a hole drilled in the back. The controller compared this signal to the desired set points with the error between these signals being sent to a proportional power controller. The power controller varied the voltage across the heaters and thus the heat input to keep the error signal as small as possible. Typically, the specimen temperature varied only  $\pm 2$  degrees Fahrenheit after it reached the equilibrium temperature. The maximum time required to bring the specimen to temperature was approximately one hour. In order to keep from overheating the load cell which is directly attached to the top grip, a blower was directed on it. This system was only used when the furnace was set at 500°F and proved to be quite satisfactory by allowing only a load cell temperature of 138°F for a furnace temperature of 500°F.

### 3.5 Computer-Testing Machine Interface

The basic fatigue testing apparatus consists of two parts; a ten metric-ton MTS servocontrolled hydraulic testing machine and a Digital Equipment Corporation MINC minicomputer. The MTS machine is considered the heart of the system since it supplies the power which loads the specimen as commanded by the brain of the system, the minicomputer. This section describes the characteristics of both the testing machine and the minicomputer individually and then details the hardware which ties them together into one functioning system. The requirements for this system to then function under both load control and strain control are considered.

The MTS testing machine was a servohydraulic controlled machine composed of a load unit, a performance package and a control package. The load package was a two column,  $\pm 22$  kip frame containing a hydraulic ram with a six-inch stroke capability and a load cell matched to the frame capacity. A six-gallon per minute pump rated for 3000 psig pressure and a servovalve made up the components of the performance package. The control package was made up of a servocontroller to drive the servovalve, a feedback selector to determine the control mode and the necessary transducer conditioners to provide excitation and signal conditioning of the transducers. The whole control system was set up to operate on a  $\pm 10$  volt signal from the signal conditioners. It should be noted that the MTS machine has a function generator, counter panel and a control panel which permitted it to operate completely on its own.

The MINC minicomputer system consisted of a processor, 60 K bytes of memory, laboratory instrument module interfaces, two dual-density

floppy disks and a graphic CRT display with a separate keyboard. The three lab modules in use on the MINC were the crystal clock, digital-to-analog (D/A) converter and the analog-to-digital (A/D) converter. The last two modules are the ones that were the interface with the testing machine and send or receive the signals commanded by the FORTRAN or BASIC program currently being executed by the processor. Because of this it is important to note that the digital-to-analog signal could be operated for either a unipolar or bipolar voltage range up to 10.24 volts. However, the analog-to-digital converter could only be operated on a bipolar voltage range of  $\pm 5.12$  volts.

In order to obtain all of the data to evaluate Neuber's rule, both load-controlled tests of notched specimens and strain controlled tests of smooth specimens were required. The marriage of the MTS machine and the MINC minicomputer permits this to be done in a style which had not been attempted. For the load control case in which the feedback selector chosen was the load cell, the digital-to-analog converter was used to send a  $\pm 10$  volt signal computed by the minicomputer to the "program" connection on the front of the MTS machine. The MTS controller then attenuated this external programmer signal to provide the dynamic component of the composite load command. The static component for the composite load was manually determined by using the set-point potentiometer on the MTS controller. In all of the tests conducted, the set-point was adjusted to zero mean load. In the load-control case, the minicomputer then read in the actual load signal into an analog-to-digital converter after the machine had stabilized. However, since the MTS machine sent out a  $\pm 10$  volt signal and the analog-to-digital converter could only accept a  $\pm 5$  volt signal, a two to one voltage divider was placed between



the two as an interface to the A/D. Other D/A signals were sent to the ISG and A/D signals received before the next load signal was sent to the MTS machine.

For the strain-controlled tests of the smooth specimens, the feedback selector was turned to external. The extensometer discussed earlier was used in the feedback loop, however, an excitation source needed to be provided and the output signal required some conditioning. The excitation of the bridge on the extensometer was provided by a VE-20A strain indicator manufactured by Vishay Inc. This strain indicator not only provided the excitation but also conditioned the output signal, however, the signal was still very small. Because of this, the analog output from the strain indicator was sent through a Tektronix differential amplifier with a gain of 100. This amplifier also had a high frequency filter which was used to further improve the signal fed from the output of the amplifier to the input of the MTS external connection. The input to the MTS machine from the extensometer was to be approximately 3000 microstrain per volt. As mentioned, this was the feedback signal. The command signal again came from the minicomputer and was connected to the MTS machine at the program connection. For this case, the MTS span control was set at the maximum position of 1000 and the command signal from the minicomputer was adjusted to send out a voltage signal on the D/A converter that was equal to the strain desired on the specimen based on the extensometer calibration factor. Once the machine has stabilized, the signal from the load cell was fed through the voltage divider and into the A/D converter just as before. The signals were sent until either all of the data was obtained or the specimen had fractured.

## CHAPTER IV

### SOFTWARE

As mentioned in the previous chapter, the intelligent controller/data acquisition system was the MINC minicomputer. This chapter describes the computer programs which were developed to control the tests and store the data collected. The first section is concerned with the programs required to control the tests of the notched specimens and also compute the strain as measured by the ISG. The second section deals with the programs used in smooth specimen testing while the final section describes the programs which were used in analyzing the data generated by both sets of tests.

#### 4.1 Notched Specimen Programs

There were three programs used in running notched specimens. One program called NØTCH6.FØR was the actual controlling program while the other two programs, JUNK.BAS and VIEW1.BAS, were used only as a means to obtain input data for NØTCH6. Two other programs written in assembly language and named AIN and AØUT were used internally by NØTCH6 to exchange data between the central processing unit and either the analog-to-digital converter or the digital-to-analog converter. The function of each of these programs is discussed in detail below.

There were three major duties of the NØTCH6.FØR program. First, it must transmit and receive the signals required to control the MTS machine. Second, data necessary to control the ISG must be exchanged,

and computations using this data must be made to determine strains. Finally, the appropriate data must be stored in a compact form.

In order to understand the manner in which NØTCH6 controls the load imposed on the specimen, a brief review of the MTS control system is necessary. As stated in the previous chapter, the MTS machine's servocontrols worked off a  $\pm 10$  analog signal and had two basic inputs, the set point and the span. The set point control which determined the mean load on the specimen and was adjusted to zero load for all notched specimens. The second control, the span, actually regulated the portion of an external input signal that was seen by the signal comparator. The total input to the signal comparator was the sum of the signals from both the span and the set point controls. The difference between the input signal and the feedback signal from the load cell at the comparator determined the size and direction of the load which was applied to the specimen by the hydraulic ram in order to bring this difference to zero. However, if the signals at the comparator varied more than a predetermined amount, an interlock shut off the hydraulic system.

The NØTCH6. program controlled the load on the specimen by sending a variable voltage signal to the "program" BNC connection on the front of the MTS control panel. This variable voltage signal was in the form of a triangular wave with peaks at + 10 volts and - 10 volts. By adjusting the span control to the appropriate point any variable load from zero pounds to  $\pm 20,000$  pounds could be applied to the specimen. For all of the cases run, the triangular wave was stopped at sixty discrete points so that measurements could be taken with the ISG. Depending on the load, however, the step change in voltage at the comparator could result in a value exceeding the maximum error signal

allowed by the interlock. Since this would result in a shutdown of the machine, the output signal from the MINC's digital-to-analog converter was modified to include several intermediate voltage steps between the main steps where other measurements are made. These intermediate steps were made in rapid succession to minimize total cycle time, but were slow enough to allow the MTS to respond to each one. For the loads used it was found that ten intermediate steps provided a smooth load transition.

The analog-to-digital converter on the MINC was used to record the signal coming from the load cell on the MTS machine. This signal was proportional to the output load signal, but varied from it depending on the position of the span control. Also, for loads in excess of 10,000 pounds, the signal would be greater than the  $\pm 5$  volts permitted by the A/D. To alleviate this problem, a two-to-one voltage divider was placed between the output of the load cell and the input to the A/D. Therefore, the load recorded was the actual load on the specimen.

The second duty of the MINC minicomputer was to control the ISG which was considerably more difficult than controlling the MTS load. However, this task had already been accomplished by Sharpe during the development of the ISG system. This initial software version was written in assembly language for a small minicomputer and had a resolution of .004 microns, a range of .14 microns and an error band of  $\pm 5\%$ . The basic principle of this small displacement program was to scan both the upper and lower fringes, locate all of the maxima and minima of each fringe pattern and then compare the extreme locations of subsequent scans so that the magnitude of the fringe shift could be determined. The fringe scans were performed by using a minicomputer to increment the servocontrolled mirror through 256 positions while measuring the

voltage from the PMT's at each mirror position. A sliding average was performed on this raw PMT data to eliminate noise before a direct comparison of these averaged voltage values was used to find the extrema points. Simply subtracting mirror positions at the extrema points of the PMT signal from each other at two different loads, averaging these values for both the upper and lower fringes and dividing by the extrema spacing at zero load provided the normalized fringe motion used in equation 3.3. With the other values of this equation being fixed, the displacement or strain between the indentations could be determined for a given load increment. By summing these displacement or strain values for each load increment, the absolute value was determined. Several calibration tests of this system were made with excellent results. The resolution and accuracy of this system were more than sufficient for the cyclic measurements to be run, and in fact were used by Bofferding in his cyclic measurements. However, two problems existed with the system:

1. Unless the software was in assembly language, cyclic tests of more than a few cycles took an excessively long period of time.
2. The zero point drifted into tension during the tests, which was due to all calculations being made relative to the last load point instead of a true zero point.

Because of these two problems, new software was developed which used a slightly different strategy in finding the normalized fringe motion. This new strategy involved first finding a minimum bordered by two very bright fringes and located in a position straddling the aperture of the PMT when the servocontrolled mirrors were near the center of their sweep capability. Once this ideal minimum was found, the ISG setup was adjusted using a program named JUNK.BAS to provide the

brightest pattern. The spacing between the minima were carefully measured with the aid of the VIEW1.BAS program. This minimum straddling the PMT aperture became the chosen minimum and the software was set up to independently move the servocontrolled mirror so that the minimum remains centered on the PMT slit. This was accomplished by rotating the mirror slightly. The amount of fringe shift between loads was measured by the number of voltage steps that must be sent to the mirror to bring the chosen minimum back to the center of the PMT slit. This technique, which was used on the two channels, required that the mirrors for both the top and bottom channels be driven independently, consequently two D/A converters must be used for mirror positioning instead of only one on the original system. The advantages of this new technique far outweighed this penalty because the same strain resolution could be obtained by using only between 40 to 60 points for a mirror scan instead of the 256 required on the old system. By reducing the input data per load point, both the time to scan the additional points was saved as well as the computation time required for increased data. A second benefit of the technique was that the drift of the zero point was eliminated. This was the result of comparing the current mirror position to one chosen at zero load rather than just incrementing the current strain or displacement by the amount changed during the last load increment.

The final phase of software development for the notched specimen program was to implement a data storage scheme which would be compact but could permit easy access to the data for future testing and analysis. Since the MINC minicomputer had a dual floppy disk drive with each disk capable of storing 512 K bytes, the disk was chosen as the storage

device. For the notched specimen program, the information which required storage for each load cycle was: (1) the cycle number, (2) the load in lbs/10 for each load increment, (3) the remote strain in microstrain for each load increment, and (4) the notch strain in microstrain for each load increment. In order to conserve space all of the data was converted to integer values and stored in binary form in a direct access file. By converting to integer values only one byte was required for storage instead of the two bytes used for floating point numbers. The direct access file also permitted the data for any given cycle to be examined without having to read through the preceding cyclic data. In fact, this storage scheme permitted not only all of the notched specimen data but also the smooth specimen data for each of one thousand cycles to be stored on a single floppy disk.

As stated earlier a program written in FORTRAN and named NOTCH6.FOR was developed to incorporate the techniques described above into a central controller for both the MTS machine and the ISG. Figure 4.1 contains a simplified flowchart of this program while the actual program listing is found in Appendix B. The basics of the program as defined by the flowchart consist of initially zeroing all variables and opening the required data file. Next the various input variables are read in. These are then used to compute the appropriate loading curve for the MTS machine and other constants. After this is completed, the program runs in a loop for a specified number of cycles. The first cycle does not increment the load on the specimen so that the location of the chosen minima can be locked in. If this occurs satisfactorily, then the program begins to increment the specimen load on the next cycle. After each load increment, the mirrors are scanned through a

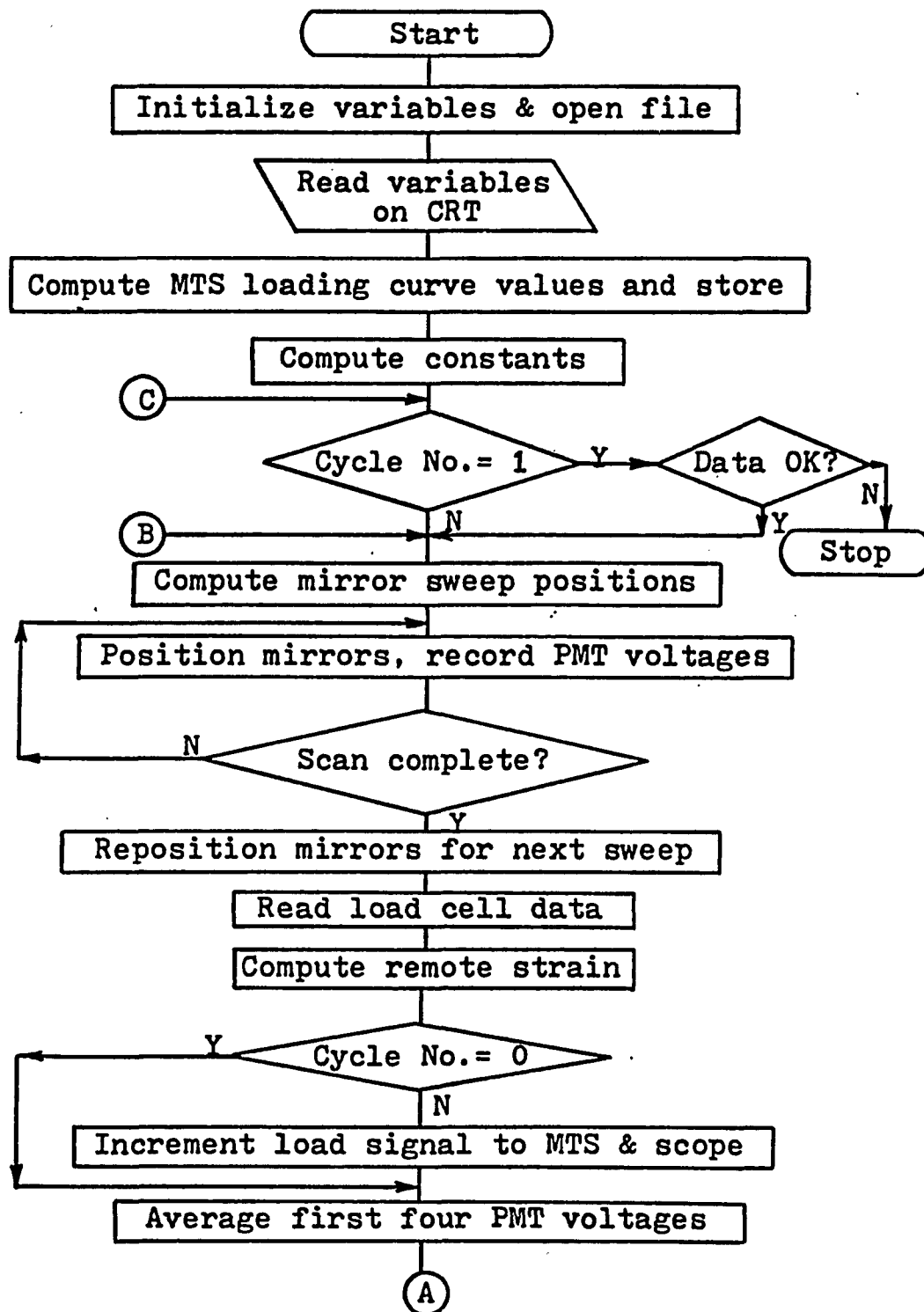


Figure 4.1. Flowchart of NOTCH6



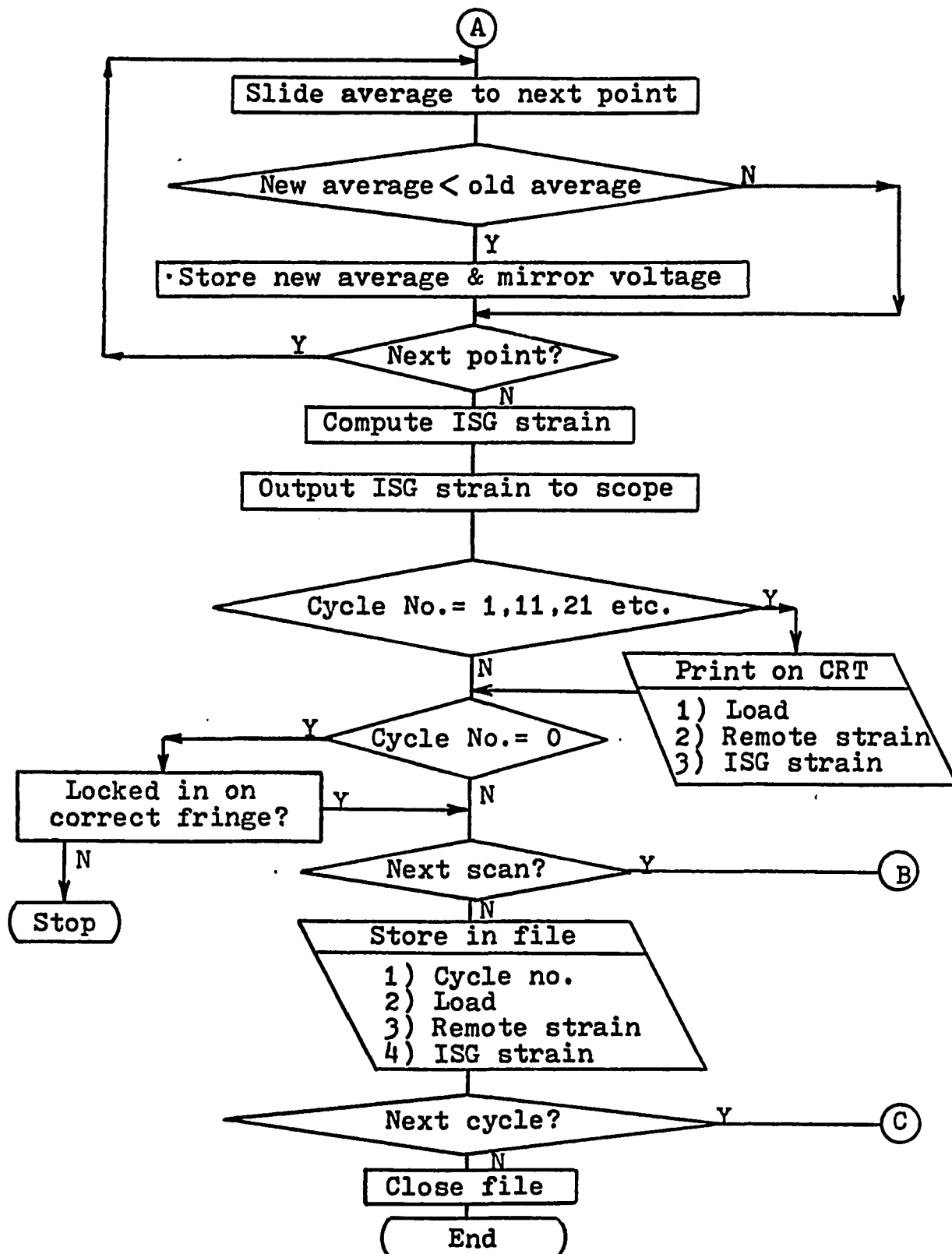


Figure 4.1. Flowchart of NOTCH6 (continued)

specified number of positions and the PMT voltage is read in for each mirror position. The load cell data is also read and used in computing the remote strain in the specimen. Once this is complete, the mirrors are repositioned for the next sweep and the load incremented on the specimen. This is done to permit the transients to die down before the next measurements are made. Computations of the strain at the notch are then made by averaging the PMT data, finding the mirror voltage at the point of minimum averaged PMT voltage, and comparing it to the one found on the first cycle. This procedure is repeated until the specimen load has experienced a completely reversed load cycle, then the data from all of these load increments are stored on the floppy disk. This is repeated until the specified number of cycles has been completed at which time the data file is closed and the test terminated.

To aid the operator in following the progress of the test, several outputs are provided for in the program. One indication of the status of the test is a plot of load versus notch strain. This is obtained by sending out both load signals and ISG strain signals at each load increment from the minicomputer. They are fed into an oscilloscope set up as an X-Y plotter. A second output medium is the CRT screen where the number of the load cycle in progress is displayed. Also, on every tenth load cycle, all of the data taken during that cycle is displayed on the screen. These two output formats from the minicomputer enable the test to be carefully monitored. One additional aid is that parallel signals from the two PMT's are fed into a dual trace oscilloscope. They permit the operator to see that the chosen minimum remains centered on the PMT aperture.

Two routines were used by the main program of NØTCH6 to input and output signals to various devices. These routines were named AIN and AØUT and are assembly language programs which were written by Rick Haag, another graduate student. AIN was used to receive data connected to the input channels of the analog-to-digital converter. AØUT provided a method of sending analog signals out from the four channels of the digital-to-analog converter.

The programs JUNK and VIEW1 were written in BASIC and used to provide input data to NØTCH6. JUNK sends out rapidly varying voltage signals to both servocontrolled mirrors resulting in the fringe pattern being continuously swept across the PMT's at the rate of 10 Hertz. This enables the fringe pattern to be adjusted until it is bright and properly situated on the aperture of the PMT. The second program, VIEW1, is used to find the minima which will be followed by NØTCH6 as well as the spacing between minima on both channels. This is accomplished by slowly scanning 256 points and plotting the resulting PMT voltages versus mirror position on the CRT. After the plot is complete for the first channel a cursor appears on the screen and is used by the operator to lock in the point on the graph which represents the chosen minimum. The cursor appears again and is moved to the location of the second minimum and then locked in. This process is repeated for the data on the second channel. The program then prints out the mirror location for the chosen minimum and the spacing between minima for both channels in a form which can be directly input to NØTCH6.

The current version of NØTCH6 which was used for all tests operated at a rate of sixty scans and load increments per cycle and a scan length of sixty mirror positions. A rate of approximately

10 cycles per minute was obtained for the speed of data input and reduction. Breaking this time down even further revealed that it took 100 milliseconds per scan with the ratio of mirror sweep time to computation time being 60/40. Using indentations spaced 100 microns apart, and the spacing between minima adjusted to approximately 100 mirror positions the sensitivity of the computer controlled ISG was 55 microstrain or a displacement of .0055 microns. The stability of the system was checked and after a fifteen-minute warmup period the reading was within  $\pm 55$  microstrain. Since the range of strain measurements was to be approximately  $\pm 1\%$ , the range of this computer controlled system was checked. Initially it was found that with the original 7 x 7 mm mirrors, a  $\pm 1\%$  strain would move the chosen minimum dangerously close to the edge of the mirror. To alleviate the possibility of losing this minimum, larger mirrors measuring 7 x 11 mm replaced the smaller ones. This resulted in measurements in excess of  $\pm 1\frac{1}{2}\%$  being made with no problems. These tests concluded the software development for the notched specimen tests.

#### 4.2 Smooth Specimen Programs

Only a single program named SMØØTH.FØR was needed for the smooth specimen testing. The main function of this program, written in FORTRAN, was to recall the stored ISG data taken at the notch and send the appropriate signal to the MTS machine to reproduce this strain in the smooth specimen. Once this had been done the MTS load cell reading was input and stored. The details of these operations are discussed below.

A copy of the program SMØØTH.FØR is included in Appendix C and a flowchart presented in Figure 4.2. The flowchart shows that first, all

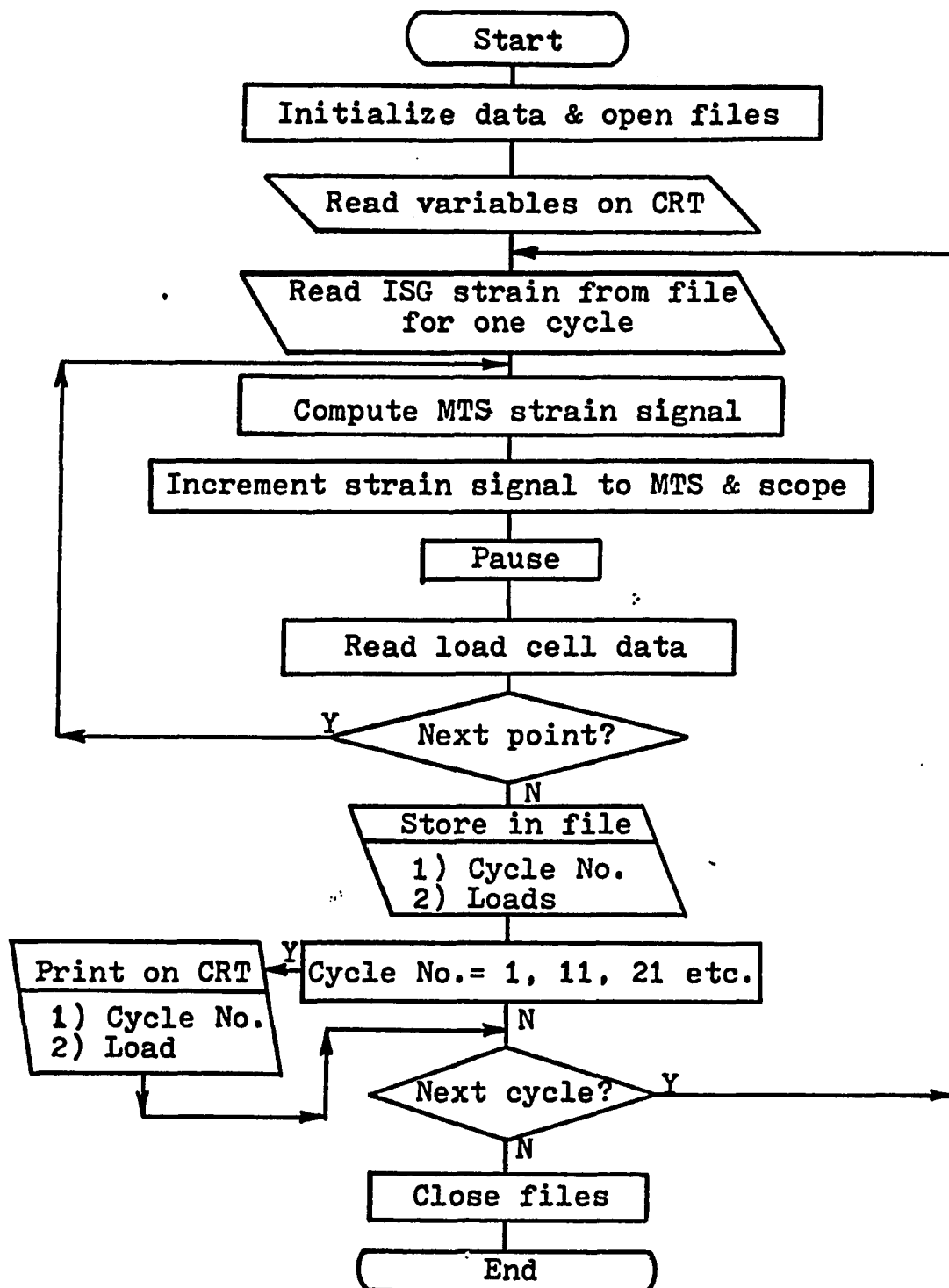


Figure 4.2. Flowchart of SMOOTH

of the variables are initialized and then two files are opened. The first file, named RESULT.DAT, is the data file in which all of the notched specimen data has been stored while the second file entitled SMØØTH.DAT is the one in which all of the smooth specimen data will be placed. Next the values of the various parameters such as the extensometer calibration factor and the number of cycles to be run are read in. With this completed, the program went into a loop in which all sixty stored notch strains for a complete load cycle were read into memory from the data file named RESULT. Using these strain values and the calibration factor for the extensometer, the voltage signal needed to impose the measured strain on the smooth specimen was computed. One by one these signals were sent out to the MTS machine and, after a small delay to eliminate any dynamic effects, the value from the load cell was read in. This was repeated until all sixty load values had been obtained, at which time they were read into the data file named SMØØTH. This entire sequence was repeated until the number of cycles specified had been completed, then both the data files were closed and the program terminated.

This program had the same operator output features found in the notched specimen program. They consisted of an X-Y plot on the oscilloscope of strain versus load and a printout on the CRT of all load and strain data every tenth load cycle.

The speed capabilities of the SMØØTH program were quite a bit faster than that of the NØTCH6 program due to reduced data transfer and computations required. However, to prevent problems from occurring by loading the specimens at two substantially different rates, a pause was placed in the program. This pause resulted in approximately twenty cycles being run in one minute which is only twice the speed of the

notched specimen data acquisition. Therefore, it is felt that sampling rate is not a factor. This concluded the software development for the smooth specimen test.

#### 4.3 Data Reduction Programs

Once both the notched specimen data and smooth specimen data had been collected and stored on a floppy disk, several different analyses were made. Four programs were written in BASIC to perform the required data reduction and were named ANAL1, ANAL2, ANAL3 and ANAL4. These programs are described in detail below; but for them to make all of the necessary computations, large amounts of data concerning the properties of the specimens was required. To provide this data in a convenient fashion, an additional program entitled STORE was written. The function of this program was to prompt the operator to input various information about the specimen used in generating the data stored on a particular disk. Such things as notched and smooth specimen numbers, number of good data cycles stored, and other physical properties like specimen cross sectional area, were requested. After obtaining all of this data, the program opened a sequential data file named TEST.DAT on the data storage disk, placed the data into this file and then closed it. Therefore, this file provided a source of basic specimen information for any analysis program.

There were four different ways in which the data generated was to be evaluated. The first was to view the notch strain, as measured by the ISG on the notched specimen, plotted versus the remote stress for any cycle. This function was performed by the program named ANAL4, which either plotted the notch strain and remote stress on the CRT or

printed out the values for any cycle chosen. A second, very similar task was carried out by the ANAL1 program. The output format was the same, the only difference being that the notch stress obtained from the smooth specimen test was plotted versus the notch strain. ANAL2 was used to compute the stress concentration factor, strain concentration factor and the geometric mean of these two factors for selected cycles of the test. To accomplish this, data from both the notched and smooth specimens was analyzed. The output from this program consisted of either a semi-log plot on the CRT of the appropriate concentration factor versus cycles or a printout of cycle numbers and concentration values. The fourth program computed the same three concentration factors, but only for the initial tensile loading points on the first cycle. These concentration factors were then plotted versus notch strain by the ANAL3 program. These four programs provided nearly all of the data reduction required.

All four of the programs described above are listed in Appendix D. Due to the many similarities between the programs, only a general description of the programming philosophy will be presented here. The first step in each of the programs was to open the three data files named TEST, RESULT and SMOOTH stored on each data disk. Next, various physical property information on the specimens was input from the TEST data file. The cycles at which the various computations were to be made were then input from either a specified array or operator input. For each specified cycle, the appropriate load or strain data was retrieved from the data files. Finally, after all of the values have been assembled, the required computations were made. The operator was then given the choice of plotting the data on the CRT or using the printer to output



all of the values in tabular form. Once this was complete, the files were closed and the program terminated.

## CHAPTER V

### EXPERIMENTAL PROCEDURES

In the previous chapters, details of the specimens to be used have been given, as well as, the associated hardware and software used in testing the specimens. This chapter explains the procedures which were used during the actual tests. First, the general alignments and calibration of the testing machine are described, then the procedures used in testing the notched specimens and smooth specimens at room temperature are detailed. Next, the adjustments needed to run the same specimens at an elevated temperature are discussed. Finally, an assessment of the experimental error is presented.

Before testing of any kind was done, the MTS testing machine was calibrated and aligned. In November, 1980, a service technician from MTS calibrated the load cell on the machine against a master load cell with known calibration standards. The results of this calibration revealed only minor differences between the initial and final settings. Next, the load frame and grips were checked for alignment, which is critical because any out of plane bending would cause inaccuracies in the ISG measurements and possible specimen buckling. First the crosshead and ram of the MTS machine were moved to the final location for all testing. Then the grips were loosely inserted into the load frame where they were still free to rotate. Alignment was accomplished with an extra notched specimen of 7475 aluminum instrumented with strain gages on both sides.

The strains from both gages were recorded both before and after installation into the grips. Data from both gages was also recorded as the specimen and grips were rotated in 45° increments through a complete rotation. An analysis of the strain reading for the various grip positions quickly pointed out the direction in which the load cell attached to the crosshead had to be moved to center it above the ram. After this adjustment was made, the alignment check was repeated to insure it had not been disturbed during retightening of the adjusting nut. With the MTS machine calibrated and aligned, testing was ready to begin.

#### 5.1 Notched Specimen Tests

The principal measurement made using the notched specimen is the strain at the edge of the notch. Therefore, before any testing was conducted, the ISG was calibrated against a strain gage. This was done by using the blank alignment specimen which already had strain gages bonded to it. A small area adjacent to the strain gage was carefully polished to a mirror finish and two indentations were placed 100 microns apart in this area. These indentations were carefully aligned to insure that they were along the same axis as that of the strain gage, since they were to form the gage for the ISG. Also, since there were no notches on this specimen and both the strain gage and indentations were located in the center part of the specimen's gage length, the strain gradient was assumed to be uniform. This specimen was then loaded into the grips and the ISG system adjusted to align the fringe pattern with the photomultiplier tubes. The MTS machine was used to manually load the specimen from zero load to 6000 lb. tension, back through zero to 6000 lb.

compression and finally back to zero. These load steps were taken in 1000 lb. increments, and at each increment both the strain gage reading and the ISG reading were recorded. Figure 5.1 shows a plot of strain gage versus ISG strain. From this plot it is obvious that the ISG strain is consistently lower than the actual strain. Repeated tests showed that the ISG hardware and software were both functioning correctly. Also, a second alignment check revealed no measureable misalignment.

As mentioned earlier in the description of the ISG, rigid-body motion that is not parallel to the load axis leads to errors in strain measurement. If the specimen moves away from the laser in a direction parallel to the incident beam, the resulting fringe motion is equivalent to a negative strain. Each test specimen was checked in the elastic region at room temperature prior to testing, and each showed a similar low calibration. It was concluded that the test machine was misaligned, but consistently so. Therefore, it was decided that all strains measured by the ISG would be adjusted upwards 13% to account for the low readings.

With the ISG calibrated, everything needed for testing of the notched specimens was ready. The first step consisted of preparing the specimens by polishing a small area at the edge of the notch where the indentations for the ISG were placed. The polishing procedure consisted of a light sanding to knock off the high spots with 400 grit paper and finishing with a 600 grit paper. The final sanding was done parallel to the longitudinal axis of the specimen to keep any diffuse light from being reflected on the photomultiplier tubes. After sanding the area, it was buffed to a mirror finish using a 5-micron aluminum oxide solution and a buffing wheel attached to a high speed grinding tool.

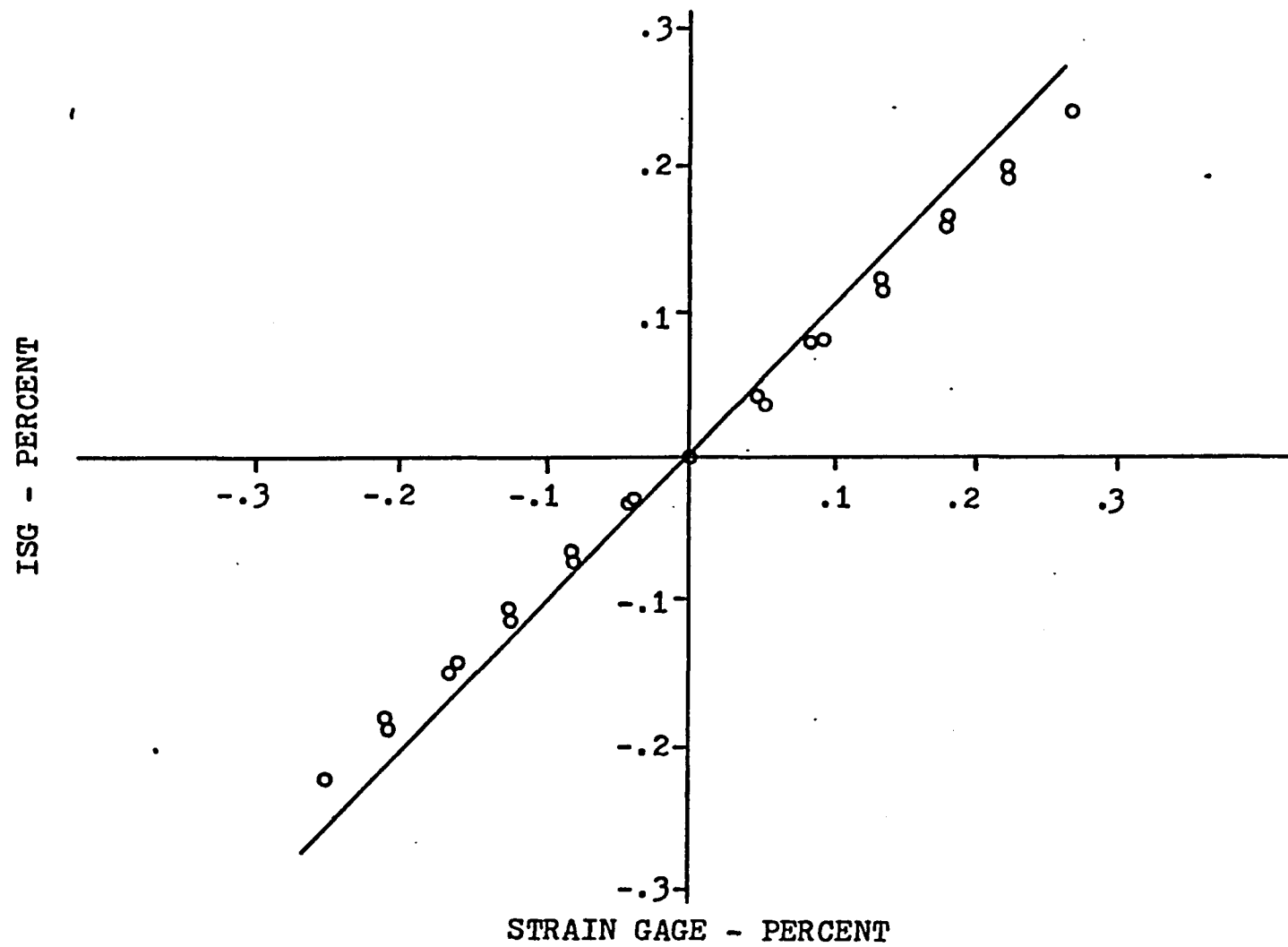


Figure 5.1. Calibration Curve for the Interferometric Strain Gage

Care was taken not to round the corners at the edge of the notch by only buffing lightly in those areas. Next, the polished area was washed down with methanol to remove any residue from the surface. Finally, two indentions were placed in the polished area 50 microns from the edge of the notch using a Vickers hardness tester. The pyramidal indentations were approximately 17 microns on a side and were located along the axis of the specimen 100 to 150 microns apart.

The second step in running the tests involved mounting the specimen in the grips, aligning the ISG system and then performing a calibration check. The specimen installation was straightforward and so was the initial ISG alignment. After initially finding the fringes, several software aids were available to lock in the sharpest pattern. One of these aids was the program called JUNK.BAS, which sets up the servocontrolled mirrors to continuously scan the fringe pattern and display it on the oscilloscope. This permits the effectiveness of slight adjustments to be seen quantitatively on the oscilloscope. Once the best fringe pattern has been chosen, a second program named VIEW1.BAS is used to find and place the minimum that would be followed in the center of the mirror. This is useful because it provides information needed by the actual test program and also because it centers the pattern, thus, preventing it from moving off one edge of the mirror during testing. Once everything has been carefully adjusted, a calibration test was run manually. This test involved loading the specimen to approximately 20 to 30% of its test load in several increments and recording the load, remote strain and local strain at the notch at each point. The load was a complete cycle going into both tension and compression and was chosen to be small so that the material at the edge of the notch would

remain in the elastic region. The purpose of these tests was to experimentally measure the stress concentration factor for the notch of each specimen. This test also permitted the effects of the notch machining technique to be evaluated.

The final step in testing a notched specimen is the actual test and data collection. After the test load had been decided upon, the span control on the MTS machine was set to limit the maximum specimen load which was cycled between tension and compression around zero load. The machine interlocks were also set at this time to insure that if a malfunction occurred, the specimen and grips would not be damaged. The floppy disk to be used for data collection was also initialized at this time with data pertaining to the specimen to be tested. This data was the specimen number, indentation spacing, notch geometry and test temperature and was coded in the volume ID in the following form:

Volume ID = A, B, C, D

where, A = specimen number,

B = indentation spacing,

C = notch geometry; H = hole, E = ellipse, S = slot,

D = test temperature; R = room temp., E = elevated temp.

The only remaining step was to run the test program called NØTCH6.FØR. This program prompts the operator for all information needed and then begins execution. For all of the notched tests conducted, sixty load increments were made for each load cycle with data being recorded at each increment. These tests were conducted for a maximum of one thousand cycles or until the load-strain curve showed a crack had been initiated, at which time the data files were closed and the test stopped. The approximate speed of the tests was 10 load cycles per minute.

## 5.2 Smooth Specimen Tests

Since the ISG was not used for the smooth specimen tests, the procedure was quite a bit simpler. The extensometer described in Chapter III served as the feedback device for the MTS machine in these tests, and therefore its calibration was required. This calibration was very similar to that performed for the ISG. A smooth specimen blank was machined from the 7475 aluminum, and strain gages were mounted on both sides of it. The extensometer was then fastened to this specimen and the entire assembly loaded into the MTS machine. After zeroing everything, small increments of load were applied and readings from both the strain gage and extensometer recorded. Figure 5.2 shows a plot of this data. From this data a calibration constant of  $2960 \mu\text{in/in/volt}$  was obtained.

The actual test of a smooth specimen consisted only of mounting the extensometer on the specimen using the two springs and then placing the assembly in the grips. The floppy disk on which the local notch strain data had been stored in the earlier notched specimen test was placed in the appropriate disk drive. To insure that all components were operating correctly, the span control on the MTS machine was set at 100 and the SMØØTH.FØR program was run for approximately 30 to 35 cycles. This actually loaded the specimen to 10% of the strain measured at the notch and then recorded the load input from the MTS load cell. Since this strain was still well below any plastic strain, the calibration of specimen was checked using Hookes' law. If everything checked out satisfactorily, the SMØØTH.FØR program was run after turning the span control to 1000. This subjected the smooth specimen to the full notch strain load while recording the load required to do so. The test



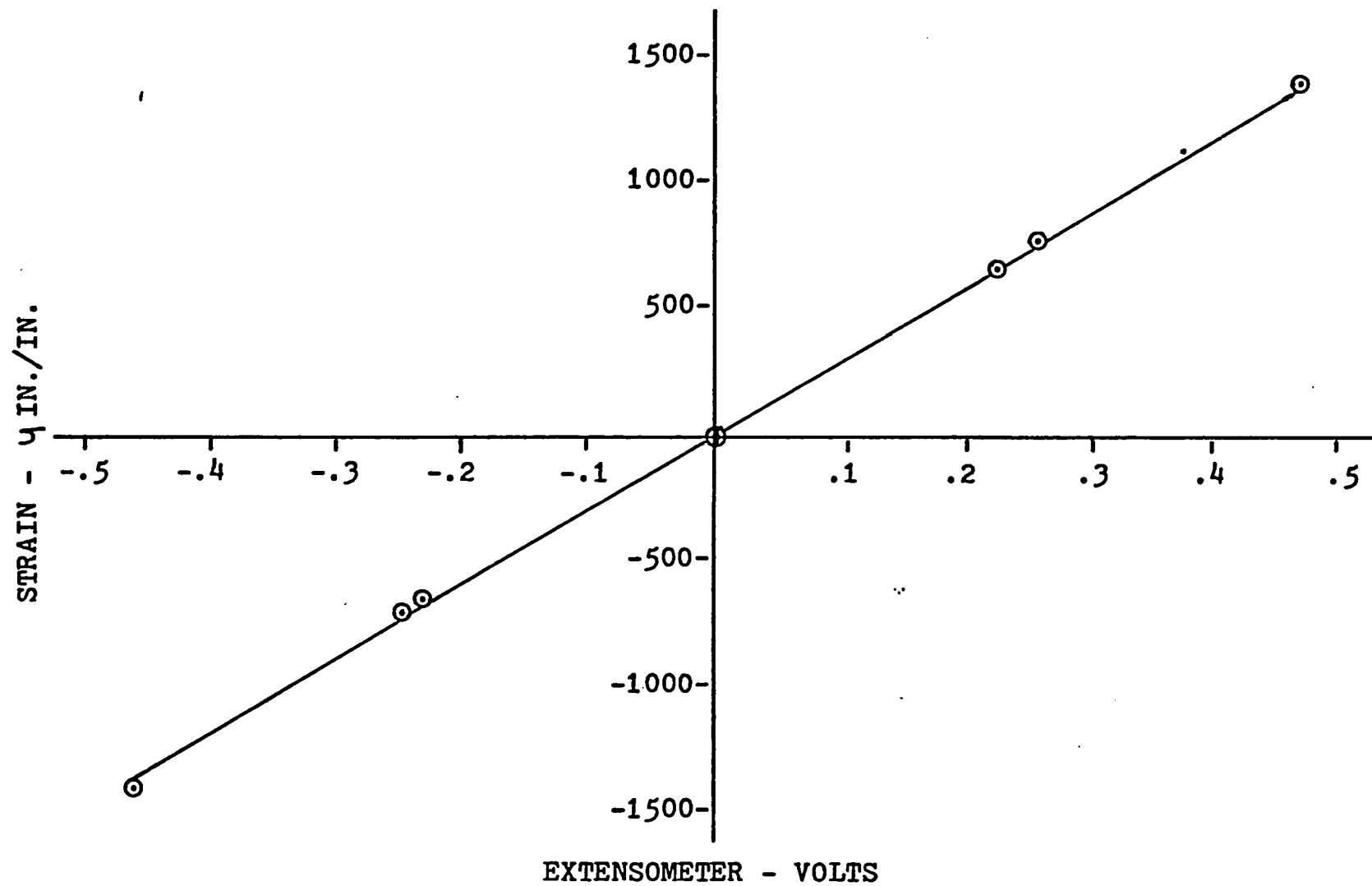


Figure 5.2. Calibration Curve for the Extensometer

continued until either all of the usable notched specimen data has been sent or until the specimen cracked or fractured. At that time all data files were closed and the test terminated.

### 5.3 Elevated Temperature Tests

The aforementioned procedures for conducting both the notched specimen test and the smooth specimen tests required only slight modifications for elevated temperature testing. Basically all that had to be done was to install a thermocouple on the specimen surface and attach it to the temperature controller. The furnace was then placed around the specimen and grips, and wired to the power controller.

The attachment of the thermocouple is accomplished by stretching a stainless steel spring around the specimen and hooking both ends of the spring together. The thermocouple is then slipped under this spring which serves to hold it in contact with the specimen surface during testing. Two different size springs are used; one for the notched specimens, and the second for the smooth specimens. The chromel-alumel thermocouple was then attached to the temperature controller using a plug type connector.

As described in Chapter III, the high temperature furnace was designed in two pieces to facilitate specimen installation and removal. Placement of the heater around the specimen and grips required only that the front half of the furnace having the quartz view ports be set on the lab jacks so that these ports are situated facing the ISG. The back half was then placed on the lab jacks and the two halves brought together around the grips and fastened using the four toggle clamps. A power cord from the temperature control unit was then attached to the terminal

strip located on the rear heater; this completed the control circuit.

To bring the specimen to temperature, the set point of the temperature controller was dialed in and the start button pushed. For the aluminum specimens which were tested at 300°F, the heater takes approximately 30 minutes to reach the setpoint. Once the setpoint is reached, the controller keeps the specimen within  $\pm 2^\circ\text{F}$  during the entire tests. The 500°F temperature used in testing the steel specimens required approximately one hour to heat up.

No problems were encountered in aligning the ISG through the heater ports for the elevated notched specimen tests. In fact, it required no additional effort over that for a room temperature test. The only problem with the high temperature tests was that the load cell had to be kept below 250°F to be operational. Since the grip was directly attached to the load cell, it conducted heat right into the cell. Therefore, all of the 500°F tests required that additional cooling be supplied to the load cell. This was provided by a small blower directed at the load cell. Temperature in the load cell never exceeded 130°F with this system. No additional cooling was required for the 300°F tests. At the completion of the tests the temperature controller was turned off and the back half of the heater removed to permit a faster cool down.

#### 5.4 Experimental Accuracy

In following the testing procedures detailed in the previous sections, error was introduced at each measurement. This section quantifies that error so that the accuracy of the overall experiment could be estimated. Two causes for error were evaluated, the first was due to

the accuracy of the measurements and the second was concerned with the fact that one dimensional measurements were being made of a two dimensional system.

The two major sources of experimental error were the measurements of notch strain and notch stress. In measuring notch strain, the ISG was used which has an accuracy of  $\pm 55$  microstrain for room temperature measurements. However, at 500°F the accuracy decreased to  $\pm 110$  microstrain. This resulted in an error of 3.67% for steel specimens in which the maximum notch strain was approximately 3000 microstrain. The measurement of the load needed in computing the notch stress was accurate to  $\pm 1$  bit in the minicomputer. This corresponded to a measurement of  $\pm 0.005$  volts at the minicomputer; however, because the voltage divider was used in this measurement, the minicomputer could actually detect only  $\pm 0.010$  volts from the MTS machine. A measurement of  $\pm 0.010$  volt on the MTS machine was equal to  $\pm 20$  lbs or a stress of  $\pm 667$  psi in a smooth specimen. Since most of the smooth specimen stress measurements of the 2024 aluminum were approximately 40 ksi, an error of 1.67% was possible. Other sources of error such as specimen misalignment and out of plane rigid body motion of the specimen were taken into account during the ISG calibration test. After making a small allowance for these other factors, it is concluded that the accuracy of the experimental measurements used in evaluating Neuber's rule was  $\pm 10\%$ .

A second source of error was due to the fact that one dimensional stress and strain measurements were taken near the notch where two dimensional stresses and strains exist. An approximation of this error was made by computing the two dimensional values for a hole in an infinite plate using equations derived from the theory of elasticity.

For the circular hole geometry, an error of only 1.5% was calculated. However, in making the same computations for the keyhole slot geometry, the error was found to be 10.8%. These error values should be considered when evaluating the results in the following chapter.

## CHAPTER VI

### RESULTS

A total of twenty-one notched specimens and twenty-one smooth specimens were tested using the equipment and techniques described in the earlier chapters. This chapter attempts to compress the voluminous data accumulated from all of these tests into a form which would permit easier evaluation of the parameters studied during the experiments. There are six sections in this chapter with each section describing a different way of examining the data. The first section presents an overview of the entire testing program and lists the various parameters studied during the program. Next, some raw data obtained from a notched specimen is presented. The third section considers the cyclic properties of the materials by analyzing the smooth specimen data for various cycles. Neuber's original premise is evaluated in section four, while a cyclic form of the relation is considered in section five. Section six examines a second cyclic form of Neuber's relation incorporating the fatigue properties of the material.

#### 6.1 Specimen Log

Each of the twenty-one notched and smooth specimens tested are listed in Table 6.1 along with other pertinent data. The first column lists the notched specimen number used in the load controlled tests while the number of the smooth specimen used in inferring the stress at the notch is listed in column two. With these specimen numbers, the location

Table 6.1  
Specimen List

Notched Specimen No.	Smooth Specimen No.	Material	Notch Geometry	Load lbs.	Temperature OF	Stress Concentration Factor	Notched Specimen Cycles	Smooth Specimen Cycles
201	220	AL 2024	Hole	5500	Room	2.75	1000	335
203	214	AL 2024	Hole	5500	Room	2.58	1000	647
202	217	AL 2024	Hole	5500	300	2.80	1000	570
204	219	AL 2024	Hole	5500	300	2.78	1000	660
211	221	AL 2024	Slot	4200	Room	3.93	350	330
208	216	AL 2024	Slot	4200	Room	3.96	600	395
210	218	AL 2024	Slot	4200	300	3.97	519	159
109	116	CRS 1018	Hole	8100	Room	3.28	400	400
112	113	CRS 1018	Hole	8100	Room	2.81	1000	1000
111	119	CRS 1018	Hole	8100	500	3.25	1000	1000
110	117	CRS 1018	Hole	8100	500	3.25	1000	1000
103	114	CRS 1018	Slot	5500	Room	4.88	1000	1000
102	115	CRS 1018	Slot	5500	Room	4.65	1000	1000
104	118	CRS 1018	Slot	5500	500	5.18	1000	1000
705	717	AL 7475	Hole	6000	Room	3.29	1000	300
712	714	AL 7475	Hole	6000	Room	2.86	1000	468
708	718	AL 7475	Hole	6000	300	2.82	1000	396
709	720	AL 7475	Hole	6000	300	2.68	551	326
702	716	AL 7475	Slot	2000	Room	3.96	1000	1000
704	715	AL 7475	Slot	4000	Room	3.94	750	557
703	719	AL 7475	Slot	4000	300	4.44	580	34

of a particular specimen within the original material can be found using the layout drawings found in Chapter II. The third column denotes the material from which the specimen was machined and the fourth column provides the notch geometry. The alternating component of the load used in testing the notched specimens is listed in the next column and the temperature at which both the smooth and notched specimens were testing is defined in column six. In column seven, the stress concentration factor which was measured experimentally during an initial calibration test of the notched specimen is presented. This concentration factor was computed using the gross cross-sectional area of the specimen and incorporated the use of the ISG calibration factor. The final two columns list the number of cycles for which good data was recorded in testing the notched and smooth specimens. It should be noted that the notched specimen tests were carried out for a maximum of 1000 cycles or until good data was no longer available due to specimen cracking. Also, the smooth specimens were run until they either failed or the stored notch strain data became unusable.

After viewing the information presented in Table 6.1, two things should be apparent. The first thing is that neglecting the tests of the slotted geometry at elevated temperature, every test save one was duplicated. This duplication was performed to insure that the results obtained from this technique were repeatable, and thus add credibility to the tests. A second observation is that even for carefully machined specimens, the measured stress concentration factors are extremely scattered. Since this scatter is primarily between materials, it probably is the result of rounding off the sharp corners near the notch during the polishing step. Another possible cause is that the



distance of the indentations from the notch varies due to the difficulty of distinguishing the edge of a notch at high magnification (400x).

One fact not shown in the table is that cracks were found near the notch at the termination of the experiment in eighteen of twenty-one tests. This indicates that the tests were indeed low-cycle fatigue tests. Also, it should be noted that equipment failures resulted in the early termination of only two experiments. Notched specimen number 709 was removed from the testing machine after only 551 cycles because of a failure in the power supply for the servocontrolled mirrors. The second equipment failure occurred on cycle number 35 of smooth specimen number 703's test. On this cycle the extensometer slipped; resulting in the buckling of the specimen.

## 6.2 Notch Strain vs. Remote Stress

All of the loads were chosen so that the stress and strain far removed from the notch remained perfectly elastic. Therefore, a plot of the remote strain versus the remote stress would be a straight line with a slope equal to the elastic modulus. However, the loads were also of a magnitude to result in plastic strain near the notch. In order to view this phenomenon, plots of notch strain versus remote stress using data taken from a notched specimen test were made. A typical plot for a 1018 steel specimen containing a hole is shown in Figure 6.1. This plot contains data taken on the first, tenth and thousandth cycle.

Only a small plastic strain was obtained even though the stress concentration factor was 2.81 and the remote stress for the specimen was equal to 36.2 ksi. Apparently, the elastic limit was exceeded at the edge of the notch, but the plastic zone must have been much smaller than

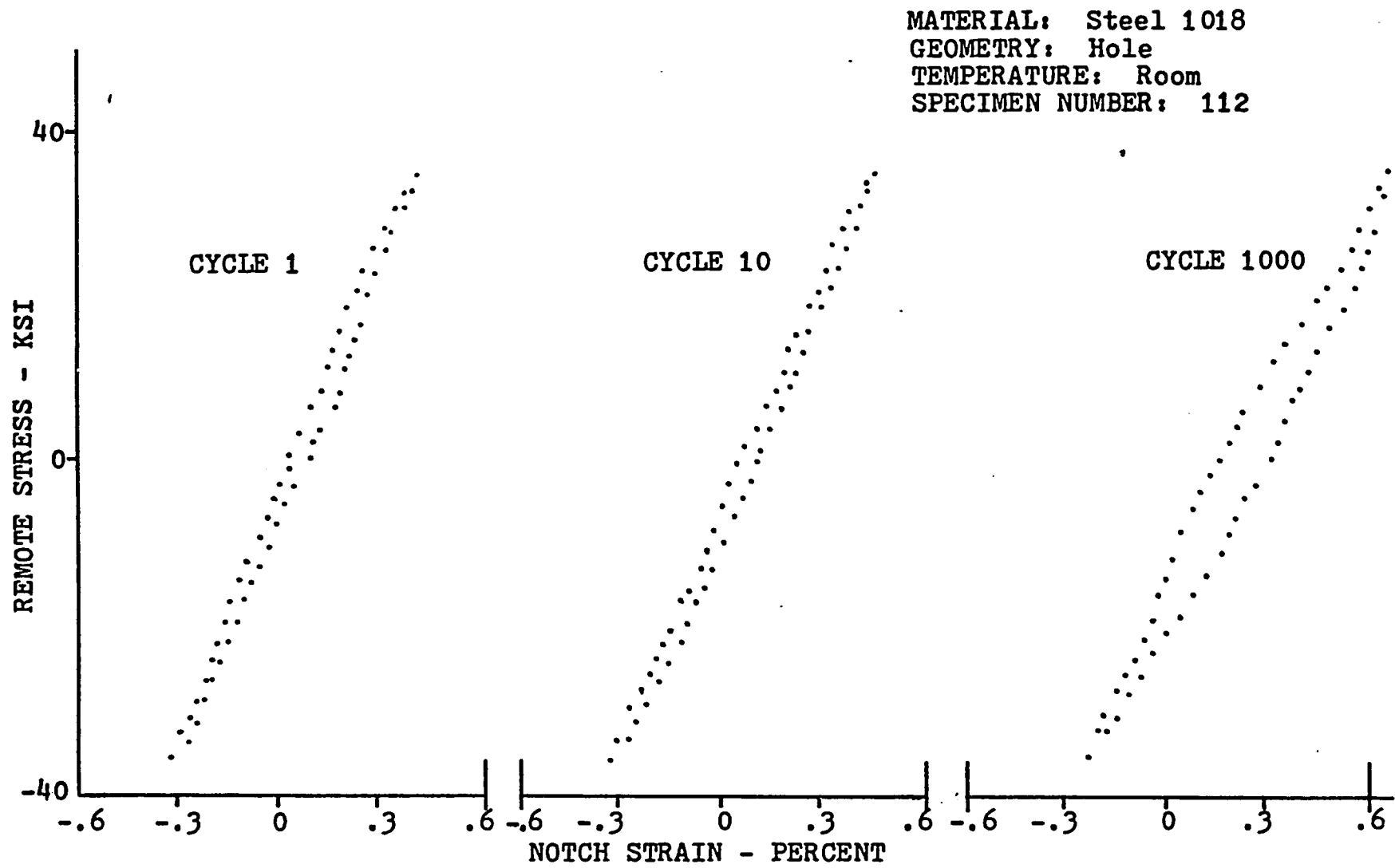


Figure 6.1. Notch Strain vs. Remote Stress

the gage length of the ISG, thus resulting in only a small plastic strain. As stated earlier, this plot is typical of that obtained for other materials and geometries.

### 6.3 Notch Strain versus Notch Stress

Since some plastic strain was recorded at the notch by the ISG, it was expected that during the strain controlled smooth specimen tests, the measured stress would exceed the yield stress of the material. Plots of the controlling notch strain and the measured notch stress for three smooth specimen tests are shown in Figure 6.2 through 6.4. Figure 6.2 presents the plots of a 2024 aluminum smooth specimen which has been subjected to the same strains found near a hole in a notched specimen tested at room temperature. Data for the first tenth and hundredth cycles are shown. The other two figures represent similar data for the 1018 cold rolled steel specimen and the 7475 aluminum specimen respectively. Note that the smooth specimen data in Figure 6.3 corresponds to the notched specimen data in Figure 6.1.

In viewing the data, two important points are quickly noticed. The first is that the load measured at the peak strain of each specimen is above the proportional limit of the material. This results in a cyclic stress-strain curve having a relatively large hysteresis loop. The second point observed is that the peak measured load is affected by the number of cycles to which the specimen for a given material has been subjected. In the case of the 2024 aluminum, the load value increases as the number of cycles placed on the smooth specimen were accumulated. This phenomenon indicates that the 2024 aluminum is a cyclic strain hardening material. A similar review of the data for the 1018 steel

MATERIAL: ALUMINUM 2024  
GEOMETRY: Hole  
TEMPERATURE: Room  
SPECIMEN NUMBER: 220

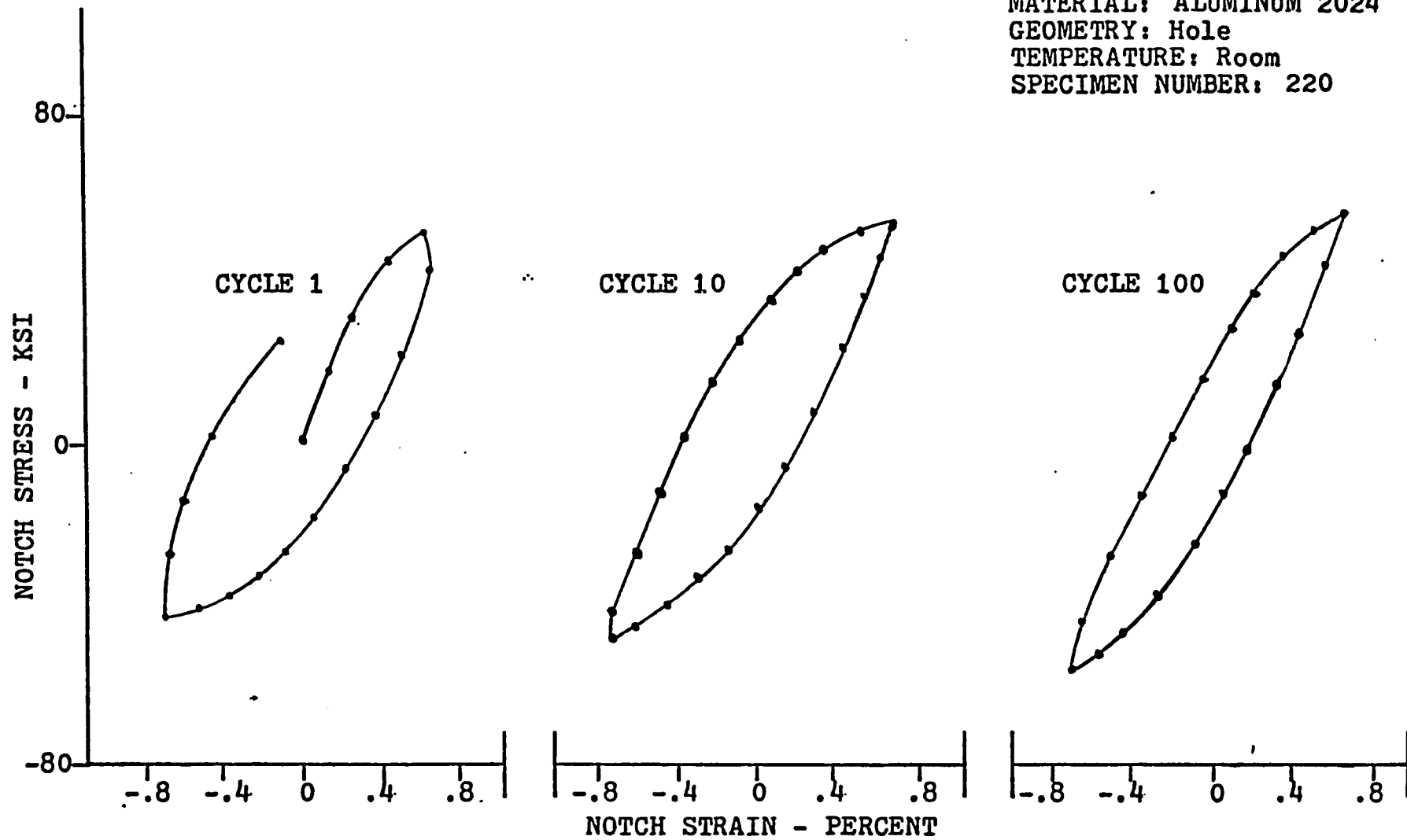


Figure 6.2. Notch Strain vs. Notch Stress - AL 2024

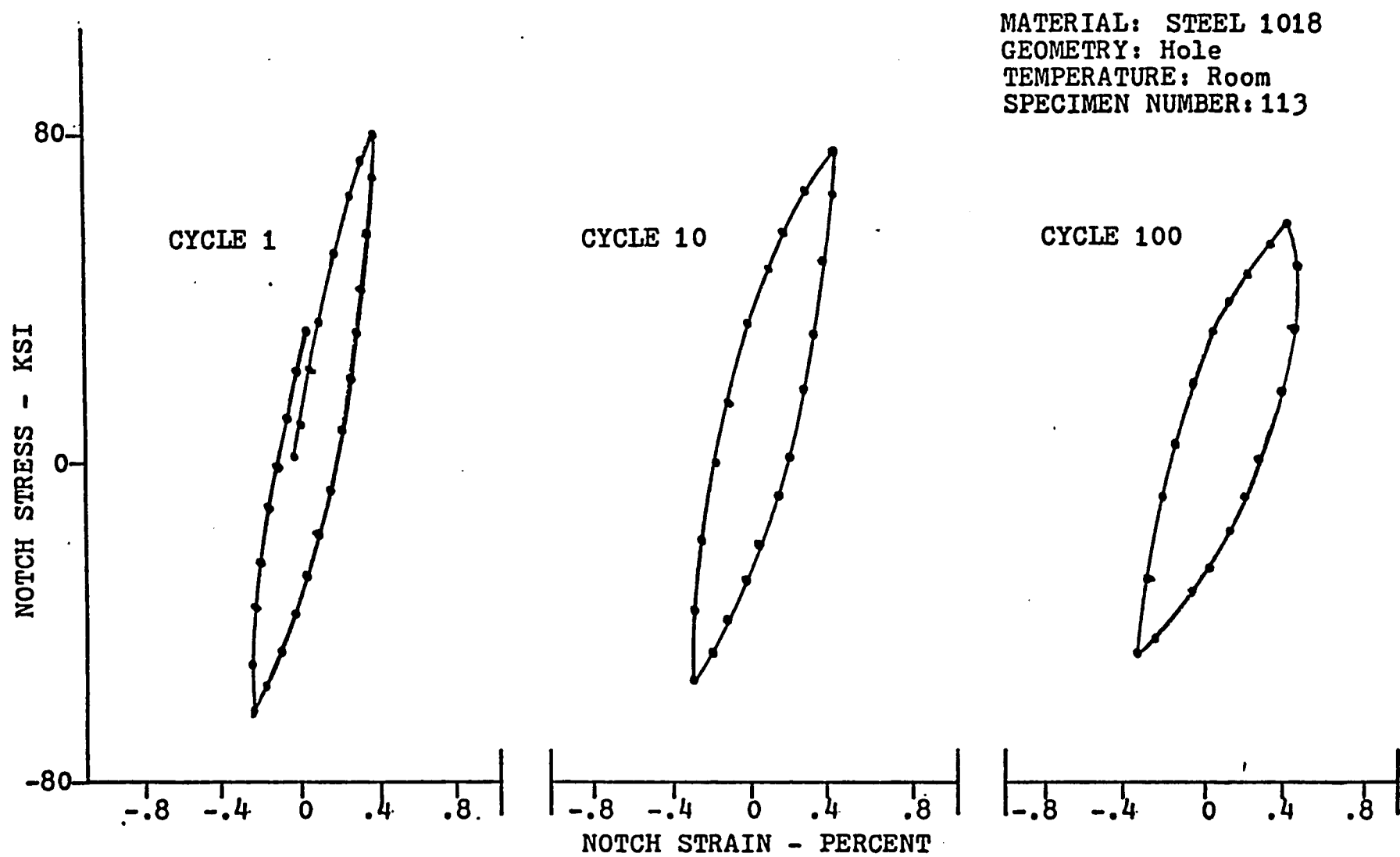


Figure 6.3. Notch Strain vs. Notch Stress - Steel 1018

MATERIAL: ALUMINUM 7475  
GEOMETRY: Hole  
TEMPERATURE: Room  
SPECIMEN NUMBER: 714

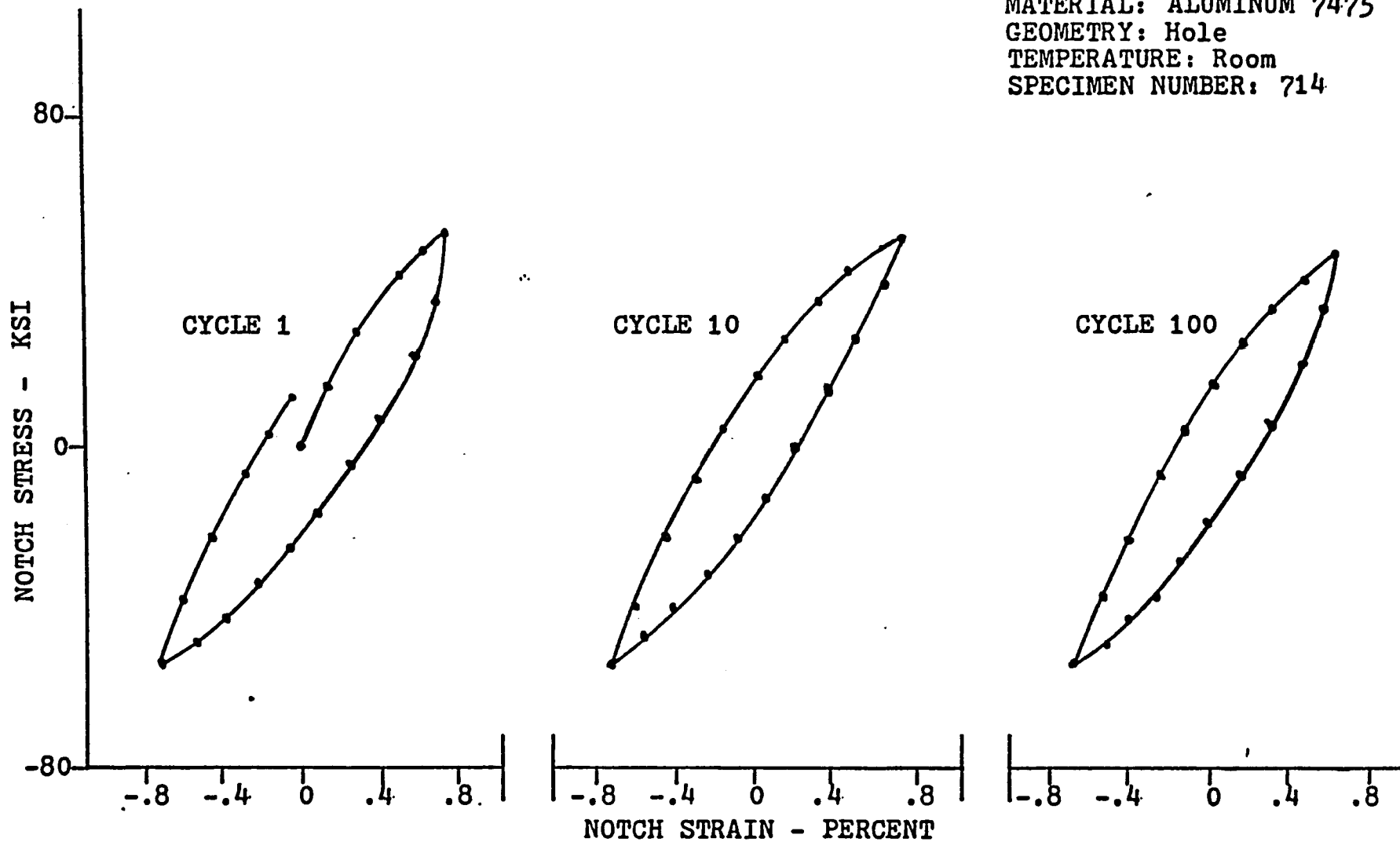


Figure 6.4. Notch Strain vs. Notch Stress - AL 7475

indicates that it is a cyclic strain softening material. The notch stress versus notch strain plots of the third material, 7475 aluminum, shows little variation with cycle number. Therefore, this aircraft grade aluminum is considered to be a cyclic stable material.

#### 6.4 Notch Strain Versus Neuber's Parameter

As stated in Chapter I, Neuber's original paper was concerned with stress and strain concentration factors near a notch for a specimen experiencing monotonic loading. This is precisely what was obtained during the initial phase of the first loading cycle when the load was increased from zero into tension. In an effort to evaluate Neuber's original premise, the data for this initial loading was plotted in Figures 6.5 through 6.7.

Figure 6.5 shows the relationship between the stress concentration factor and the notch strain for 2024 aluminum specimens containing two different notch geometries and tested at both room and elevated temperature. The stress concentration factor is obtained by dividing the stress in the smooth specimen at any given load increment by the remote stress measured at the same load increment on the notched specimen. This value is then normalized by dividing by the stress concentration factor measured during the calibration check of the particular specimen. The general trend observed from this plot is that at small values of notch strain where the entire specimen is elastic, the stress concentration factor is very close to the theoretical value. At very low strain values there is some deviation from this trend due to the experimental error discussed in the previous chapter. However, as the material goes into the plastic range at the notch, the stress concentration decreases. This is exactly what Neuber predicted would occur.

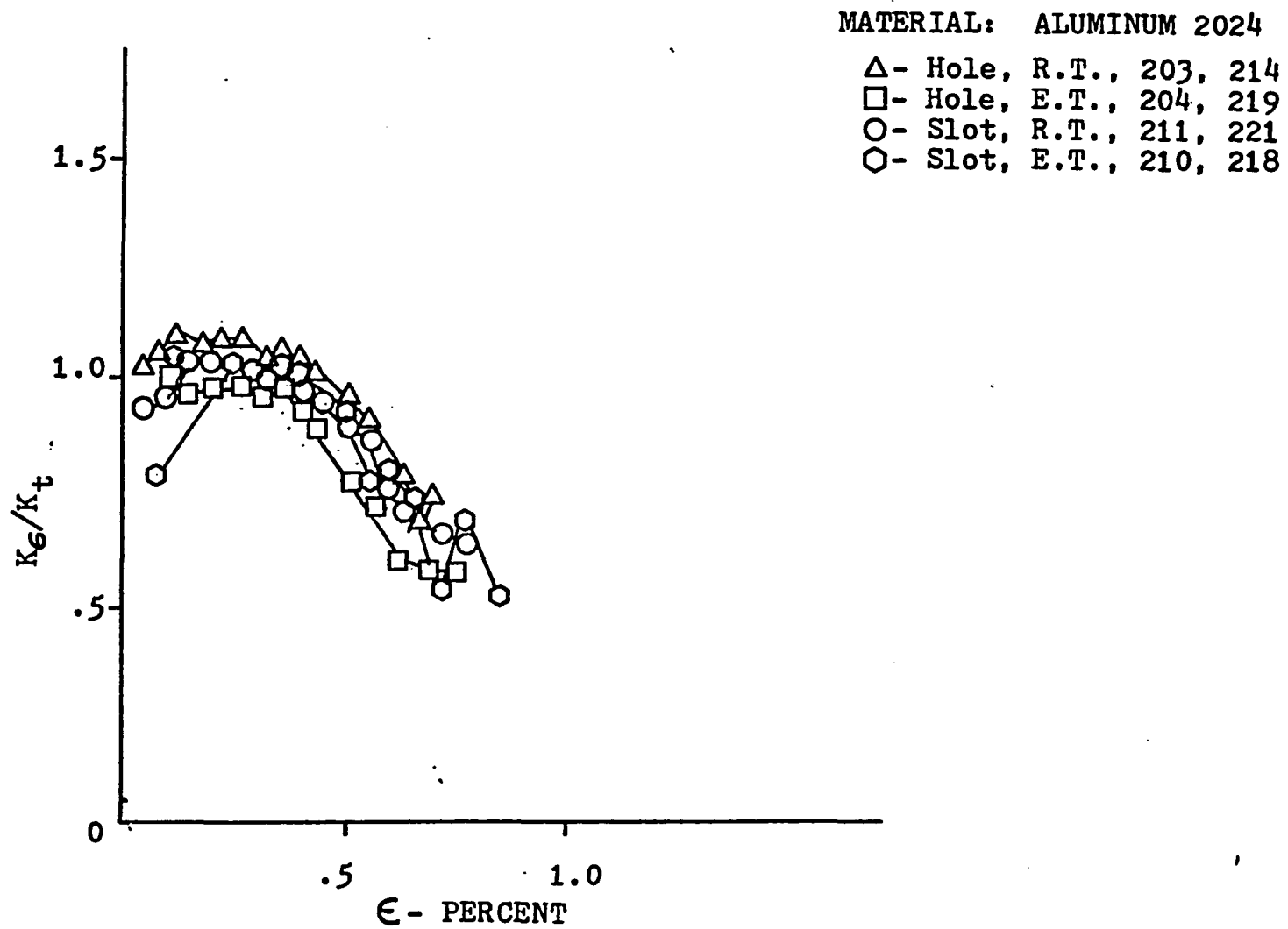


Figure 6.5. Stress Concentration vs. Notch Strain - 1st Quarter Cycle



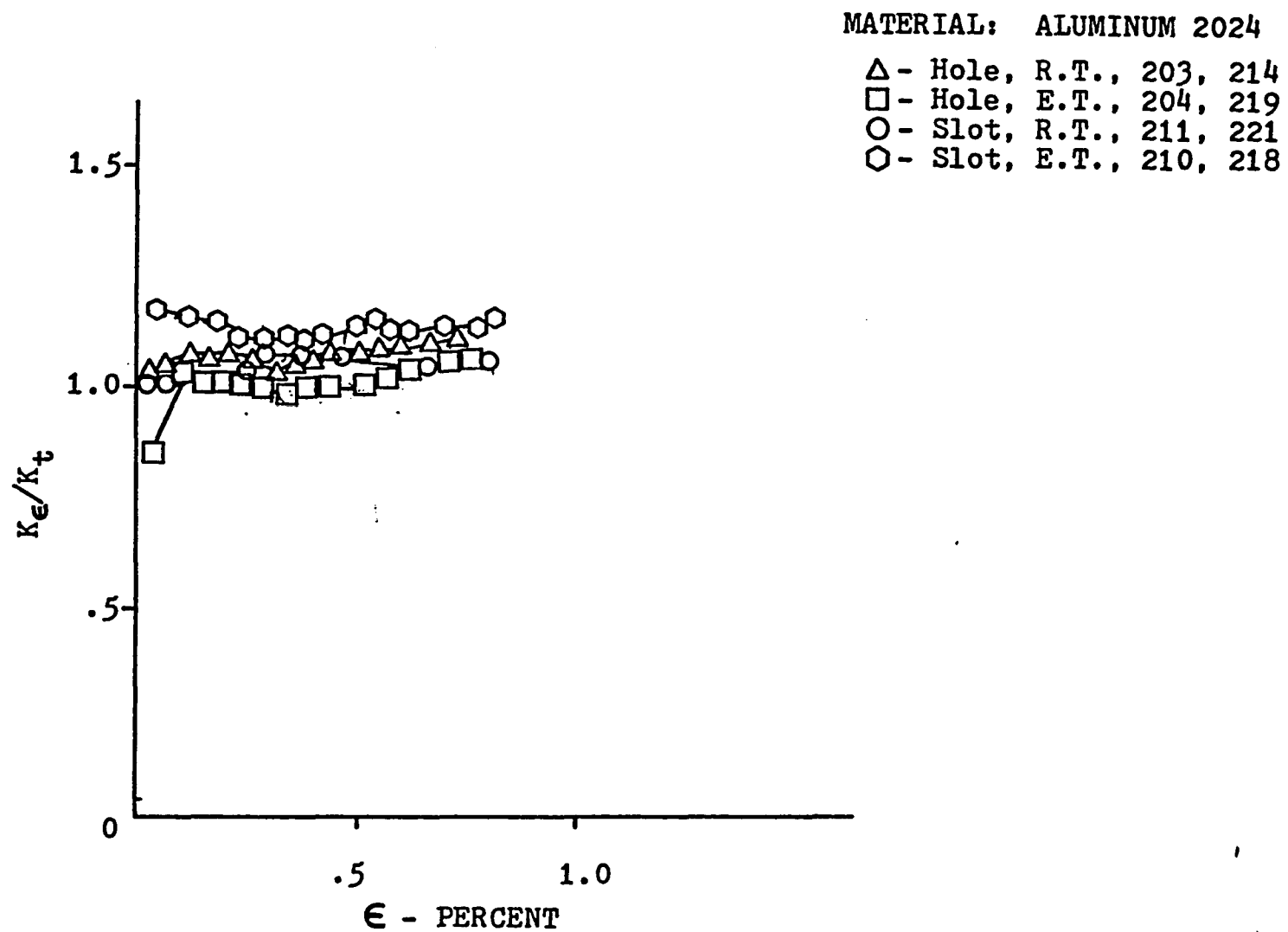


Figure 6.6. Strain Concentration vs. Notch Strain - 1st Quarter Cycle

MATERIAL: ALUMINUM 2024

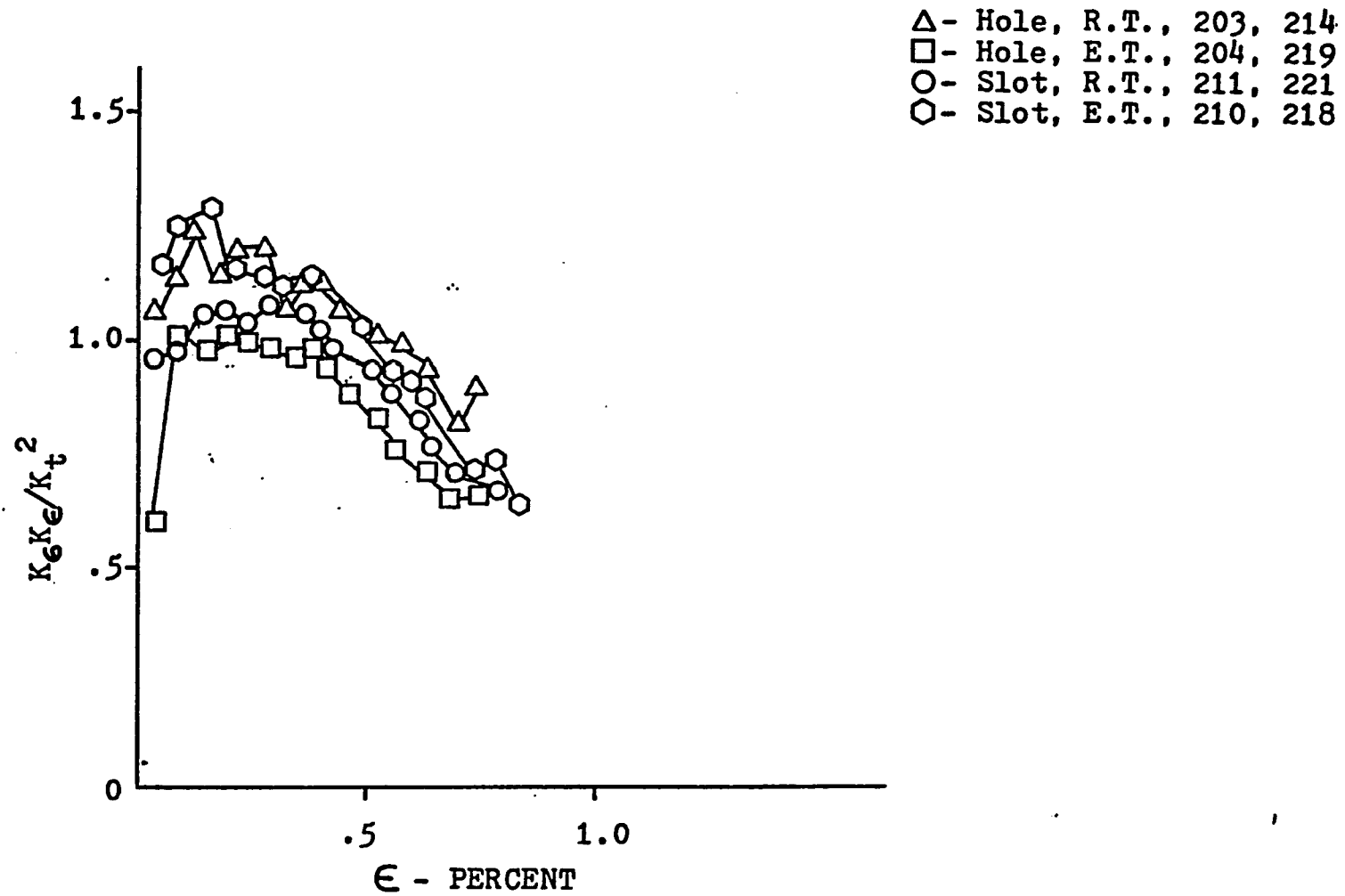


Figure 6.7. Neuber's Parameter vs. Notch Strain - 1st Quarter Cycle

The plot shown in Figure 6.6 is very similar to the previous one except that the strain concentration factor instead of the stress concentration factor is plotted versus the notch strain. This strain concentration factor is computed by dividing the measured ISG strain at the notch by the remote strain away from the notch and then normalizing the value by the calibration test stress concentration factor. This plot reveals that the strain concentration factor does not vary appreciably with notch strain. In fact, even as the material at the notch goes into the plastic region only a very slight increase in the strain concentration factor is noticed.

The plot shown in Figure 6.7 just combines the two previous plots in the manner suggested by Neuber. He stated that the geometric mean of the stress and strain concentration factors should equal the theoretical stress concentration factor. This implies that the Neuber parameter, which was obtained by multiplying the stress and strain concentration factors together and dividing by the calibration test stress concentration factor squared, should be essentially equal to one for all values of notch strain. However, since the strain concentration was approximately equal to one for all notch strain values, the Neuber parameter curve clearly follows the stress concentration factor curve. This results in some deviation from Neuber's predicted response at larger strains. Also, it should be noted that the data obtained for other materials and temperatures provided similar results.

## 6.5 Concentration Factors Versus Cycles

The previous section dealt with only the monotonic loading case, while this section extends the same idea to the cyclic loading case.

The same three parameters described above, the stress concentration factor, the strain concentration factor and Neuber's parameter are plotted versus the number of loading cycles the specimen has undergone. However, these parameters are computed slightly different from the previous factors. Instead of using the absolute value of the stress or strain, the range of stress or strain between the maximum tensile load and the maximum compressive load is used. This value is again normalized by dividing the measured stress concentration factor into it. The Neuber parameter is then computed as above but using the new stress and strain concentration factors.

The plots of these three parameters versus cycles for each of the three materials concerned are presented in Figures 6.8 through 6.25. The first six figures are for the 2024 aluminum specimen, the next six are the plots obtained for the 1018 steel specimens, while the last six plots contain only data from the 7475 aluminum tests. Within any set of plots for a particular material, the first two graphs show the stress concentration versus cycles; the next two plot strain concentration versus cycles and the final two present Neuber's parameter versus cycles. Two plots are required for each concentration factor because data from all seven specimens are plotted. A single plot would crowd the data too much, therefore, the results for the two different notch geometries are plotted separately.

After reviewing this data the following observations are apparent. First, neither the stress or strain concentration factor show any appreciable variations during the entire cyclic tests. Second, the stress concentration factor is generally below the value measured during the calibration test. This can be explained by the results of the previous

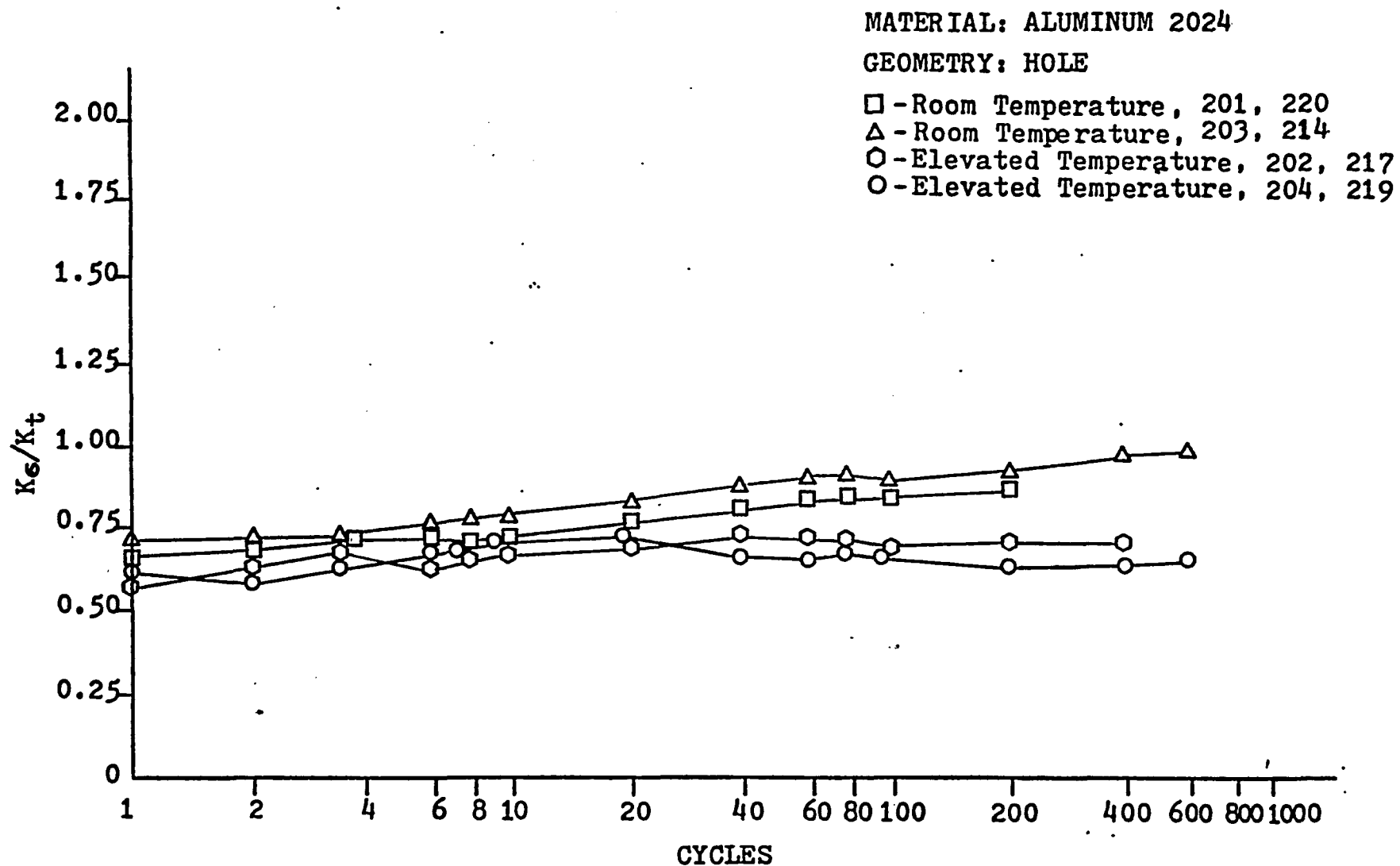


Figure 6.8. AL 2024 - Hole - Stress Concentration vs. Cycles

MATERIAL: ALUMINUM 2024

GEOMETRY: SLOT

□ - Room Temperature, 211, 221

△ - Room Temperature, 208, 216

○ - Elevated Temperature, 210, 218

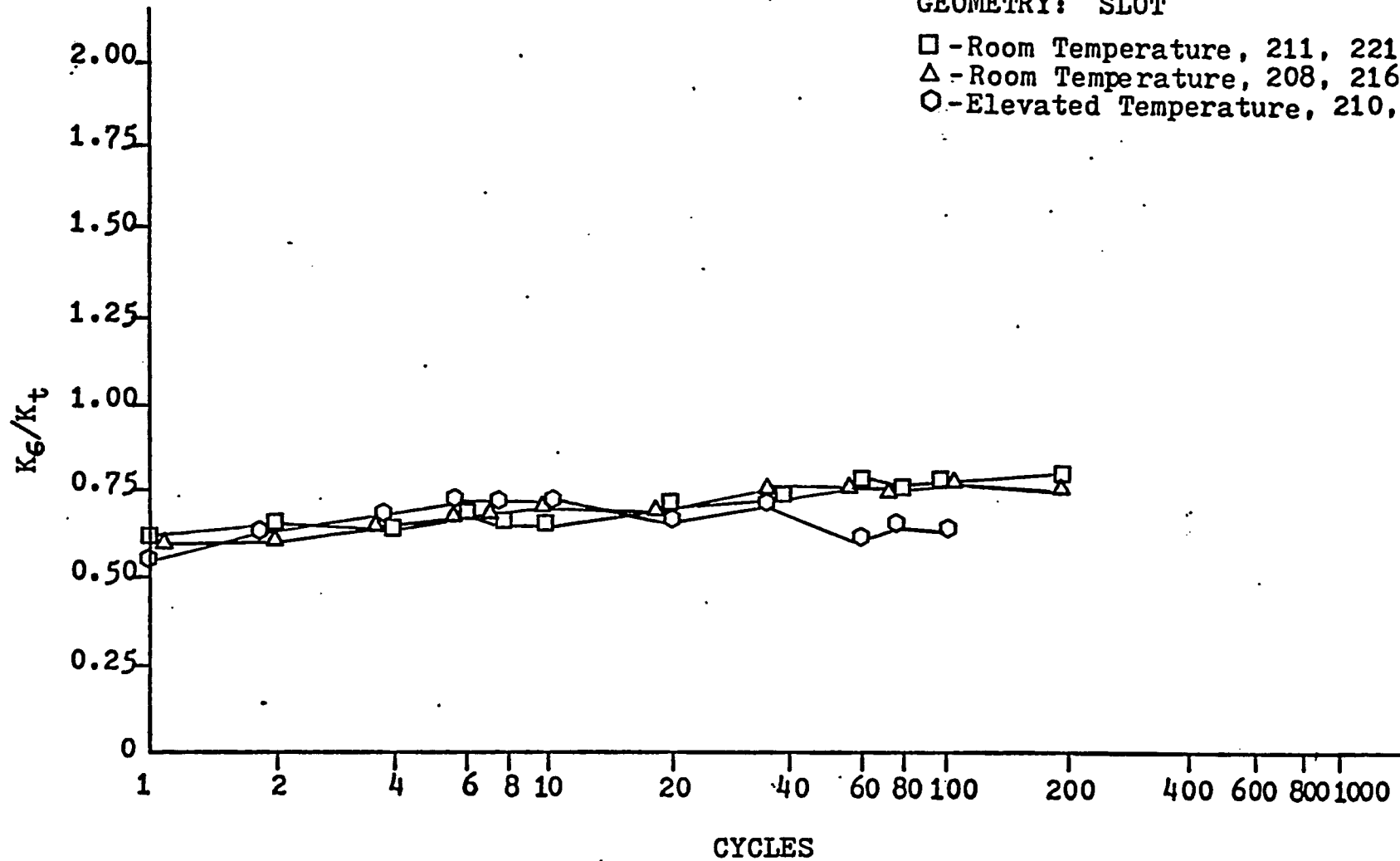


Figure 6.9. AL 2024 - Slot - Stress Concentration vs. Cycles

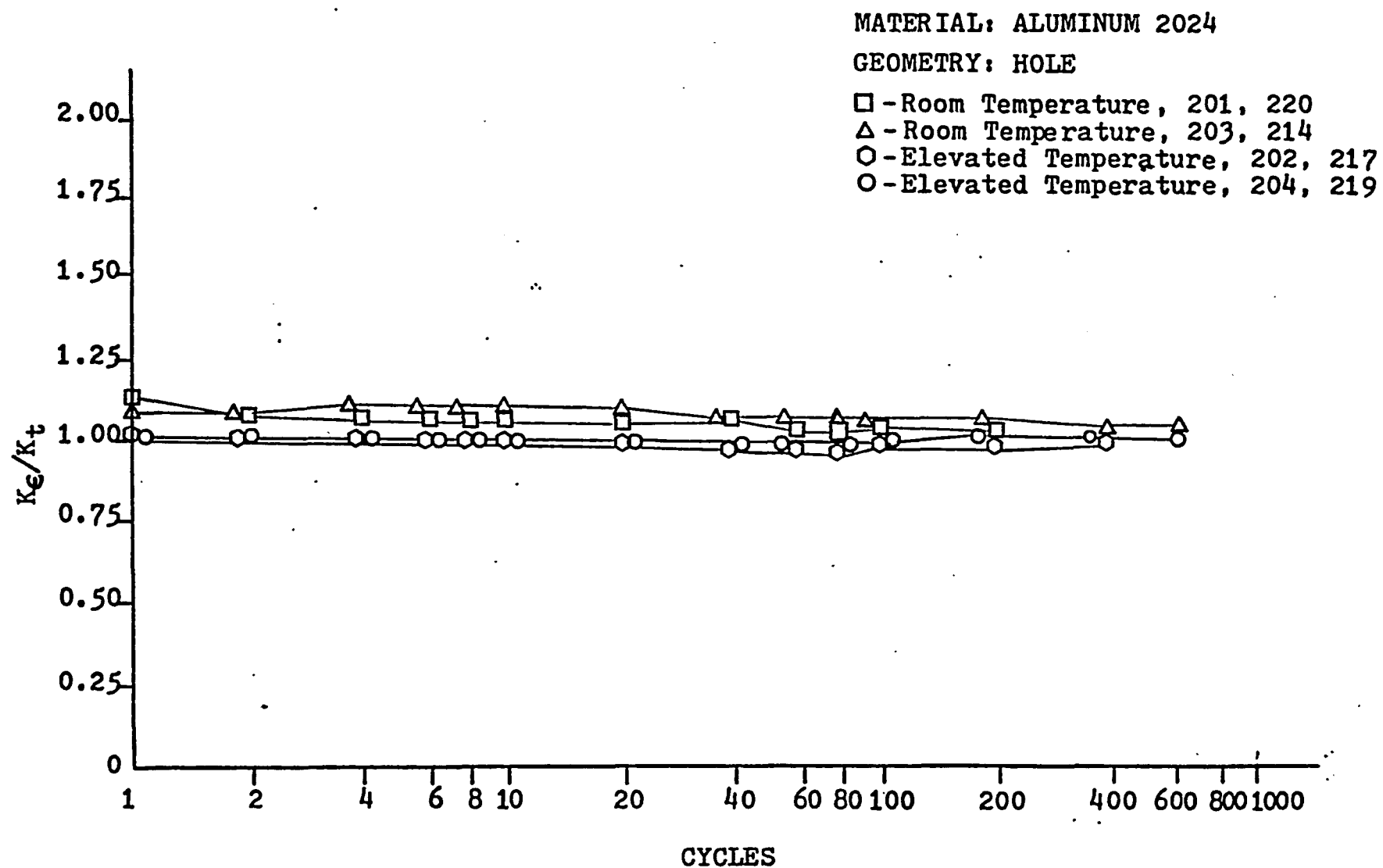


Figure 6.10. AL 2024 - Hole - Strain Concentration vs. Cycles

MATERIAL: ALUMINUM 2024

GEOMETRY: SLOT

□ - Room Temperature, 211, 221

△ - Room Temperature, 208, 216

○ - Elevated Temperature, 210, 218

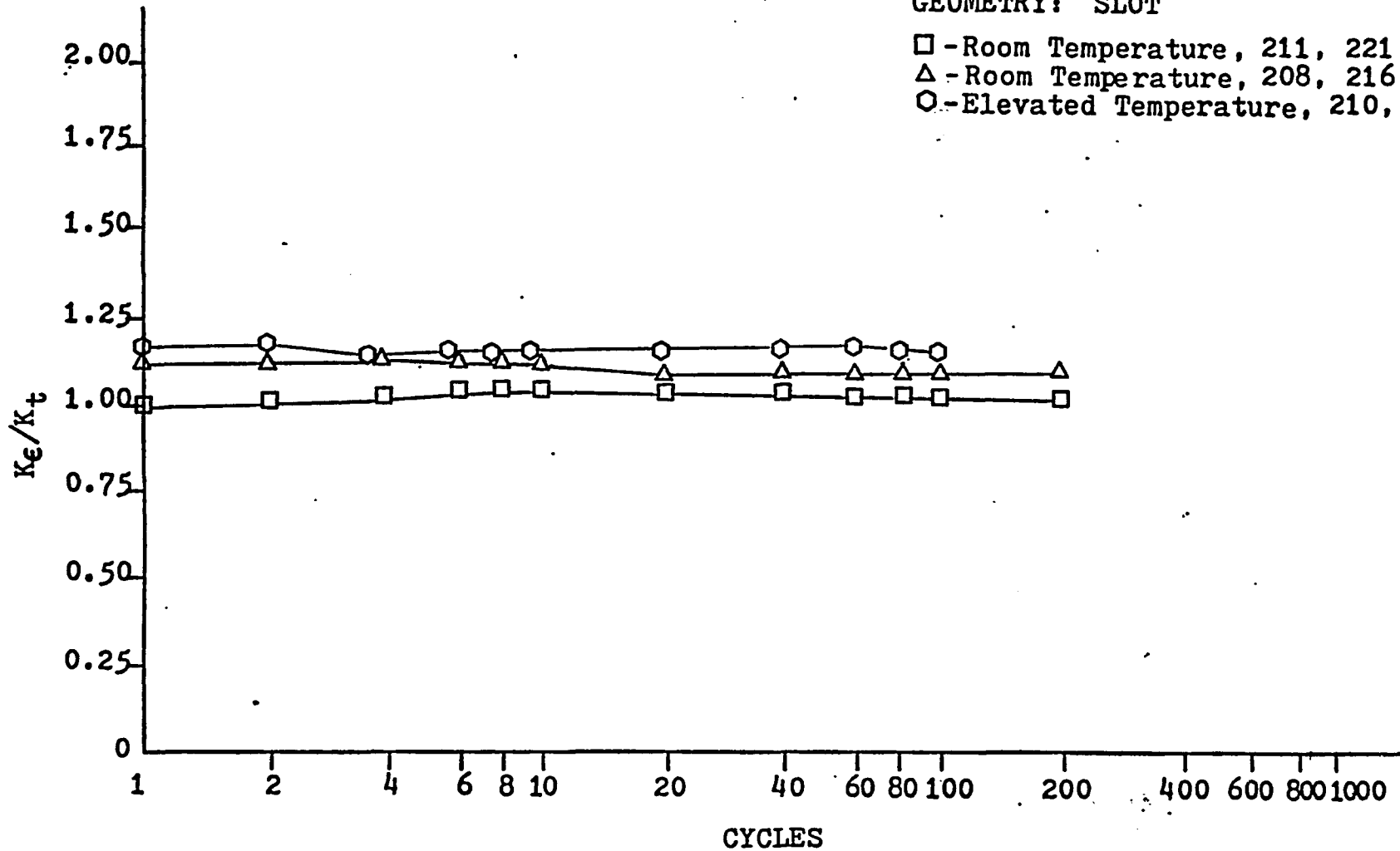


Figure 6.11.. AL 2024 - Slot - Strain Concentration vs. Cycles



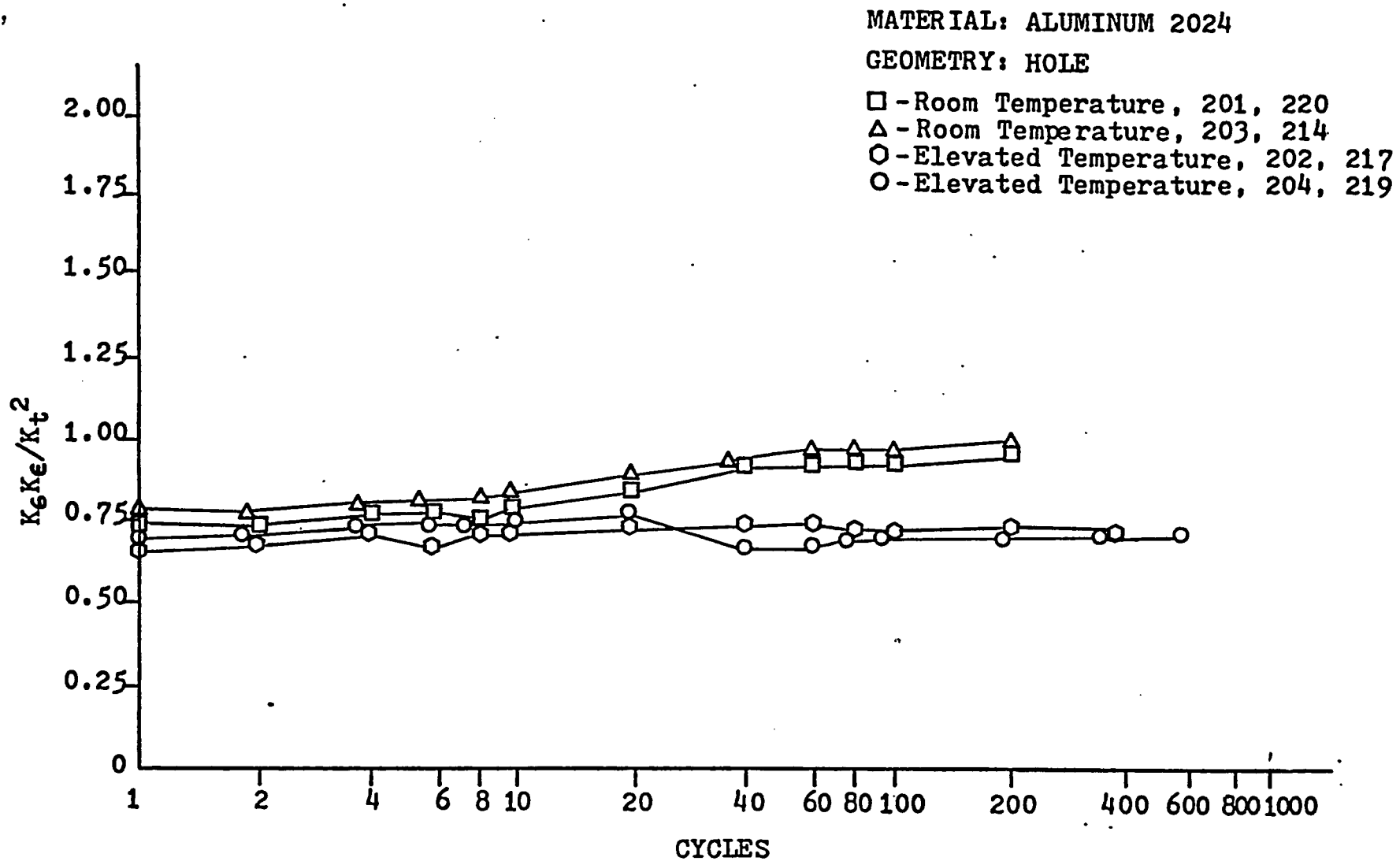


Figure 6.12. AL 2024 - Hole - Neuber's Parameter vs. Cycles

MATERIAL: ALUMINUM 2024

GEOMETRY: SLOT

□ - Room Temperature, 211, 221

△ - Room Temperature, 208, 216

○ - Elevated Temperature, 210, 218

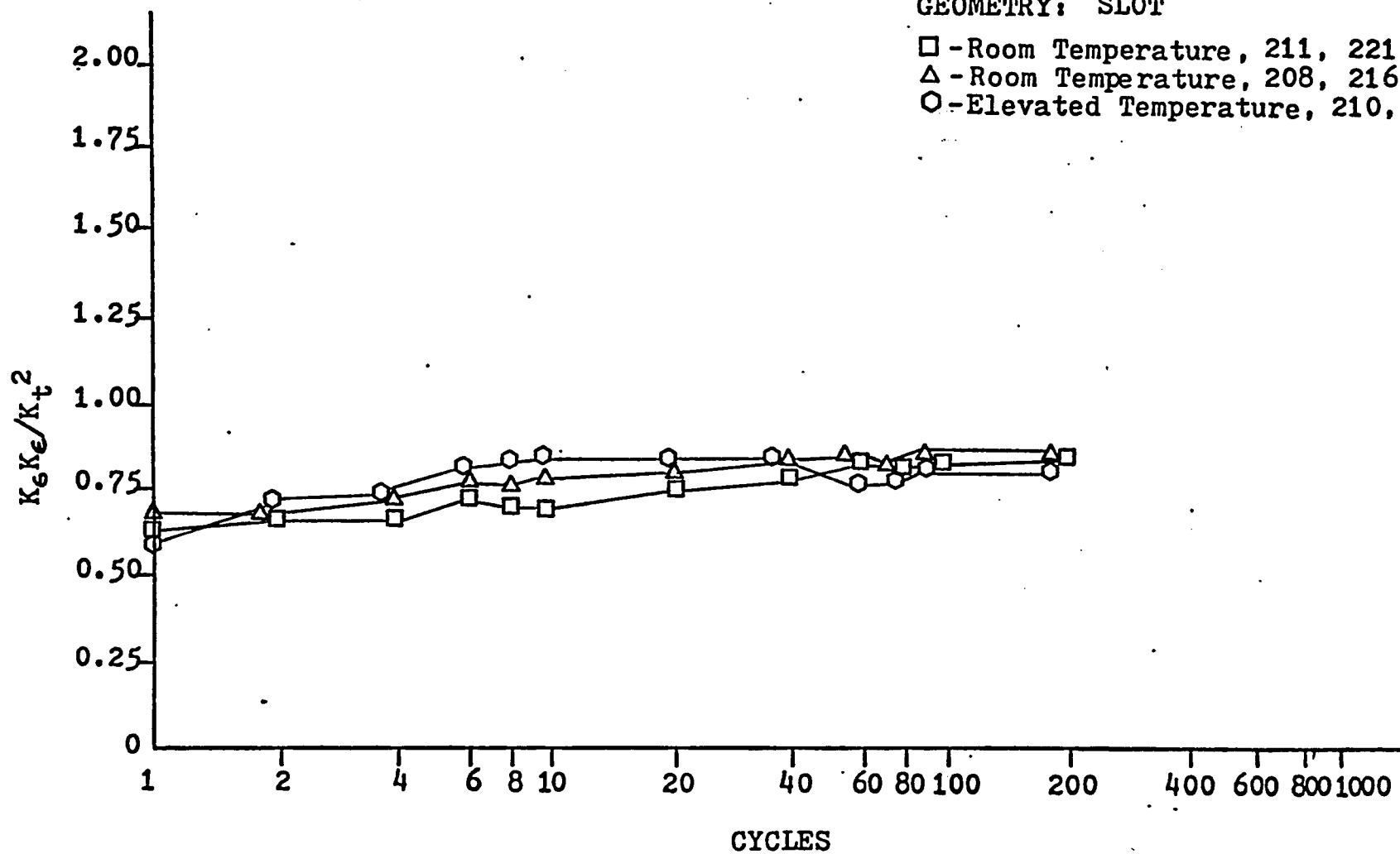


Figure 6.13. AL 2024 - Slot - Neuber's Parameter vs. Cycles

MATERIAL: STEEL 1018

GEOMETRY: HOLE

□ - Room Temperature, 109, 116

△ - Room Temperature, 112, 113

○ - Elevated Temperature, 111, 119

○ - Elevated Temperature, 110, 117

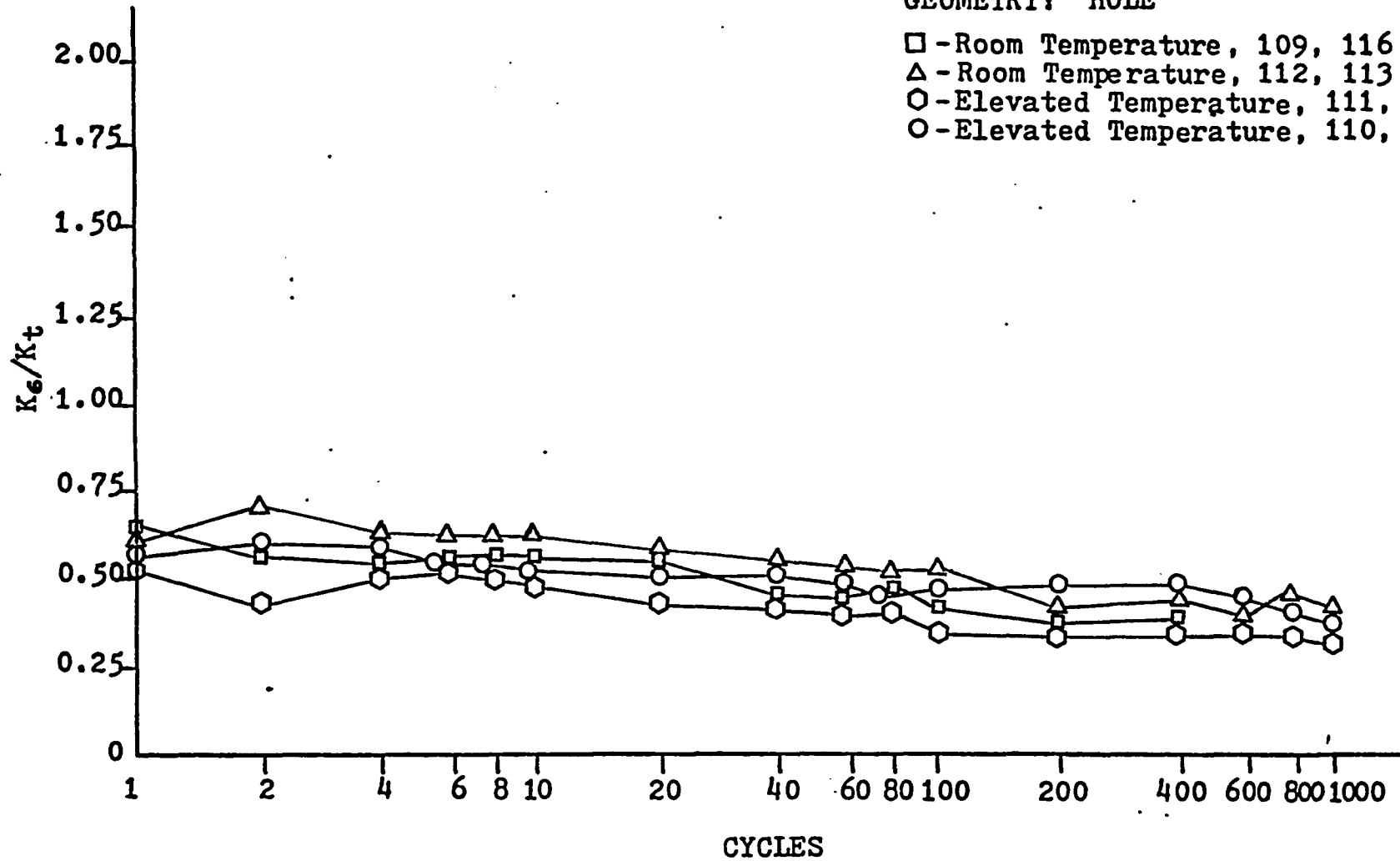


Figure 6.14. CRS 1018 - Hole - Stress Concentration vs. Cycles

MATERIAL: STEEL 1018

GEOMETRY: SLOT

□ - Room Temperature, 103, 114

△ - Room Temperature, 102, 115

○ - Elevated Temperature, 104, 118

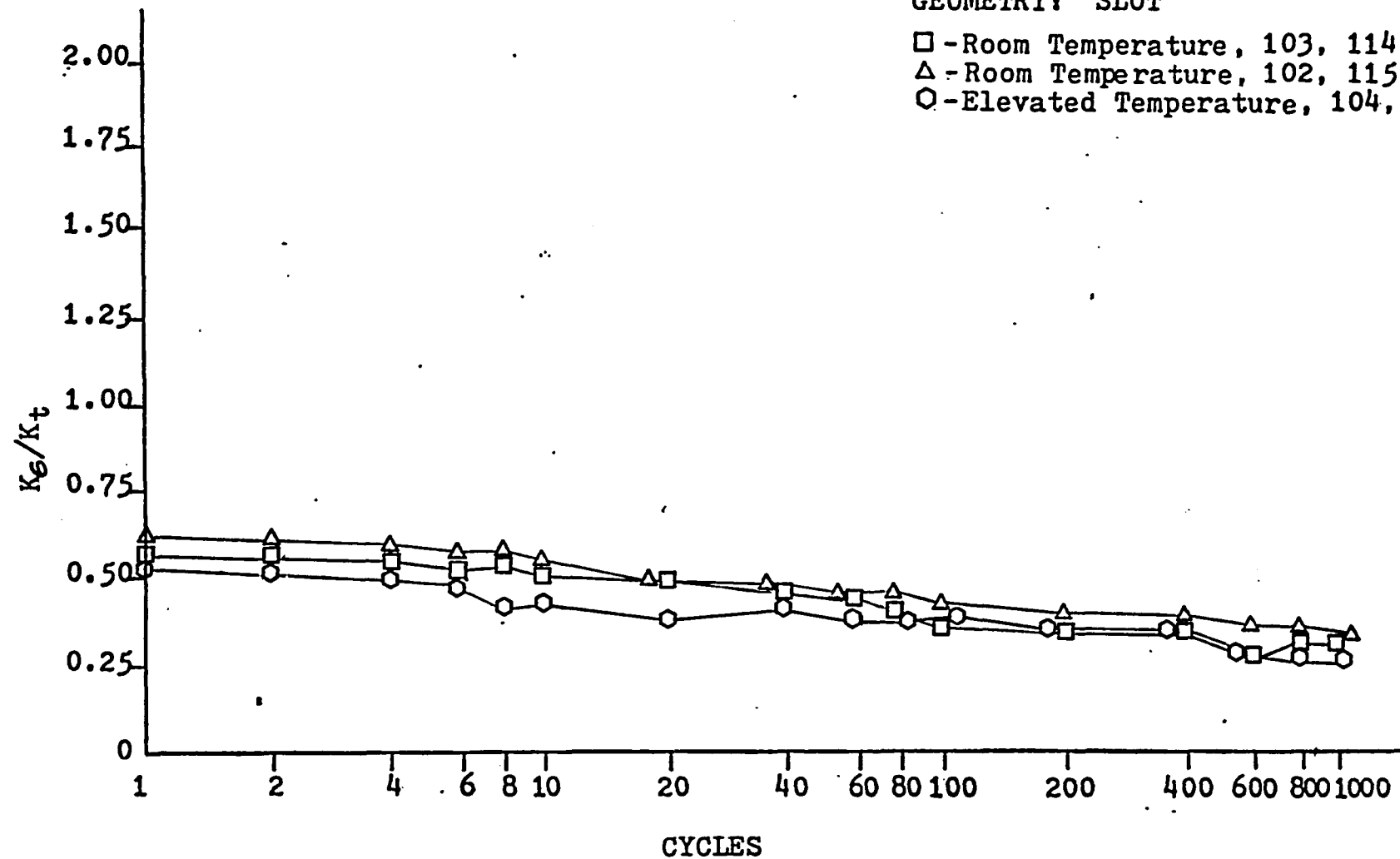


Figure 6.15. CRS 1018 - Slot - Stress Concentration vs. Cycles

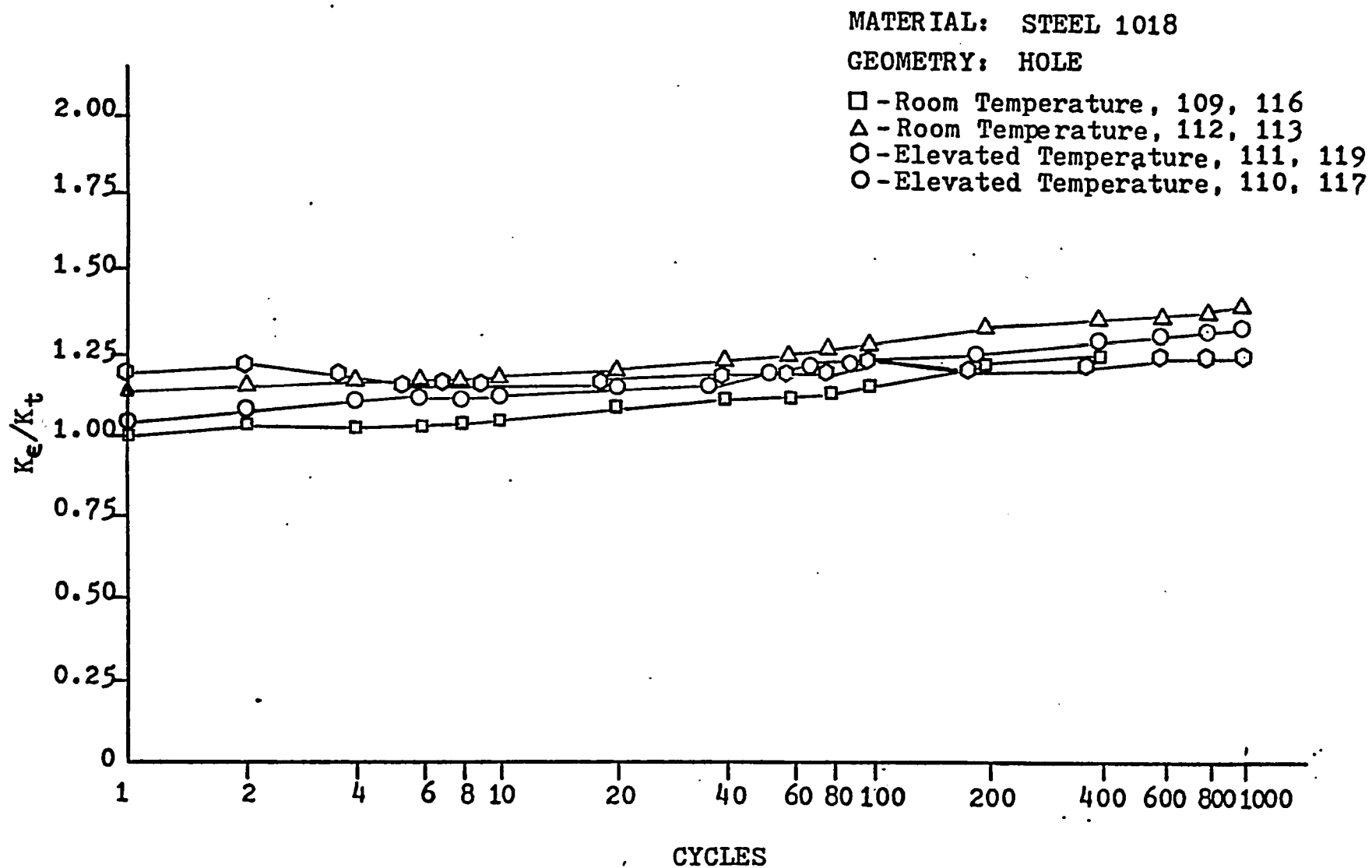


Figure 6.16. CRS 1018 - Hole - Strain Concentration vs. Cycles

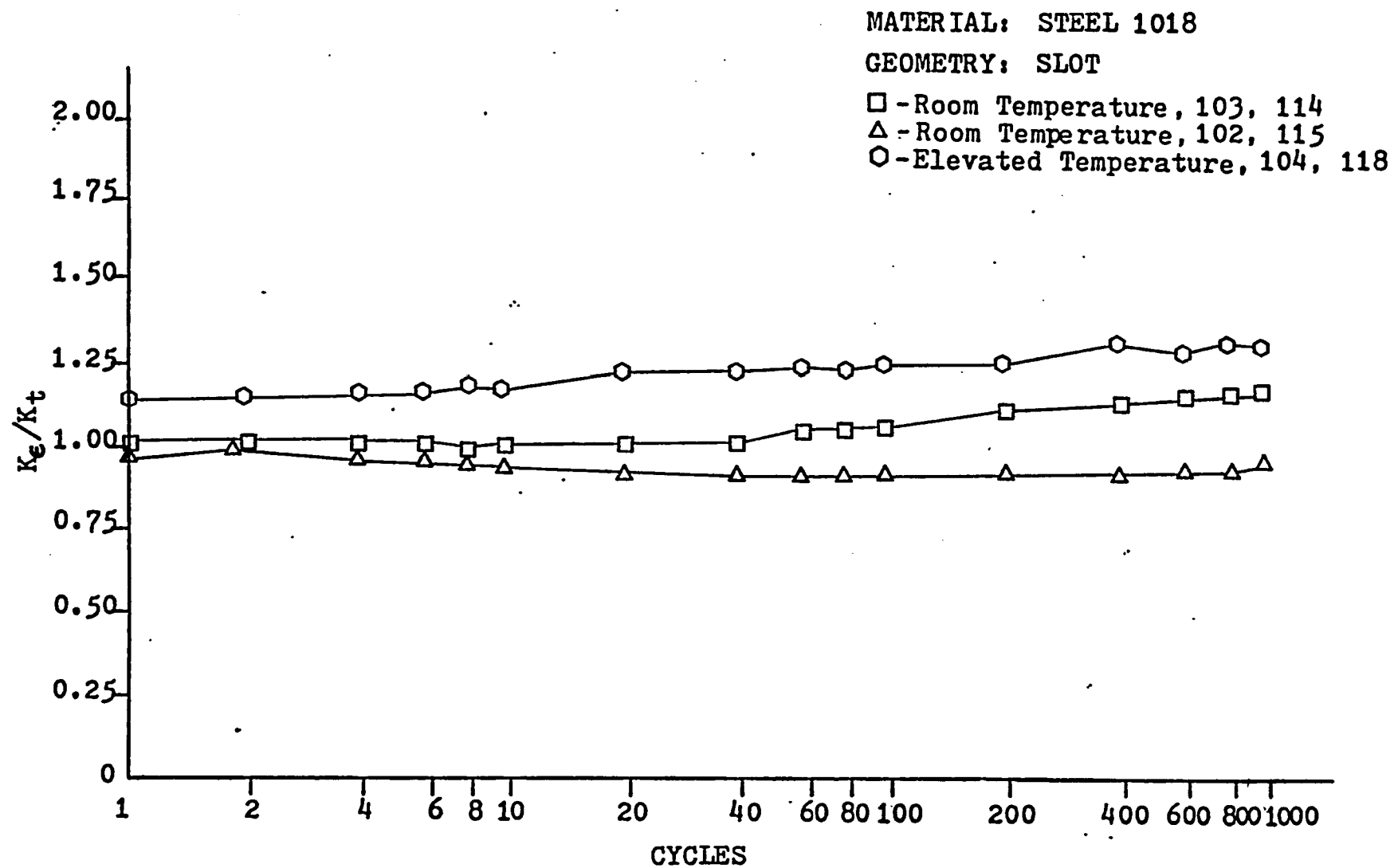


Figure 6.17. CRS 1018 - Slot - Strain Concentration vs. Cycles

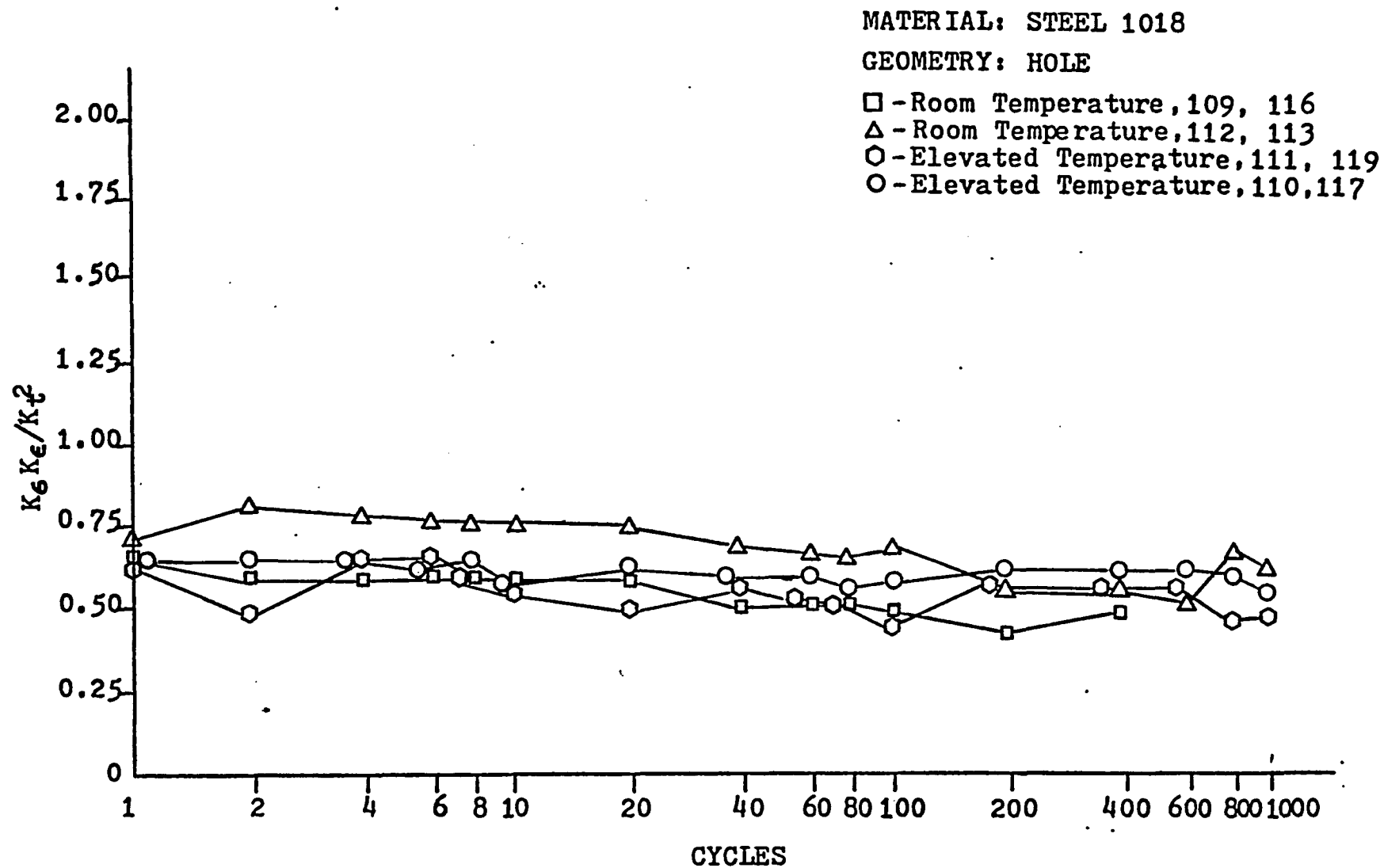


Figure 6.18. CRS 1018 - Hole - Neuber's Parameter vs. Cycles

MATERIAL: STEEL 1018

GEOMETRY: SLOT

□ - Room Temperature, 103, 114

△ - Room Temperature, 102, 115

○ - Elevated Temperature, 104, 118

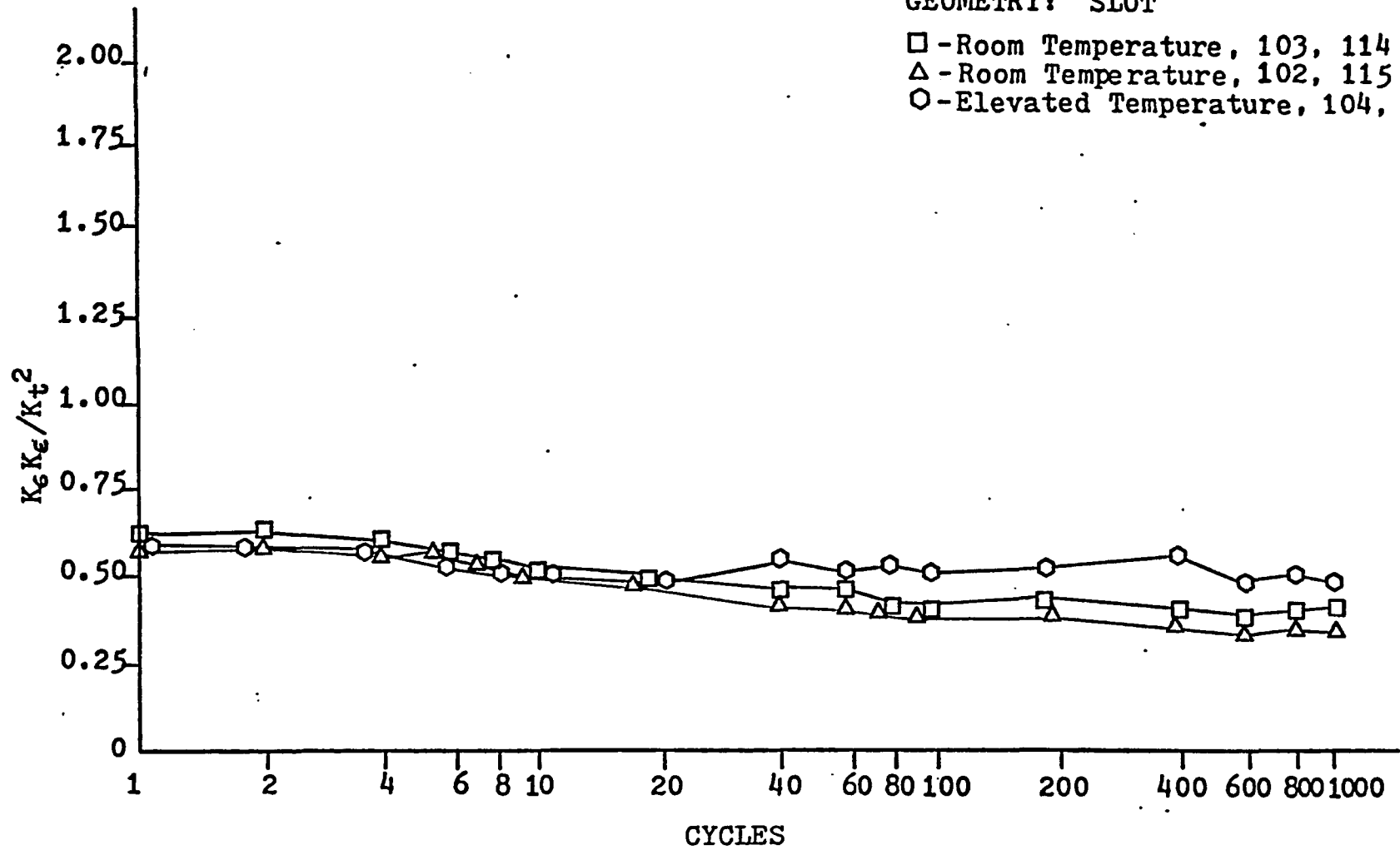


Figure 6.19. CRS 1018 - Slot - Neuber's Parameter vs. Cycles



MATERIAL: ALUMINUM 7475

GEOMETRY: HOLE

□ - Room Temperature, 705, 717

△ - Room Temperature, 712, 714

○ - Elevated Temperature, 708, 718

○ - Elevated Temperature, 709, 720

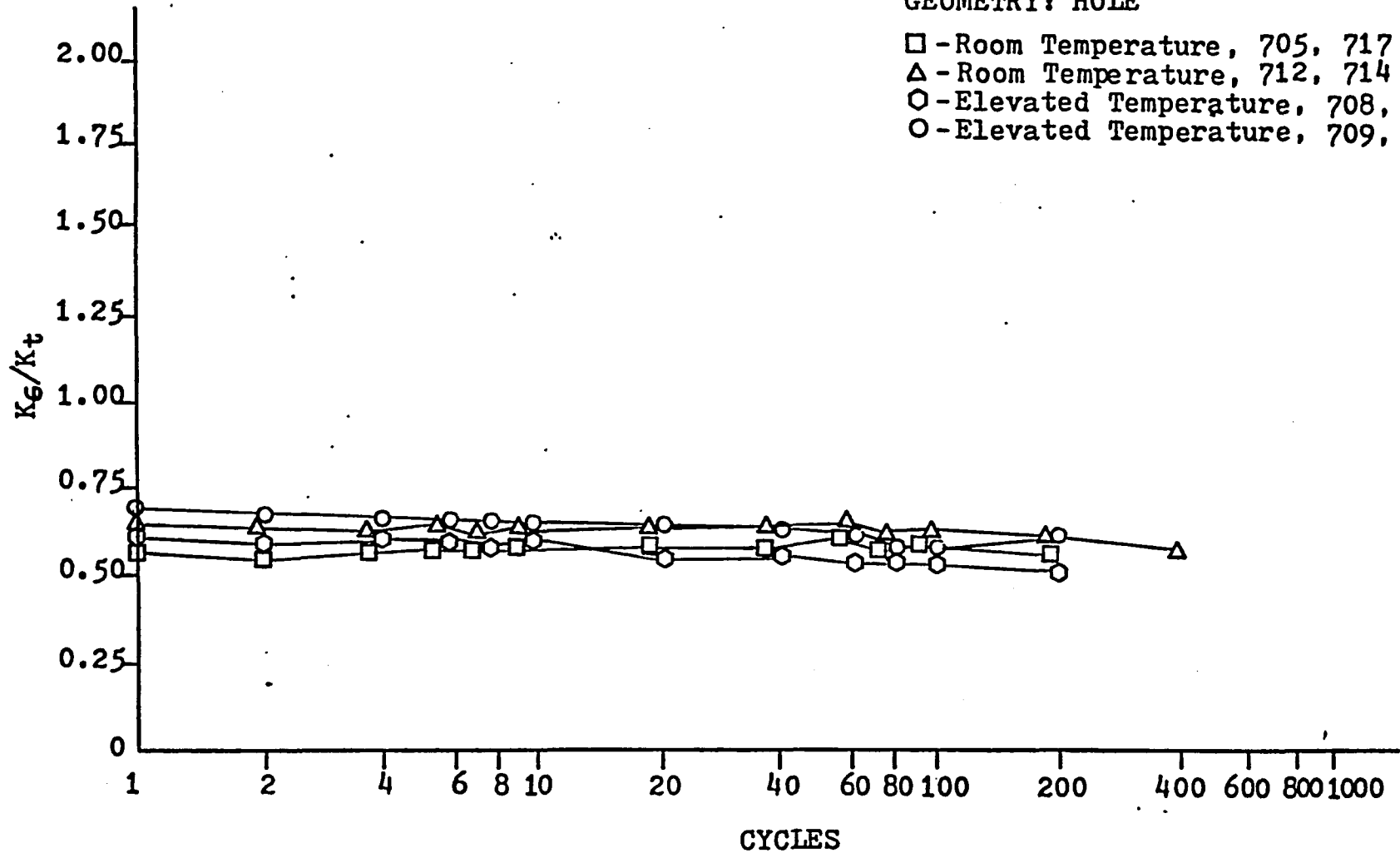


Figure 6.20. AL 7475 - Hole - Stress Concentration vs. Cycles

MATERIAL: ALUMINUM 7475

GEOMETRY: SLOT

□ - Room Temperature, 702, 716

△ - Room Temperature, 704, 715

○ - Elevated Temperature, 703, 719

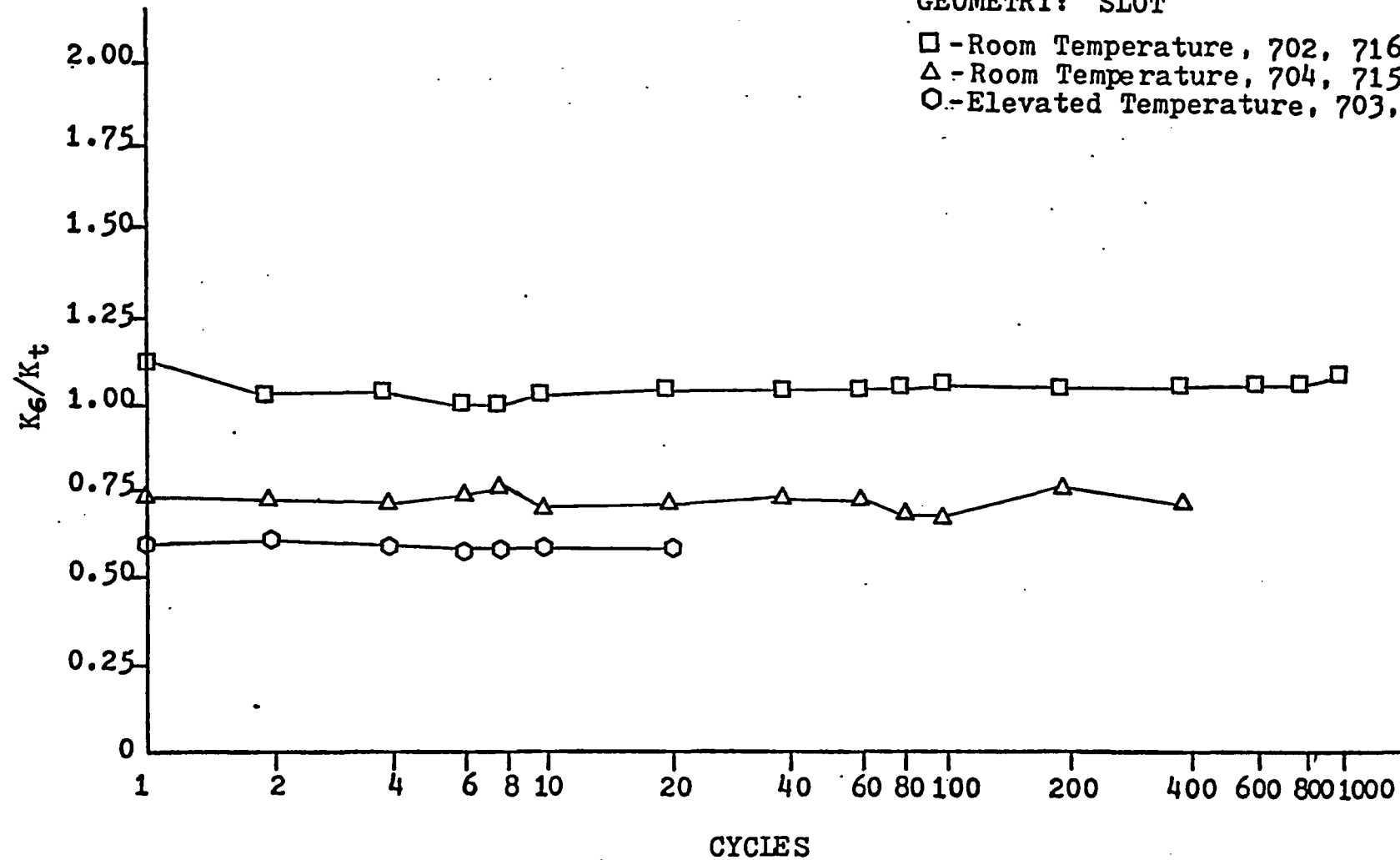


Figure 6.21. AL 7475 - Slot - Stress Concentration vs. Cycles

MATERIAL: ALUMINUM 7475

GEOMETRY: HOLE

□ - Room Temperature, 705, 717

△ - Room Temperature, 712, 714

○ - Elevated Temperature, 708, 718

○ - Elevated Temperature, 709, 720

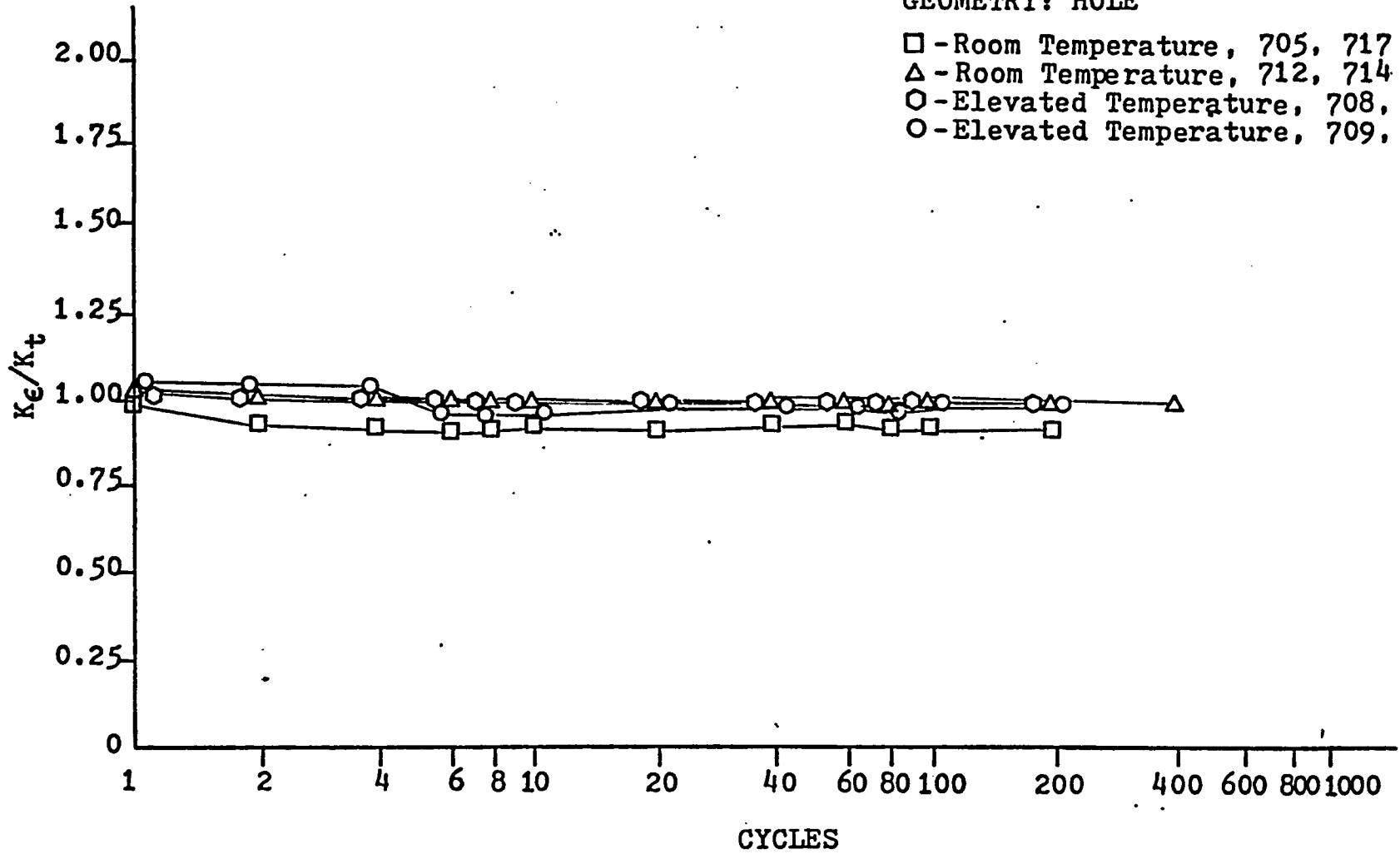


Figure 6.22. AL 7475 - Hole - Strain Concentration vs. Cycles

MATERIAL: ALUMINUM 7475

GEOMETRY: SLOT

□ - Room Temperature, 702, 716

△ - Room Temperature, 704, 715

○ - Elevated Temperature, 703, 719

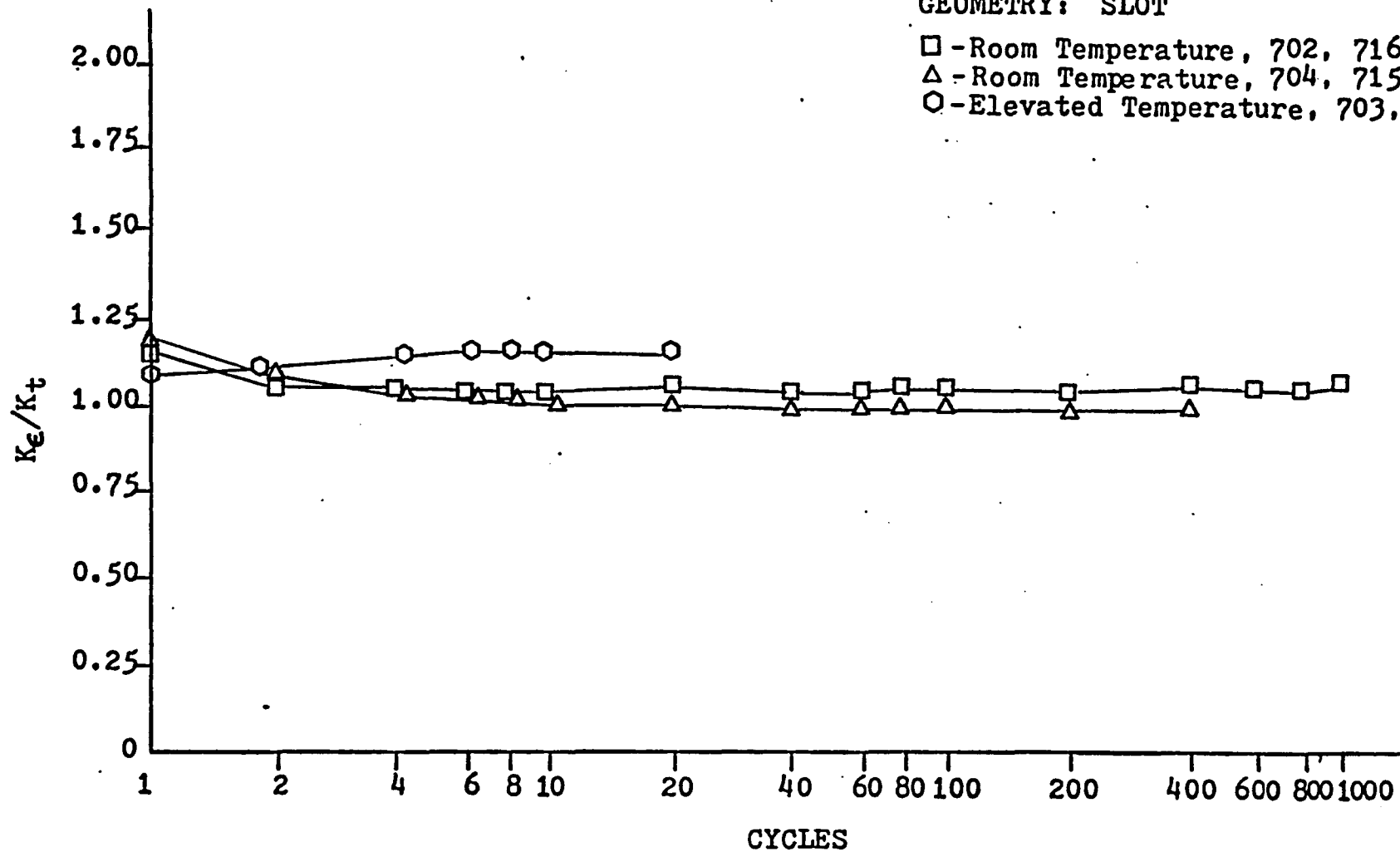


Figure 6.23. AL 7475 - Slot - Strain Concentration vs. Cycles

MATERIAL: ALUMINUM 7475

GEOMETRY: HOLE

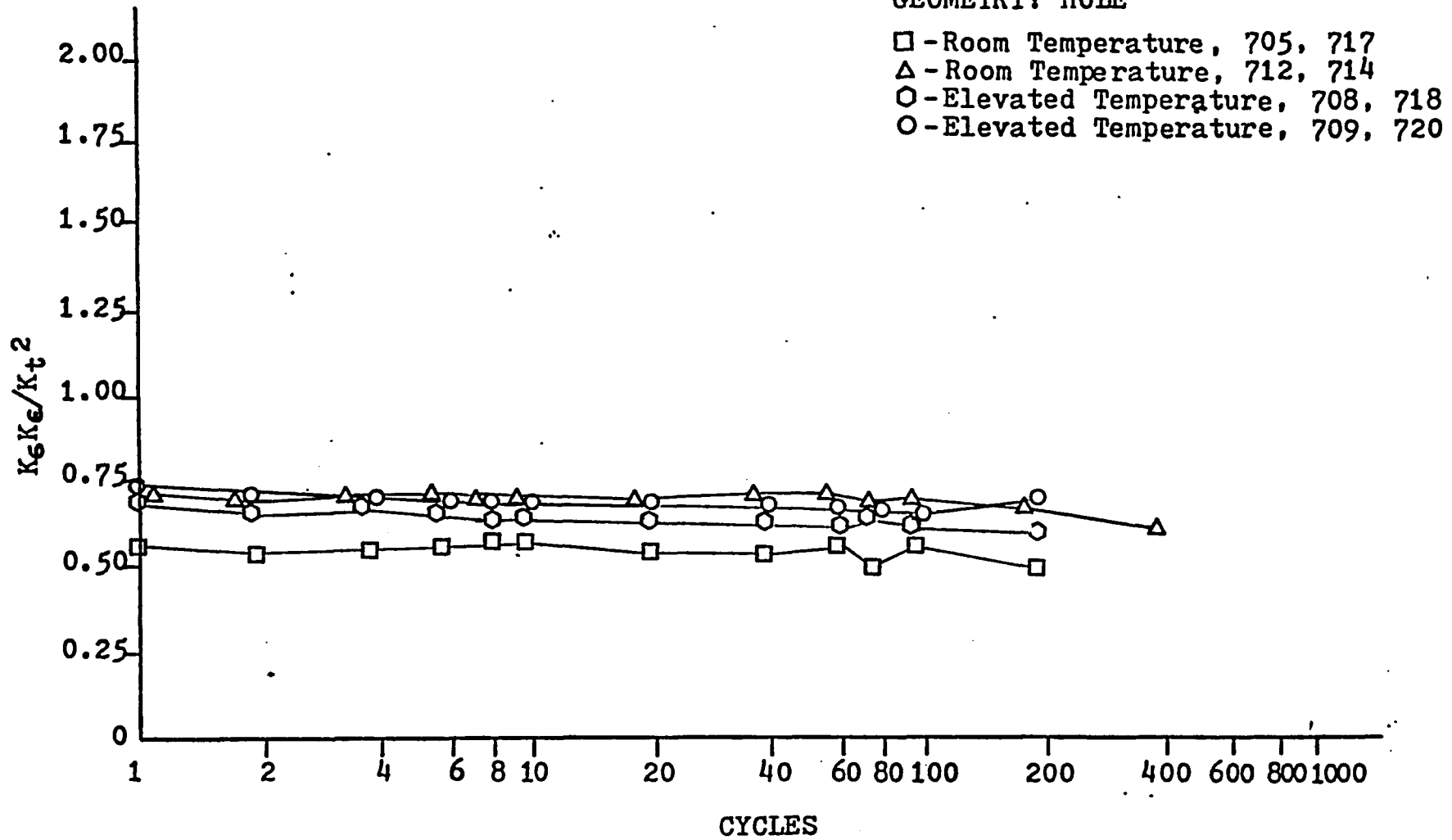


Figure 6.24. AL 7475 - Hole - Neuber's Parameter vs. Cycles

MATERIAL: ALUMINUM 7475

GEOMETRY: SLOT

□ - Room Temperature, 702, 716

△ - Room Temperature, 704, 715

○ - Elevated Temperature, 703, 719

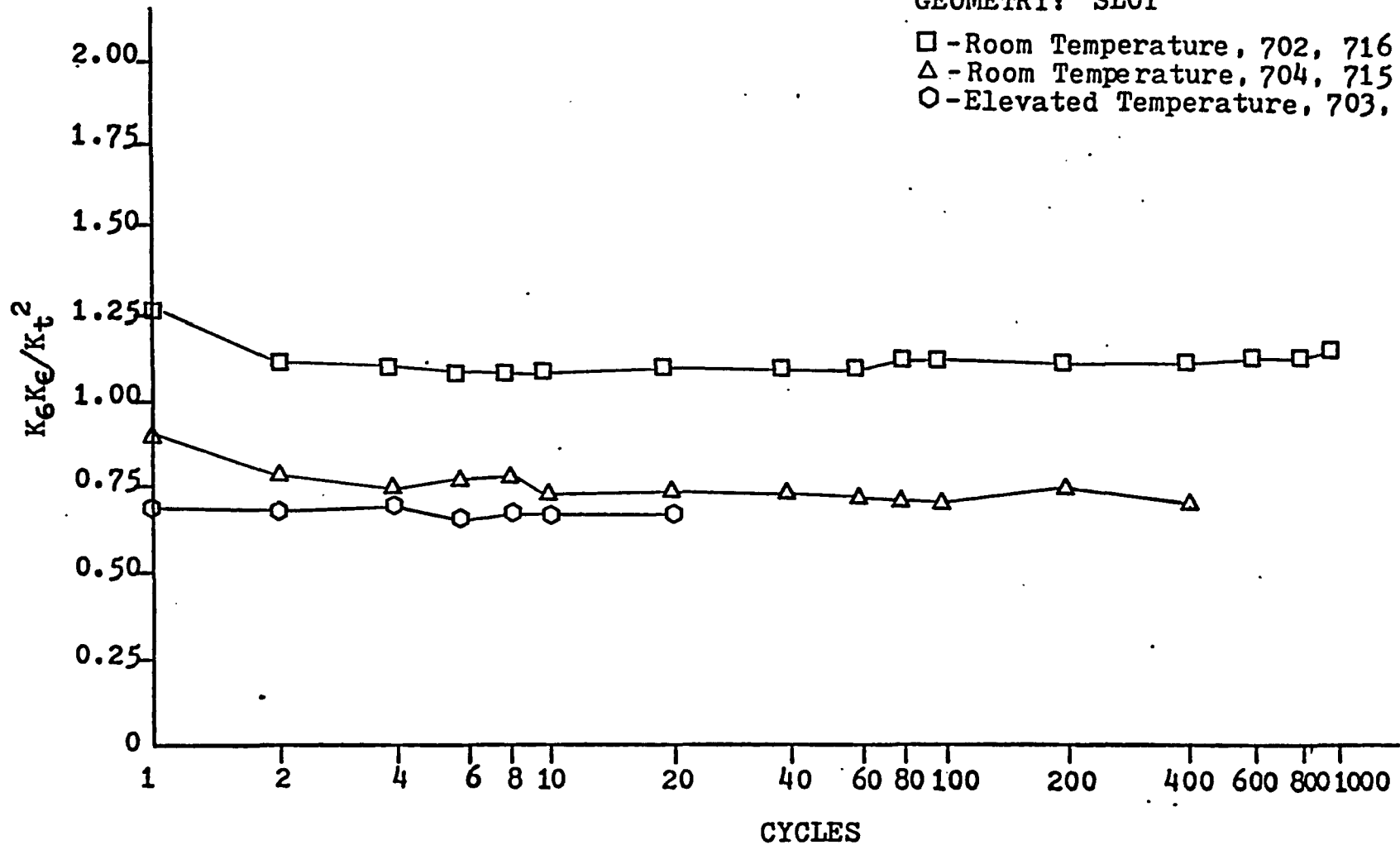


Figure 6.25. AL 7475 - Slot - Neuber's Parameter vs. Cycles

section in which the stress concentration factor dropped off considerably as the material at the notch became nonlinear. Since these cyclic values are taken at the points of maximum load where the material in the vicinity of the notch has gone beyond the elastic range, the stress concentrations are expected to be below the theoretical value. Third, the strain concentration factor remains nearly equal to one at all times. This is also in agreement with the findings of the previous section. Finally, the normalized Neuber's parameter is below 1.0 in all but one case.

### 6.6 Fatigue Notch Factor Versus Cycles

The last section evaluated Neuber's basic ideas when applied to cyclic loading; however, no allowance was made for the generally known fact that both the notch geometry and material greatly affect the fatigue strength of a part. In this section a brief look is taken at what happens when such things are considered. This is accomplished by obtaining a fatigue notch factor from the stress concentration factor measured during the calibration test. The fatigue notch sensitivity of a material and geometry relate the stress concentration factor to the fatigue notch factor. Peterson defines this relationship in the following formula:

$$K_f = q(K_t - 1) + 1 \quad 6.1$$

where,  $K_f$  = fatigue notch factor

$K_t$  = stress concentration factor

$q$  = fatigue notch sensitivity

The best method for arriving at a value of the notch sensitivity is by testing both notched and unnotched specimens of the material in question. However, this technique is really not that practical, so other means of approximating notch sensitivity have been defined. One of

the more popular techniques is given by Peterson in the formula shown below:

$$q = \frac{1}{1 + a/r} \quad 6.2$$

where,  $a$  = material constant

$r$  = notch radius

For the three materials used,  $a = 0.02$  for both aluminums and  $a = 0.0092$  for the 1018 steel. Figure 6.26 plots Neuber's parameter versus cycles for a 2024 aluminum specimen containing a hole. However, the Neuber's parameter is not normalized using the stress concentration factor, instead a horizontal line is drawn across the graph representing the stress concentration factor. This factor was then used in equations 6.1 and 6.2 to compute a fatigue notch factor which is also plotted in Figure 6.26. The same data is plotted for both a 1018 steel specimen and a 7475 aluminum specimen on Figures 6.27 and 6.29 respectively.

These three plots are generally representative of the other data obtained for all specimens containing holes and the steel specimens containing the keyhole slot geometry. Figure 6.26 shows that Neuber's parameter slightly exceeds the fatigue notch factor after approximately twenty cycles, but it is always below the stress concentration factor. In the other two plots Neuber's parameter is always below the fatigue notch factor. For these cases, the use of the fatigue notch factor in Neuber's cyclic rule generally produces better results than the use of the stress concentration factor. However, when the same analysis is performed on the keyhole slot data for either of the aluminum materials, the results are quite different. Figure 6.29 shows a plot of a 2024 aluminum specimen containing a keyhole slot, which is typical for all aluminum



MATERIAL: Aluminum 2024  
GEOMETRY: Hole  
TEMPERATURE: Room  
SPECIMEN NUMBER: 201, 220

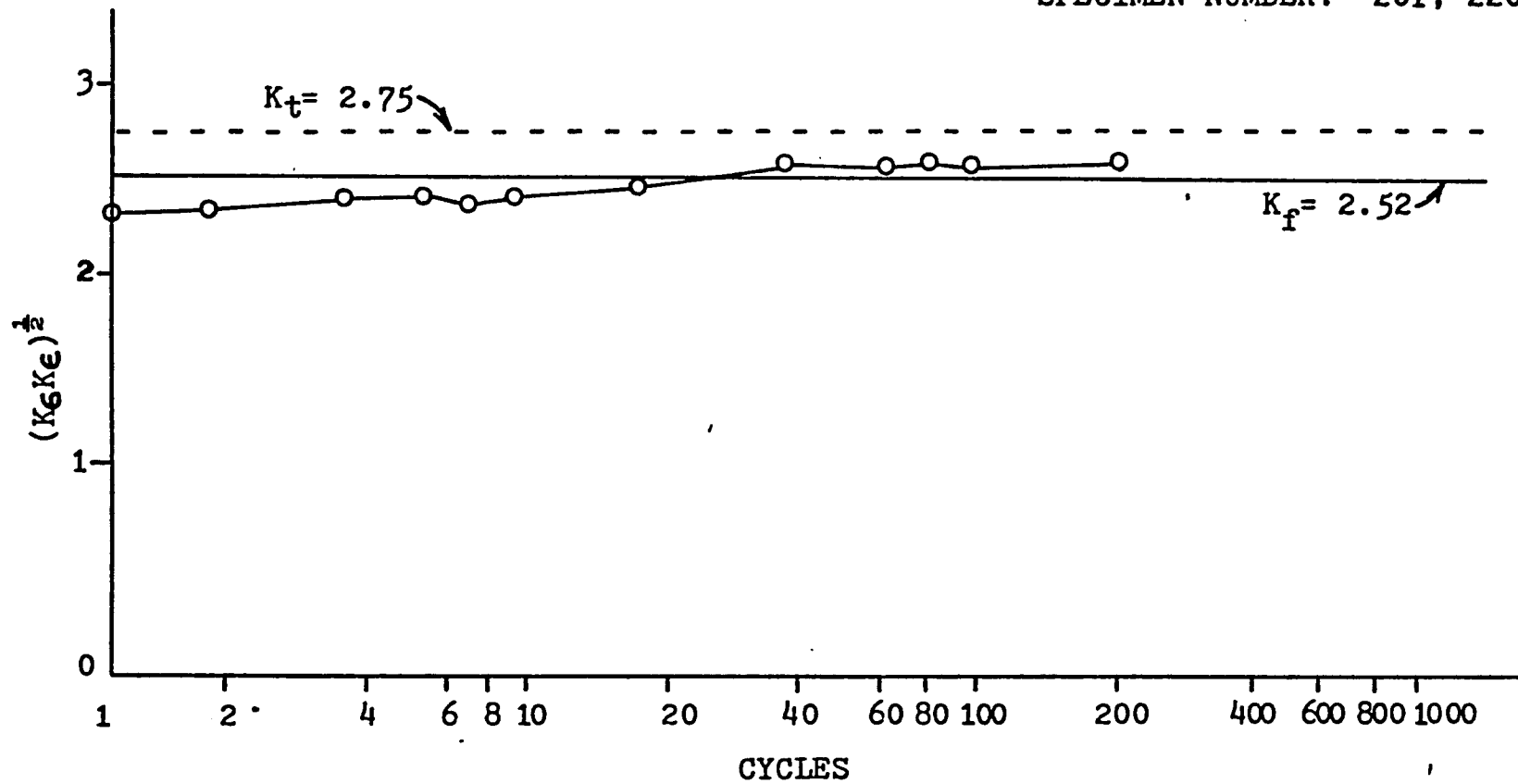


Figure 6.26. Neuber's Parameter vs. Fatigue Notch Factor - AL 2024

MATERIAL: Steel 1018  
GEOMETRY: Hole  
TEMPERATURE: Room  
SPECIMEN NUMBER: 112, 113

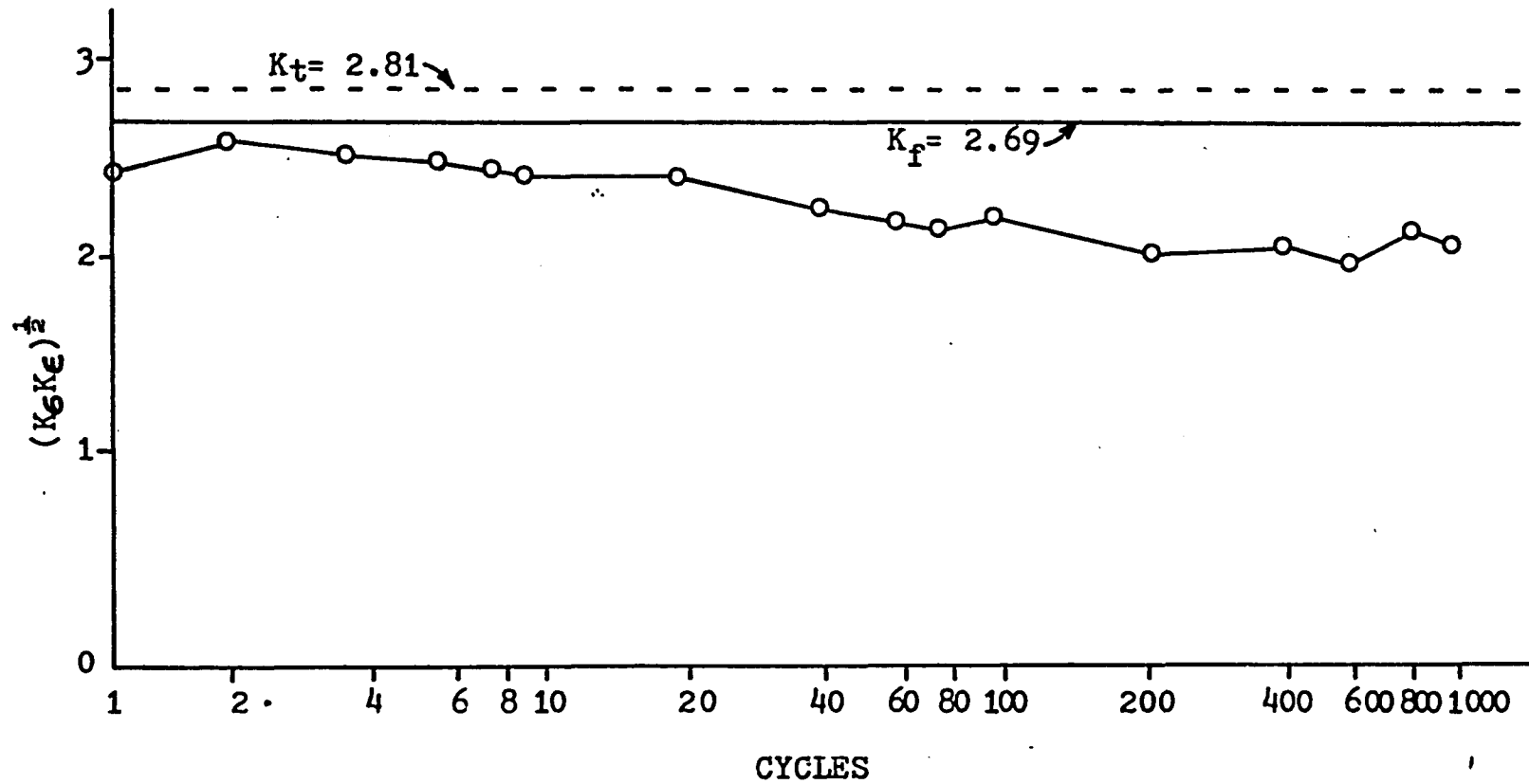


Figure 6.27. Neuber's Parameter vs. Fatigue Notch Factor - Steel 1018

MATERIAL: Aluminum 7475  
GEOMETRY: Hole  
TEMPERATURE: Room  
SPECIMEN NUMBER: 712, 714

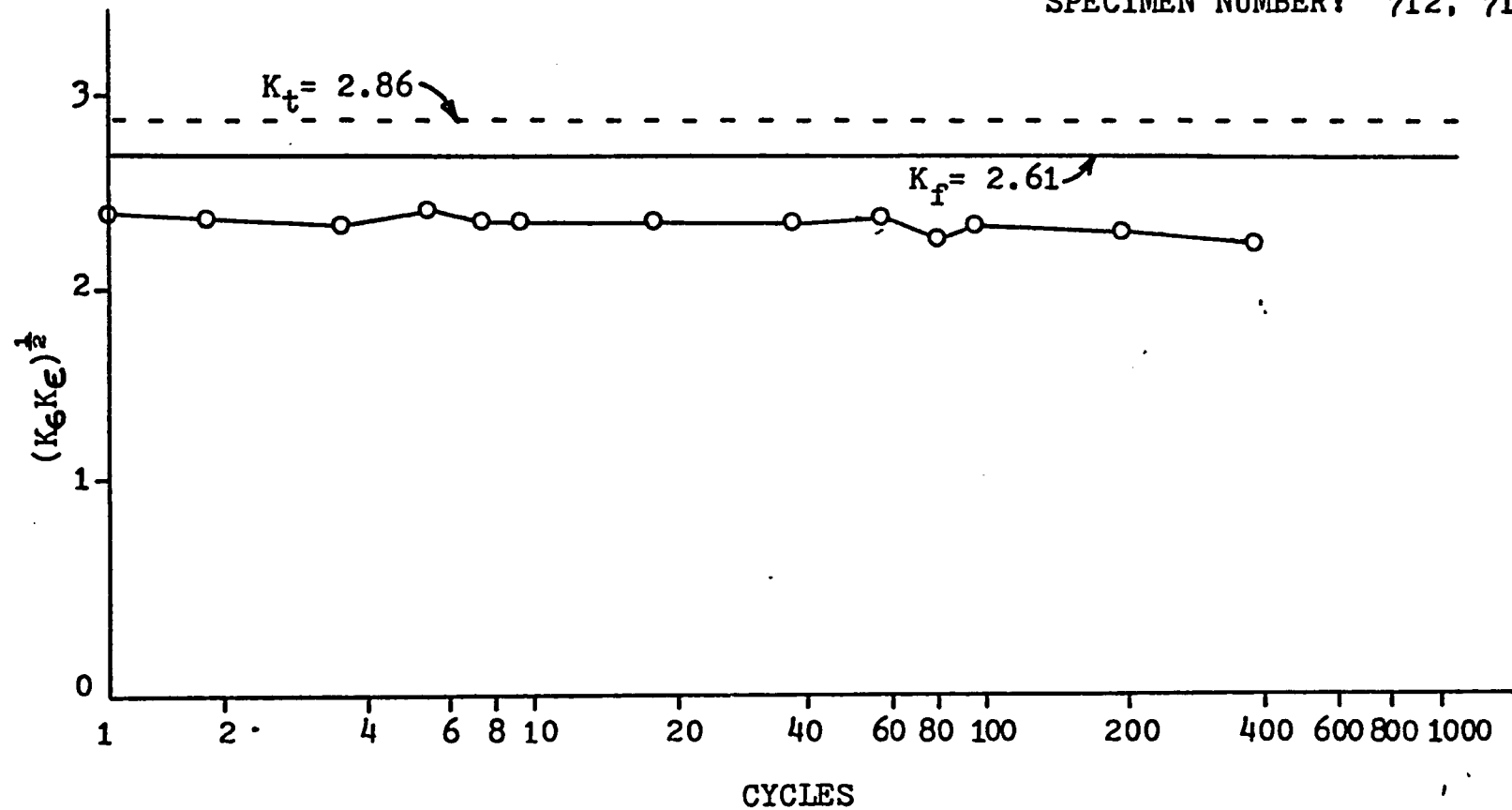


Figure 6.28. Neuber's Parameter vs. Fatigue Notch Factor - AL-7475

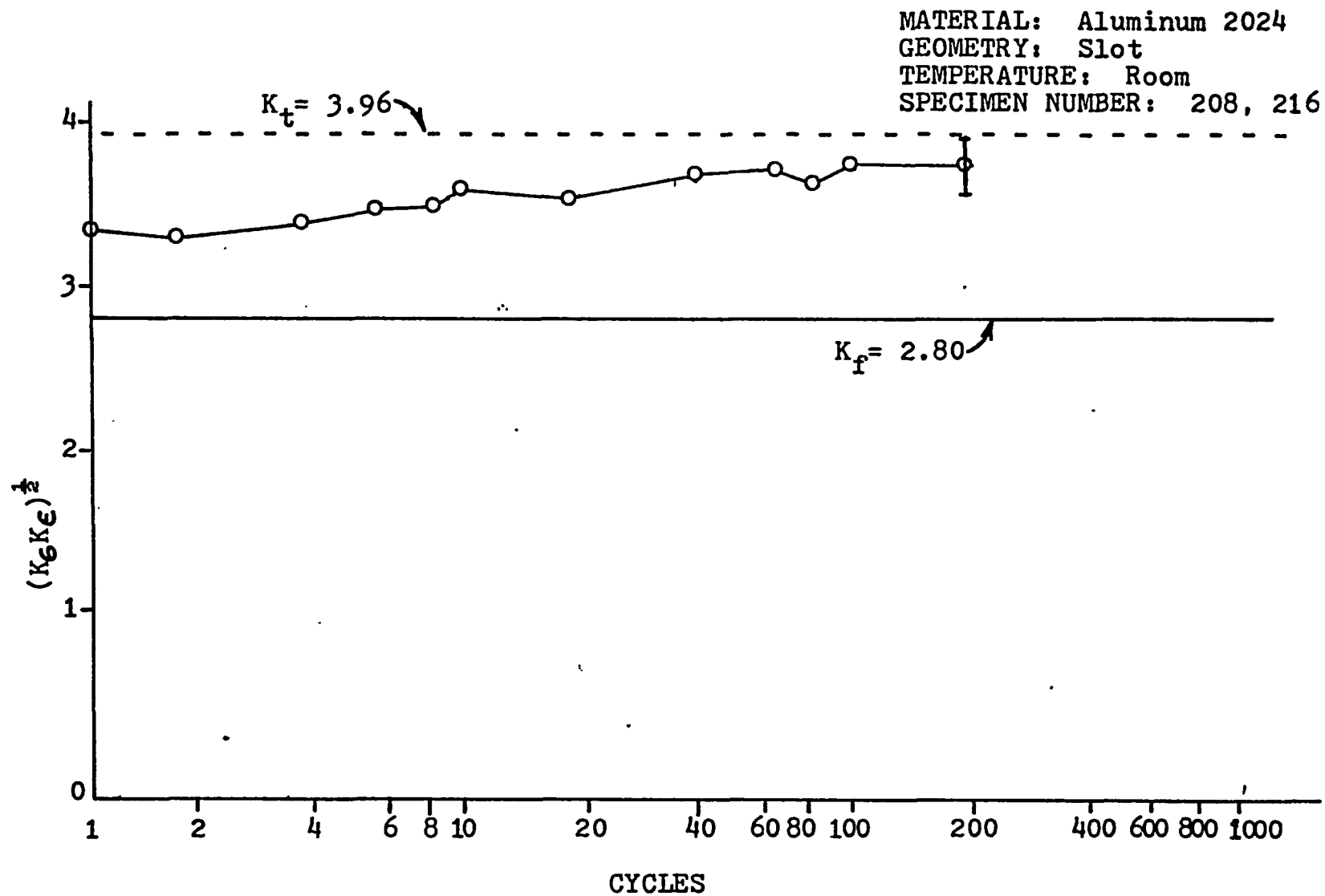


Figure 6.29. Neuber's Parameter vs. Fatigue Notch Factor - AL-2024

specimens containing the same notch geometry. This figure reveals that Neuber's parameter exceeds the fatigue notch factor at every point and by as much as 30%, but it never exceeds the stress concentration factor. This implies that the use of the fatigue notch factor in place of the theoretical stress concentration factor in Neuber's cyclic rule will not always yield conservative results, especially when sharp notches are considered.

As a final point, the significance of experimental error is addressed. In the previous chapter, the error was determined to be  $\pm 4\%$  for the notch strain measurement and  $\pm 2\%$  for the notch stress measurement. Also, a  $\pm 4\%$  error for general misalignment was included. This latter error was added to that for the notch strain measurement and used in computing the error band for the data in Figure 6.29. This error band was found to be  $\pm 5\%$  and is displayed by a bar on the last data point of Figure 6.29.

## CHAPTER VII

### CONCLUSIONS

The preceding chapters have described a series of fatigue tests which were conducted using specimens of three different materials, containing two notch geometries and tested at two temperatures. Based upon the data recorded during these tests and presented in this work, the following conclusions are drawn.

First, Neuber's cyclic rule should be evaluated using the theoretical stress concentration factor rather than the fatigue notch factor to insure conservative results. Test data tabulated in the previous chapter showed that near a sharp notch, the geometric mean of the stress and strain concentration factors could be greater than the fatigue notch factor; therefore, for design purposes no consideration should be given to the notch sensitivity of a particular material.

Second, Neuber's cyclic rule, when applied to notched specimens undergoing completely reversed cyclic loading, generally yields conservative results. The basis for this conclusion was that within the range of experimental error, the data from all twenty-one cyclic tests supported Neuber's rule. These tests were conducted in three materials which were cyclicly hardening, cyclicly softening and cyclicly stable. Each material contained two different notch geometries with stress concentration factors of 3.1 and 5.82. Also, each material and notch geometry was tested at both room temperature and a moderately elevated

temperature. Since Neuber's cyclic rule yielded conservative results for every combination of these three parameters, it is considered to apply in general.

Third, the interferometric strain gage is ideally suited for measuring large strains near notches on materials undergoing cyclic loading at room and elevated temperature. Essentially no problems were encountered with the ISG during the entire notched specimen testing program. Also, duplication of tests showed that the system had good repeatability.

## BIBLIOGRAPHY

1. "Standard Definitions of Terms Relating to Fatigue Testing and the Statistical Analysis of Fatigue Data," Part 10, 1976 Annual Book Of ASTM Standards. Philadelphia: American Society for Testing and Materials, 1976.
2. Neuber, H. "Theory of Stress Concentration for Shear-Strained Prismatical Bodies With Arbitrary Nonlinear Stress-Strain Law," Journal of Applied Mechanics, 28(1961), 544-550.
3. U. S. Joint Publications Research Service, trans., Theory of Notch Stresses: Principles for Exact Calculations of Strength With Reference to Structural Form and Material, by Heinz Neuber. Washington, D.C.: Office of Technical Services, 1961.
4. Topper, T. H., R. M. Wetzell, and JoDean Morrow. "Neuber's Rule Applied to Fatigue of Notched Specimens," Journal of Materials, 4(1969), 200-209.
5. Leis, B. N., C. V. B. Gowda, and T. H. Topper. "Some Studies of the Influence of Localized and Gross Plasticity on the Monotonic and Cyclic Concentration Factor," Journal of Testing and Evaluation, 1(1973), 341-348.
6. Crews, J. H., and H. F. Hardrath. "A Study of Cyclic Plastic Stresses at a Notch Root," Experimental Mechanics, 6(1966), 313-320.
7. Krempl, E. E. "Influence of Stress/Strain Concentration and Mean Stress on the Low-Cycle Fatigue Behavior of Three Structural Steels at Room Temperature," GEAP-5726 (1968).
8. Krempl, E. E. "The 550°F Notched High-Strain Fatigue Behavior of Three Low-Strength Structural Steels," GEAP-10090 (1969).
9. Krempl, E. E. "The Effect of Stress Concentration on the Low-Cycle Fatigue of Three Low-Strength Structural Steels at Room Temperature and 550°F," GEAP-10170 (1970).
10. Conle, A. and H. Nowack. "Verification of a Neuber-based Notch Analysis by the Companion-Specimen Method," Experimental Mechanics, 17(1977), 57-63.
11. Bofferding, C. H. "A Study of Cyclic Stress and Strain Concentration Factors at Notch Roots Throughout Fatigue Life," Unpublished Master's thesis, Michigan State University, 1980.



12. Fuchs, H. O., and R. I. Stephens. Metal Fatigue in Engineering. New York: John Wiley and Sons, 1980.
13. A.S.M.E. Boiler and Pressure Vessel Code Case N47-17, New York: American Society of Mechanical Engineers, 1980.
14. Maiya, P. S. "Effects of Notches on Crack Initiation in Low-Cycle Fatigue," Materials Science and Engineering, 38(1979) 289-294.
15. Severud, L. K. "Background to the Elastic Creep-Fatigue Rules of the ASME B & PV Code Case 1592," Nuclear Engineering and Design, 45(1978) 449-455.
16. Peterson, R. E. Stress Concentration Factors. New York: John Wiley and Sons, 1974.
17. Sharpe, W. N., Jr., "Development and Application of an Interferometric System for Measuring Crack Displacements," Final Report on Grant NSG 1148, 1976.

APPENDIX A

STRAIN GAGE SPECIFICATIONS

FOR THE EXTENSOMETER

STRAIN GAGE SPECIFICATIONS  
FOR THE EXTENSOMETER

Strain Gages: Micro-Measurements WK-09-125PC-350

Gage Factor = 2.005

Resistance = 350 ohms

Gage Length = .125 inches

Adhesive: Micro-Measurements M Bond 610

Cure Temperature = 325°F for 1 hour

Postcure Temperature = 550°F for 2 hours

Solder: Micro-Measurements 570-28R

Solidus/Liquidus Temperature = 565/574°F

Lead Wire: Micro-Measurements 126-FWK Stranded silver plated  
copper wire Kapton polyimide  
insulation

Temperature Range: -452 to 600°F

APPENDIX B  
COMPUTER PROGRAM LISTING  
NOTCH6.FOR

```

C
C      NOTCH6.FOR
C
C      THIS PROGRAM CONTROLS BOTH THE ISG AND MTS
C      MACHINE IN A TEST WHICH CYCLICLY LOADS A
C      NOTCHED SPECIMEN AND RECORDS THE STRAIN AT
C      THE NOTCH AND THE REMOTE STRESS AND STRAIN.
C      THIS DATA IS STORED IN A FILE NAMED RESULT.DAT.
C
      INTEGER V1,V2,T1,B1
      INTEGER Q,S6,S5,R6,R5,V3,V4
      DIMENSION NL1(100),NT2(100),NT1(100)
      DIMENSION T1(64),B1(64),V1(64),V2(64),Q(800)
      OPEN (UNIT=1,NAME='SY1:RESULT.DAT',ACCESS='DIRECT',
*      INITIALSIZE=900,RECORDSIZE=91)
      CALL AOUT(0,0,1)
      CALL AOUT(0,1,1)
      CALL AOUT(0,2,1)
      CALL AOUT(0,3,1)
      WRITE(7,11)
11      FORMAT(1X,'HOOK UP MTS MACHINE')
      WRITE(7,10)
10      FORMAT(1X,'NO. OF POINTS PER SCAN')
      READ(5,15)N1
      WRITE(7,*)N1
15      FORMAT(15)
      WRITE(7,20)
20      FORMAT(1X,'NO. OF SCANS PER CYCLE')
      READ(5,15)N2
      WRITE(7,*)N2
      WRITE(7,22)
22      FORMAT(1X,'NO. OF POINTS AVERAGED')
      READ(5,15)NAV

```

```

WRITE(7,*)NAV
WRITE(7,24)
24  FORMAT(1X,'NO. OF INTERMEDIATE LOAD STEPS')
    READ(5,15)NP3
    WRITE(7,*)NP3
    WRITE(7,30)
30  FORMAT(1X,'MIN. LOCATION - CHANNEL 1')
    READ(5,15)NP1
    WRITE(7,*)NP1
    WRITE(7,40)
40  FORMAT(1X,'MIN. SPACING - CHANNEL 1')
    READ(5,15)ND1
    WRITE(7,*)ND1
    WRITE(7,50)
50  FORMAT(1X,'MIN. LOCATION - CHANNEL 2')
    READ(5,15)NP2
    WRITE(7,*)NP2
    WRITE(7,60)
60  FORMAT(1X,'MIN. SPACING - CHANNEL 2')
    READ(5,15)ND2
    WRITE(7,*)ND2
    WRITE(7,65)
65  FORMAT(1X,'CROSS SECTIONAL AREA')
    READ(5,75) AREA
    WRITE(7,*) AREA
    WRITE(7,67)
67  FORMAT(1X,'MODULUS OF ELASTICITY')
    READ(5,76) EM
    EM=EM/1000000.
    WRITE(7,*) EM
76  FORMAT(E10.2)
    WRITE(7,70)
70  FORMAT(1X,'INDENTATION SPACING')

```

```

      READ(5,75)D0
      WRITE(7,*)D0
75    FORMAT(F10.4)
      WRITE(7,80)
80    FORMAT(1X,'REFLECTED ANGLE')
      READ(5,75)A0
      WRITE(7,*)A0
      JF1=N2/4
      N2=JF1*4
      DO 100 J=1,JF1
      DO 100 JK=1,NP3
      I=(NP3*(J-1))+JK
      Z2=I
      Z3=JF1*NP3
      Z1=(Z2/Z3)*2000
      Q(I)=Z1
      Q(I+(NP3*JF1))=2000,-Z1
      Q(I+(2*NP3*JF1))=-Z1
100   Q(I+(3*NP3*JF1))=-2000,+Z1
      CALL ADUT(Q(NP3*N2),2,1)
      S6=NP1*8-1024
      R6=NP2*8-1024
      S0=(ND1+ND2)*4
      A0=A0*3.1416/180.
      C=.6328/(2*D0*S0*SIN(A0))
      S5=S6
      R5=R6
      JT=1
      J8=0
26    FORMAT(1X,5(E13.6,2X))
      DO 250 NY=1,1001
      NC=NY-1
      IF(NC.NE.2)GO TO 32

```

```

WRITE(7,35)
35  FORMAT(1X,'CONTINUE? (Y=1,N=2)')
    READ(5,15)NC9
    IF(NC9.EQ.1)GO TO 32
    STOP
32  WRITE(7,34)NC
34  FORMAT(1X,I5)
    DO 200 NX=1,N2
    DO 210 I=1,N1
    T1(I)=S5-8*((N1/2)-I)
210  B1(I)=R5-8*((N1/2)-I)
    DO 220 J=1,N1
    CALL ADUT(T1(J),0,1)
    CALL ADUT(B1(J),1,1)
    CALL AIN(V1(J),0,1)
    CALL AIN(V2(J),1,1)
220  CONTINUE
    JS=N1/2
    CALL ADUT(T1(JS),0,1)
    CALL ADUT(B1(JS),1,1)
    CALL AIN(NL1(NX),3,1)
    NT2(NX)=(NL1(NX)*10)/(AREA*EH)
    IF(J8.NE.1)GO TO 560
    K=(NX-1)*NP3
    DO 230 NS=1,NP3
    CALL ADUT(Q(K+NS),2,1)
230  CONTINUE
560  M3=0
    N3=0
    DO 563 KJ=1,NAV
    M3=V1(KJ)+M3
563  N3=V2(KJ)+N3
    V3=M3

```



```

V4=N3
S5=T1(1)
R5=B1(1)
N9=N1-NAV-1
DO 240 KK=2,N9
V3=V3+V1(KK+NAV-1)-V1(KK-1)
V4=V4+V2(KK+NAV-1)-V2(KK-1)
IF(V3.GE.N3)GO TO 620
M3=V3
S5=T1(KK)
620 IF(V4.GE.N3)GO TO 650
N3=V4
R5=B1(KK)
650 CONTINUE
240 CONTINUE
S1=((S6-S5)+(R5-R6))*C*1000000.
C WRITE(7,95)S5,S6,R5,R6,S1
95 FORMAT(1X,4I10,1X,F12.5)
NT1(NX)=S1+.5
NS1=NT1(NX)/8
CALL ADUT(NS1,3,1)
IF(J8.NE.1)GO TO 800
IF(NC.NE.JT)GO TO 800
IF(NX.EQ.N2)JT=JT+10
WRITE(7,33)NL1(NX),NT2(NX),NT1(NX),S5,R5
33 FORMAT(1X,5I6)
800 CONTINUE
IF(NY.NE.1)GO TO 200
IF(NX.NE.N2)GO TO 200
J8=1
S6=S5
R6=R5
WRITE(7,90)

```

```
90    FORMAT(1X,'START? (Y=1,N=2)')
      READ(5,15)NP9
      IF(NP9.EQ.1)GO TO 200
      STOP
200   CONTINUE
      IF(NC.EQ.0)GO TO 250
      WRITE(1'NC)NC,(NL1(KS),NT2(KS),NT1(KS),KS=1,N2)
250   CONTINUE
      CLOSE (UNIT=1)
      END
```

APPENDIX C  
COMPUTER PROGRAM LISTING  
SMOOTH.FOR

```

C
C      SMOOTH.FOR
C
C      THIS PROGRAM USES THE ISG DATA TAKEN ON THE
C      NOTCHED SPECIMENS TO CONTROL THE MTS MACHINE
C      UNDER STRAIN CONTROL. IT RECORDS THE LOAD DATA
C      AND STORES IT IN A FILE NAMED SMOOTH.DAT.
C
      DIMENSION NL1(60),NT2(60),NT1(60),NL2(60),NST(60)
      REAL KOR
      OPEN (UNIT=1,NAME='SY1:RESULT.DAT',TYPE='OLD',
*      ACCESS='DIRECT',READONLY,RECORDSIZE=91)
      OPEN (UNIT=2,NAME='SY1:SMOOTH.DAT',ACCESS='DIRECT',
*      INITIALSIZE=260,RECORDSIZE=31)
      JT=1
      KOR=1.133
      CALL AOUT(0,0,1)
      CALL AOUT(0,1,1)
      CALL AOUT(0,2,1)
      CALL AOUT(0,3,1)
      WRITE(7,11)
11      FORMAT(1X,'HOOK UP MTS MACHINE')
      WRITE(7,20)
20      FORMAT(1X,'CLIP GAGE CAL. FACTOR')
      READ(5,1)CGCF
      WRITE(7,*)CGCF
1      FORMAT(F10,4)
      WRITE(7,30)
30      FORMAT(1X,'NO. OF CYCLES')
      READ(5,2)NCY
2      FORMAT(I5)
      WRITE(7,*)NCY
      WRITE(7,40)

```

```

40    FORMAT(1X,'START ? (Y=1,N=2)')
      READ(5,2)NGO
      IF(NGO.EQ.1)GO TO 99
      STOP
99    CONTINUE
      DO 100 K=1,NCY
      READ(1,K)NC,(NL1(KS),NT2(KS),NT1(KS),KS=1,60)
      WRITE(7,110)NC
110   FORMAT(1X,I5)
      DO 150 L=1,60
      NST(L)=(NT1(L)/CGCF)*200*KOR
      CALL AOUT(NST(L),2,1)
      CALL AOUT(NST(L),3,1)
      CALL ISLEEP(0,0,0,3)
      CALL AIN(NL2(L),3,1)
150   CONTINUE
      WRITE(2'NC)NC,(NL2(KS),KS=1,60)
      IF(JT.NE.K)GO TO 100
      WRITE(7,120)(NT1(KY),NL2(KY),KY=1,60,3)
120   FORMAT(1X,2I6)
      JT=JT+10
100   CONTINUE
      CLOSE(UNIT=1)
      CLOSE(UNIT=2)
      END

```

## **APPENDIX D**

### **DATA REDUCTION PROGRAMS**

```

1 REM
2 REM          ANAL1.BAS
3 REM
4 REM  THIS PROGRAM PLOTS NOTCH STRAIN
5 REM  VERSUS NOTCH STRESS.
6 REM
10 DIM Y(100),X(100)
20 DIM Z(100)
30 OPEN 'SY1:RESULT.DAT' AS FILE #1
40 DIM #1,AZ(182000)
50 OPEN 'SY1:SMOOTH.DAT' AS FILE #3
60 DIM #3,BZ(65000)
70 OPEN 'LP:' FOR OUTPUT AS FILE #2
80 L=60
90 OPEN 'SY1:TEST.DAT' AS FILE #4
100 INPUT #4,D1$,D2$,D3
102 INPUT #4,D4,D5,D6%
104 INPUT #4,D7%,D8,D9
110 P$=D2$
120 L1=3*L
130 FOR J=0 TO 999
140 PRINT 'CYCLE NUMBER'
150 INPUT J
160 J=J-1
170 J1=J*(L1+2)
180 J2=J*(L+2)
190 L$=STR$(AZ(J1))
200 DISPLAY_CLEAR
210 PRINT AZ(J1),BZ(J2)
220 PRINT 'PLOT DATA? (Y=1,N=2)'
230 INPUT N9%
240 IF N9%=1% THEN 260
250 PRINT #2,'SMOOTH DATA'+ SPECIMEN NO. '+P$+' CYCLE NO. '+L$

```

```

260 I=0
270 FOR K=1 TO L1-2 STEP 3
272 F0=BZ(J2+I+1)
274 F3=(F0*10)/D4
276 F5=AZ(J1+K+2)
278 F4=(F5*1.13)/10000
280 IF N9Z=1Z THEN 310
290 PRINT AZ(J1+K),AZ(J1+K+1),AZ(J1+K+2),BZ(J2+I+1)
300 PRINT #2,F4,F3
310 IF N9Z<>1Z THEN 340
320 Y(I)=F3
330 X(I)=F4
340 I=I+1
350 NEXT K
360 IF N9Z<>1Z THEN 480
370 Y(I)=80000
380 X(I)=2
390 Y(I+1)=-Y(I)
400 X(I+1)=-X(I)
410 GRAPH('EXACT',,X(0),Y(0))
420 LABEL('BOLD','NOTCH STRESS VS. NOTCH STRAIN','STRESS')
430 X$='SPECIMEN NO. 'P$+' CYCLE NO. 'L$
440 ERASE_TEXT('-TEXT,ROW',21,1,100)
450 ERASE_TEXT('-TEXT,ROW',22,1,100)
460 ERASE_TEXT('-TEXT,ROW',23,1,100)
470 HTEXT('BOLD',22,1,X$)
480 NEXT J
490 CLOSE
500 END

```



```

1 REM
2 REM          ANAL2.BAS
3 REM
4 REM THIS PROGRAM COMPUTES AND PLOTS THE
5 REM STRESS AND STRAIN CONCENTRATION FACTORS
6 REM AND NEUBER'S PARAMETER VERSUS CYCLES.
7 REM
10 DIM RX(100),Y(17),X(17),F1(25),F2(25),F3(25),F4(25)
20 OPEN 'SY1:TEST.DAT' AS FILE #4
30 INPUT #4,D1$,D2$,D3
32 INPUT #4,D4,D5,D6%
34 INPUT #4,D7%,D8,D9
36 N6=D9
40 CLOSE #4
50 OPEN 'SY1:RESULT.DAT' AS FILE #1
60 DIM #1,AZ(182000)
70 OPEN 'SY1:SMOOTH.DAT' AS FILE #3
80 DIM #3,BZ(65000)
90 OPEN 'LP:' FOR OUTPUT AS FILE #2
100 L=60
110 L1=3*L
120 RX(0)=1
130 RX(1)=2
140 RX(2)=4
150 RX(3)=6
160 RX(4)=8
170 RX(5)=10
180 FOR M2=1 TO 2
190 FOR M1=1 TO 5
200 M3=10^M2
210 RX(M1+(5*M2))=RX(M1)*M3
220 NEXT M1
230 NEXT M2

```

```

240 FOR M4=0 TO 15
250 J=RZ(M4)-1
260 J1=J*(L1+2)
270 J2=J*(L+2)
280 IF RZ(M4)>D7% THEN 360
290 F0=AZ(J1+46)-AZ(J1+136)
300 F4=AZ(J1+48)-AZ(J1+138)
310 F5=BZ(J2+16)-BZ(J2+46)
320 F1(M4)=(F0*10)/D3
330 F2(M4)=(F1(M4)/D5)*1.00000E+06
340 F3(M4)=(F5*10)/D4
350 F4(M4)=F4*1.13
360 NEXT M4
370 PRINT 'PLOT 1)STRESS 2)STRAIN 3)NEUBER 4)STOP'
380 INPUT N9
390 ON N9 GO TO 1000,2000,3000,6000
1000 FOR M5=0 TO 15
1010 IF RZ(M5)>D7% THEN 1042
1020 Y(M5)=F3(M5)/F1(M5)
1025 Y(M5)=Y(M5)/N6
1030 X(M5)=LOG10(RZ(M5))
1040 NEXT M5
1042 Y(M5+1)=0
1044 X(M5+1)=0
1046 Y(M5+2)=2
1048 X(M5+2)=3
1050 P0$='STRESS CONCENTRATION VS. CYCLES'
1060 P1$='STRESS CONCN.'
1070 GOSUB 4000
1072 GOSUB 5000
1080 GO TO 370
2000 FOR M5=0 TO 15
2010 IF RZ(M5)>D7% THEN 2042

```

```

2020 Y(M5)=F4(M5)/F2(M5)
2025 Y(M5)=Y(M5)/N6
2030 X(M5)=LOG10(RX(M5))
2040 NEXT M5
2042 Y(M5+1)=0
2044 X(M5+1)=0
2046 Y(M5+2)=2
2048 X(M5+2)=3
2050 P0$='STRAIN CONCENTRATION VS.CYCLES'
2060 P1$='STRAIN CONCEN.'
2070 GOSUB 4000
2075 GOSUB 5000
2080 GO TO 370
3000 FOR M5=0 TO 15
3010 IF RX(M5)>D7% THEN 3042
3020 Y(M5)=(F3(M5)*F4(M5))/(F1(M5)*F2(M5))
3025 Y(M5)=Y(M5)/(N6*N6)
3030 X(M5)=LOG10(RX(M5))
3040 NEXT M5
3042 Y(M5+1)=0
3044 X(M5+1)=0
3046 Y(M5+2)=2
3048 X(M5+2)=3
3050 P0$='NEUBERS RULE VS. CYCLES'
3060 P1$='NEUBERS RULE'
3070 GOSUB 4000
3075 GOSUB 5000
3080 GO TO 370
4000 GRAPH('EXACT',,X(0),Y(0))
4010 LABEL('BOLD',P0$,P1$)
4020 X$='NOTCHED SPECIMEN NO. '+D1$
4025 Y$='SMOOTH SPECIMEN NO. '+D2$
4030 ERASE_TEXT('-TEXT,ROW',21,1,100)

```

```
4040 ERASE_TEXT('-TEXT,ROW',22,1,100)
4050 ERASE_TEXT('-TEXT,ROW',23,1,100)
4060 HTEXT('BOLD',22,1,X$)
4065 HTEXT('BOLD',23,1,Y$)
4070 RETURN
5000 PRINT 'PRINT (Y=1,N=2)'
5010 INPUT P6
5020 IF P6=1 THEN 5032
5030 RETURN
5032 PRINT #2
5034 PRINT #2
5040 PRINT #2,X$
5050 PRINT #2,Y$
5060 PRINT #2
5070 PRINT #2,P0$
5080 FOR M6=0 TO 15
5090 IF RZ(M6)>D7% THEN 5120
5100 PRINT #2,RZ(M6),Y(M6)
5110 NEXT M6
5120 RETURN
6000 DISPLAY_CLEAR
6005 CLOSE
6010 END
```

```

1 REM
2 REM          ANAL3.BAS
3 REM
4 REM THIS PROGRAM COMPUTES AND PLOTS THE STRESS AND
5 REM STRAIN CONCENTRATION FACTORS AND NEUBER'S
6 REM PARAMETER VERSUS NOTCH STRAIN.
7 REM
10 DIM RZ(100),Y(17),X(17),F1(25),F2(25),F3(25),F4(25)
20 OPEN 'SY1:TEST.DAT' AS FILE #4
30 INPUT #4,D1$,D2$,D3
32 INPUT #4,D4,D5,D6%
34 INPUT #4,D7%,D8,D9
36 N6=D9
40 CLOSE #4
50 OPEN 'SY1:RESULT.DAT' AS FILE #1
60 DIM #1,AZ(182000)
70 OPEN 'SY1:SMOOTH.DAT' AS FILE #3
80 DIM #3,BZ(65000)
90 OPEN 'LP:' FOR OUTPUT AS FILE #2
240 FOR M4=1 TO 15
250 K=M4
260 F0=AZ((3*K)+1)
270 F4=AZ((3*K)+3)
280 F5=BZ(K+1)
320 F1(M4)=(F0*10)/D3
330 F2(M4)=(F1(M4)/D5)*1.00000E+06
340 F3(M4)=(F5*10)/D4
350 F4(M4)=F4*1.13
360 NEXT M4
370 PRINT 'PLOT 1)STRESS 2)STRAIN 3)NEUBER 4)STOP'
380 INPUT N9
390 ON N9 GO TO 1000,2000,3000,6000
1000 FOR M5=1 TO 15

```

```

1020 Y(M5)=F3(M5)/F1(M5)
1025 Y(M5)=Y(M5)/N6
1030 X(M5)=F4(M5)/10000
1040 NEXT M5
1042 Y(M5+1)=0
1044 X(M5+1)=0
1046 Y(M5+2)=2
1048 X(M5+2)=1.5
1050 P0$='STRESS CONCENTRATION VS. NOTCH STRAIN'
1060 P1$='STRESS CONCN.'
1070 GOSUB 4000
1075 GOSUB 5000
1080 GO TO 370
2000 FOR M5=1 TO 15
2020 Y(M5)=F4(M5)/F2(M5)
2025 Y(M5)=Y(M5)/N6
2030 X(M5)=F4(M5)/10000
2040 NEXT M5
2042 Y(M5+1)=0
2044 X(M5+1)=0
2046 Y(M5+2)=2
2048 X(M5+2)=1.5
2050 P0$='STRAIN CONCENTRATION VS. NOTCH STRAIN'
2060 P1$='STRAIN CONCN.'
2070 GOSUB 4000
2075 GOSUB 5000
2080 GO TO 370
3000 FOR M5=1 TO 15
3020 Y(M5)=(F3(M5)*F4(M5))/(F1(M5)*F2(M5))
3025 Y(M5)=Y(M5)/(N6*N6)
3030 X(M5)=F4(M5)/10000
3040 NEXT M5
3042 Y(M5+1)=0

```

```

3044 X(M5+1)=0
3046 Y(M5+2)=2
3048 X(M5+2)=1.5
3050 P0$='NEUBERS RULE VS. NOTCH STRAIN'
3060 P1$='NEUBERS RULE'
3070 GOSUB 4000
3075 GOSUB 5000
3080 GO TO 370
4000 GRAPH('EXACT',,X(0),Y(0))
4010 LABEL('BOLD',P0$,P1$)
4020 X$='NOTCHED SPECIMEN NO. '+D1$
4025 Y$='SMOOTH SPECIMEN NO. '+D2$
4030 ERASE_TEXT('-TEXT,ROW',21,1,100)
4040 ERASE_TEXT('-TEXT,ROW',22,1,100)
4050 ERASE_TEXT('-TEXT,ROW',23,1,100)
4060 HTEXT('BOLD',22,1,X$)
4065 HTEXT('BOLD',23,1,Y$)
4070 RETURN
5000 PRINT 'PRINT (Y=1,N=2)'
5010 INPUT P6
5020 IF P6=1 THEN 5032
5030 RETURN
5032 PRINT #2
5034 PRINT #2
5040 PRINT #2,X$
5050 PRINT #2,Y$
5060 PRINT #2
5070 PRINT #2,P0$
5080 FOR M6=1 TO 15
5090 IF RZ(M6)>D7% THEN 5120
5100 PRINT #2,X(M6),Y(M6)
5110 NEXT M6
5120 RETURN

```

6000 DISPLAY\_CLEAR  
6005 CLOSE  
6010 END



```

1 REM
2 REM          ANAL4.BAS
3 REM
4 REM THIS PROGRAM PLOTS THE REMOTE STRESS
5 REM VERSUS THE NOTCH STRAIN.
6 REM
10 DIM Y(100),X(100)
20 OPEN 'SY1:RESULT.DAT' AS FILE #1
30 DIM #1,AZ(182000)
40 OPEN 'LP:' FOR OUTPUT AS FILE #2
50 L=60
60 OPEN 'SY1:TEST.DAT' AS FILE #4
70 INPUT #4,P$,D2$,D3
80 INPUT #4,D4,D5,D6%
90 INPUT #4,D7%,D8,D9
100 CLOSE #4
110 L1=3*L
120 FOR J=0 TO 999
130 PRINT 'CYCLE NUMBER'
140 INPUT J
150 J=J-1
160 J1=J*(L1+2)
170 L$=STR$(AZ(J1))
180 DISPLAY_CLEAR
190 PRINT AZ(J1)
200 PRINT 'PLOT DATA? (Y=1,N=2)'
210 INPUT N9%
220 IF N9%=1% THEN 240
230 PRINT #2,'NOTCHED DATA  SPECIMEN NO. '+P$+'  CYCLE NO. '+L$
240 I=0
250 FOR K=1 TO L1-2 STEP 3
280 F0=AZ(J1+K)
290 F1=(F0*10)/D3

```

```

300 F5=AZ(J1+K+2)
310 F4=(F5*1,13)/10000
312 IF N9Z=1Z THEN 330
314 PRINT AZ(J1+K),AZ(J1+K+1),AZ(J1+K+2)
320 PRINT #2,F4,F1
330 IF N9Z<>1Z THEN 370
340 Y(I)=F1
350 X(I)=F4
360 I=I+1
370 NEXT K
380 IF N9Z<>1Z THEN 500
390 Y(I)=50000
400 X(I)=2
410 Y(I+1)=-Y(I)
420 X(I+1)=-X(I)
430 GRAPH('EXACT',,X(0),Y(0))
440 LABEL('BOLD','REMOTE STRESS VS. NOTCH STRAIN','STRESS')
450 X$='SPECIMEN NO. 'P$+' CYCLE NO. 'L$
460 ERASE_TEXT('-TEXT,ROW',21,1,100)
470 ERASE_TEXT('-TEXT,ROW',22,1,100)
480 ERASE_TEXT('-TEXT,ROW',23,1,100)
490 HTEXT('BOLD',22,1,X$)
500 NEXT J
510 CLOSE
520 END

```

## VITA

Michael W. Guillot was born on December 27, 1951, in Baton Rouge, Louisiana. In May, 1969, he graduated from Redemptorist High School in Baton Rouge, Louisiana. He received his B. S. in Mechanical Engineering from Louisiana State University in December 1972.

In September, 1973, he started a program of study at Louisiana State University which led to his receiving a Master of Science degree in Mechanical Engineering in May, 1976. He was married to the former Ladonna Cameron on August 10, 1974.

While employed by the Ethyl Corporation, he began a course of night study in September, 1976, toward a Ph.D. degree in Mechanical Engineering. The entire year of 1980 was spent in residence at Louisiana State University, during which time research in the area of metal fatigue was conducted. After completing this research, the Ph.D. degree was granted in May, 1981.

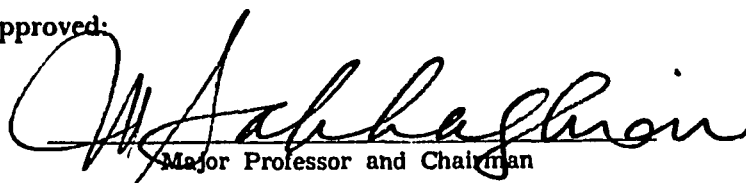
## EXAMINATION AND THESIS REPORT

Candidate: Michael Wade Guillot

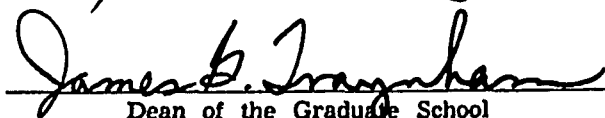
Major Field: Mechanical Engineering

Title of Thesis: An Experimental Evaluation of Neuber's Cyclic Relation at Room and Elevated Temperature

Approved:

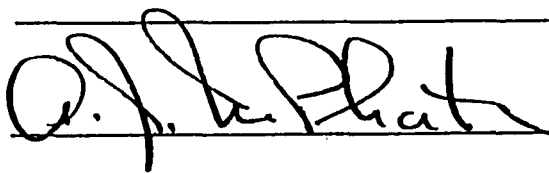


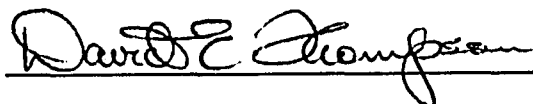
Major Professor and Chairman

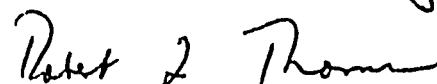


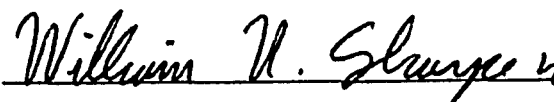
Dean of the Graduate School

### EXAMINING COMMITTEE:









Date of Examination:

May 1, 1981